STUDY OF DEEP BEAMS USING FINITE ELEMENT APPROACH

Sriharan Jasotharan

168015U

Degree of Master of Science

Department of Civil Engineering

University of Moratuwa

Sri Lanka

December 2017

STUDY OF DEEP BEAMS USING FINITE ELEMENT APPROACH

Sriharan Jasotharan

168015U

Thesis submitted in partial fulfilment of the requirements for the degree Master of Science in Civil Engineering

Department of Civil Engineering

University of Moratuwa

Sri Lanka

December 2017

DECLARATION

I declare that this is my own work and this thesis does not incorporate without acknowledgement any material previously submitted for a Degree or Diploma in any other University or institute of higher learning and to the best of my knowledge and belief it does not contain any material previously published or written by another person except where the acknowledgement is made in the text.

Also, I hereby grant to University of Moratuwa the non-exclusive right to reproduce and distribute my thesis, in whole or in part in print, electronic or other medium. I retain the right to use this content in whole or part in future works (such as articles or books)

…… Date: 18th December 2017

S.Jasotharan

The above candidate has carried out research for the Masters under my supervision.

…… Date: 18th December 2017

Prof I.R.A Weerasekera

ABSTRACT

Beams are common structural elements in most structures and generally they are analysed using classical beam theories to evaluate the stress and strain characteristics of the beam. But in the case of deep beams, higher order shear deformation beam theories predicts more accurate results than classical beam theories due its more realistic assumption regarding the shear characteristics of the beam.

In this study a hyperbolic shear deformation theory for thick isotropic beams is developed where the displacements are defined using a meaningful function which is more physical and directly comparable with other higher order theories. Governing variationally consistent equilibrium equations and boundary conditions are derived in terms of the stress resultants and displacements using the principle of virtual work. This theory satisfies shear stress free boundary condition at top and bottom of the beam and doesn't need shear correction factor.

.A displacement based finite element model of this theory is formulated using the variational principle. Displacements are approximated using the homogeneous solutions of the governing differential equations that describe the deformations of the cross-section according to the high order theory, which includes cubic variation of the axial displacements over the cross-section of the beam. Also, this model gives the exact stiffness coefficients for the high order isotropic beam element. The model has six degrees of freedom at the two ends, one transverse displacement and two rotations, and the end forces are a shear force and two components of end moments.

Several numerical examples are discussed to validate the proposed shear deformation beam theory and finite element model of the beam theory. Results obtained for displacements using the present beam theory and the finite element model are compared with results obtained using other beam theories, 2D elastic theory and 2D and 3D finite element models. Solutions obtained using the proposed beam theory and finite element model are in close agreement with the solutions obtained using 2D elastic theory and 2D and 3D finite element models of 'ABAQUS'.

Keywords: Beam theory; Finite Element; Higher order; Shear Deformation.

DEDICATION

To My Parents

ACKNOWLEDGEMENT

I would like firstly to express my deep gratitude to my supervisor Prof. Ruwan Weerasekera, for his guidance, support and encouragement during the past year. He opened a door for me to a fascinating academic world. With the wide vision on the science and engineering, he always can find an exciting research direction. He motivated to think independently and guided me wherever I needed to keep me on the track in achieving my research goals. Talking with him was always enjoyable and also inspiring, not only in the academics but also the life.

I would like to thank Dr. Chinthaka Mallikarachchi and Dr. Rangika Halwatura for their valuable feedbacks on my research which have been very helpful.

I would like to give some special thanks to my colleagues and friends. Mr. Ubamanyu and Mr. Dharmadasa who helped me whenever I face difficulties with 'ABAQUS' software in getting solutions. Also their feedbacks on my presentations and research papers related this work helped me to improve my work further.

I would like to thank Department of Civil Engineering, for providing the facilities and resources required during this period which helped me to carry out my research in a good environment. I also acknowledge Senate Research Committee (SRC), University of Moratuwa for their financial support.

Last but not least, I would like to express my gratitude to my parents for their understanding. I owe everything to my parents for what I have become.

S.Jasotharan
18.12.2017

TABLE OF CONTENT

Declaration i

Abstract ii

Dedication iii

Acknowledgement iv

Table of Content v

List of figures vii

List of Tables ix

Notations x

1. INTRODUCTION 1

1.1. Background 1

1.2. Overview of the finite element method (FEM) 2

1.3. Objectives 4

1.4. Methodology 4

1.5. Outline of this Thesis 5

2. LITERATURE REVIEW 7

2.1. Review of beam theories 7

2.2. Review of finite element models 11

2.3. Theoretical aspects related to formulation of finite element 15

2.3.1. Strong forms Vs. Weak forms 15

2.3.2. Variational methods and variational principle 16

2.3.3. Weighted residual method 16

2.3.4. Euler - Lagrange equations and boundary conditions 18

2.3.5. Finite element formulation using minimum total potential energy principle 21

3. THEORETICAL FORMULATION 23
3.1. Assumptions made in the theoretical formulation 24
3.2. Displacement field 24
3.3. Governing equations and boundary conditions 25
3.3.1. The stress resultant-displacement relations 25
3.4. General solutions for static flexure of beams 28
4. FINITE ELEMENT FORMULATION 30
4.1. Derivation of shape functions 30
4.2. Construction of weak form 34
4.3. Finite element model 35
4.3.1. Stiffness matrix terms 37
4.3.2. Load vector 39
4.4. Using the finite element model for 2D frame analysis. 39
4.4.1. Transformation from local system to global system 41
5. RESULTS AND DISCUSSION 43
5.1. Validation of the proposed theory 43
5.1.1. Numerical examples I 43
5.1.2. Comparisons and findings of the theoretical solutions 54
5.2. Validation of the finite element model 55
5.2.1. Numerical examples II 57
6. CONCLUSIONS AND FUTURE WORKS 71
6.1. Conclusions 71
6.2. Future work 72
REFERENCES 73
APPENDIX A xii
A.1. MATLAB program for stiffness matrix xii

A.2. MATLAB program to analyse the general beam problem xiv

LIST OF FIGURES

Figure 2.1-Kinematics of various beam theories 10
Figure 2.2 - Typical function y(x) and the approximate solution $y(x)$ 19
Figure 3.1-The beam under consideration 23
Figure 4.1-Genralized displacements and generalised forces on a typical element 37
Figure 4.2-Generalised displacements in the local and global coordinates ... 41
Figure 5.1-simply supported beam problem 43
Figure 5.2 -The coordinate system for 2D elasticity solution for example 1(a) 44
Figure 5.3-Transverse displacement along centre line for example 1(a)..... 45
Figure 5.4-Shear strain along centre line for example 1(a)..... 45
Figure 5.5-Shear stress variation across the depth at x = 0 for example 1(a) 46
Figure 5.6-Axial stress variation across the depth at x = 0.5L for example 1(a) 46
Figure 5.7-Transverse displacement along centre line for example 1(b)..... 47
Figure 5.8-Shear strain variation along centre line for example 1(b) 47
Figure 5.9-Transverse displacement along centre line for example 1(c)..... 48
Figure 5.10-Shear strain variation along centre line for example 1(c) 48
Figure 5.11-Shear stress variation across the depth at x = 0 for example 1(c) 49
Figure 5.12-Axial stress variation across the depth at x = 0.5L for example 1(c) 49
Figure 5.13-Cantilever beam problem 51
Figure 5.14-Transverse displacement along centre line for example 2(a)..... 52
Figure 5.15-Shear strain along centre line for example 2(a)..... 53
Figure 5.16-Transverse displacement along centre line for example 2(b)..... 53
Figure 5.17-Shear strain along centre line for example 2(b) 54

Figure 5.18 -Transverse displacement along centre line using present FE for example 1(a) 57
Figure 5.19 -Transverse displacement along centre line using 58
Figure 5.20 -Transverse displacement along centre line using present FE for example 1(a) 58
Figure 5.21-Shear strain along centre line using 59
Figure 5.22-Transverse displacement along centre line using present FE for example 1(c) 60
Figure 5.23- Transverse displacement along centre line using ABAQUS for example 1(a) 61
Figure 5.24- Transverse displacement along centre line using ABAQUS for example 1(b) 62
Figure 5.25- Shear strain along centre line using ABAQUS for example 1(a) 62
Figure 5.26- Shear strain along centre line using ABAQUS for example 1(b) 63
Figure 5.27-Stepped beam problem 64
Figure 5.28 - Shear strain along centre line for example 4 65
Figure 5.29 - Transverse displacement along centre line for example 4 65
Figure 5.30 - Results for tranverse diplacement and shear strain uisng ‘ABAQUS’ 2D model 66
Figure 5.31- Continuos beam probelem 67
Figure 5.32 -Transverse displacement along centre line for example 5 68
Figure 5.33 - Shear strain along centre line for example 5 68
Figure 5.34 - Results for tranverse diplacement and shear strain uisng 69
Figure 5.35 - Axial stress variation for thin beam 70
Figure 5.36 - Axial stress variation for deep beam 70

LIST OF TABLES

Table 5.1. Maximum value for displacements and stresses for example 1(a) ..... .50

Table5.2. Maximum value for displacements and stresses for example 1(b) 50

Table5.3. Maximum value for displacements and stresses for example 1(c) 50

NOTATIONS

A - area of cross section of beam.

b - width of beam.

D - nodal degree of freedom.

D^e - nodal degree of freedom in local coordinate system.

E - elastic modulus.

f - force vector due to distributed load.

F - force vector due to concentrated load.

f^e - force vector due to concentrated load in local coordinate system.

F^e - force vector due to concentrated load in local coordinate system.

G - shear modulus.

h - depth of beam.

I - second moment of area about centroidal axis.

K_s - shear correction factor.

L - length of beam element.

N_i - shape function.

p(x) - axially distributed load

q(x) - transverse distributed load.

S - element stiffness matrix.

S_e - stiffness matrix in local coordinate system.

T - transformation matrix.

U - strain energy.

u(x) - axial displacement at centre line of beam.

u(x, z) - axial displacement at coordinate (x, z).

V - work done by the external forces.

w(x) - transverse displacement of beam at centre line.

w(x, z) - transverse displacement at coordinate (x, z).

$\frac{dw}{dx}$ - bending rotation of cross section.

$\phi(x)$ - total rotation of cross section.

$\Phi(z)$ - function which describes the distribution of transverse shear stress along the thickness of beam.

Ω - problem domain.

Γ - boundary of domain.

Π - total potential energy.

ε_{xx} - normal strain.

γ_{xz} - shear strain.

σ_{xx} - normal stress.

τ_{xz} - shear stress

CHAPTER I

1. INTRODUCTION

1.1. Background

Beams are common structural elements in most structures and generally they are analyzed using classical or refined shear deformation theories to evaluate the static and dynamic characteristics. In the case of thin beams, the well-known elementary theory of bending (Euler-Bernoulli) [1] is commonly used to analyse the beam which gives reasonably accurate prediction of stress and strain characteristics of beam. But as the depth to span ratio increases, this elementary theory of bending produces erroneous prediction about the stress and strain characteristics of the beam. This is due to the reason that the elementary theory does not take into account the effects of shear deformation across the depth of the beam. It is based on the assumption that the section normal to neutral axis remains so during bending and after bending, implying that the transverse shear strain is zero.

As the depth to span ratio increases, the bending stress distribution across any transverse section deviates appreciably from straight line distribution used in the elementary theory of beams. Consequently, a transverse section which is plane before bending does not remain approximately plane after bending and neutral axis does not usually lie at the mid depth. Taking into account all these, Timoshenko [2] developed a first order shear deformation theory in which shear strain distribution is assumed to be constant through the thickness thus requires shear correction factor to appropriately represent the strain energy of deformation. Considering these discrepancies in the elementary theory of beam bending and first order shear deformation theory, several higher order shear deformation theories [3-11] were developed by researchers based on the assumed function for shearing stress distribution through the thickness of the beam. These theories are commonly used to predict the stress and strain characteristics of deep beams.

According to NEN-EN-1992-1-1 cl. 5.3.1 (3) [12] a deep beam is a member for which the span to overall depth ratio is bigger or equal to 3. According to ACI 318-

08: 2007 cl.10.7.1 [13] deep beams have a clear span to overall depth ratio equal to or less than 4. Dubey and Pathak [14] observed even at the span to depth ratio of 4, there is considerable influence of shear deformation on the beam.

But when the higher order theories are used to solve the practical problems (e.g. Continuous beam with various support and loading conditions), obtaining the exact analytical solution to those governing differential equations becomes a difficult task. In such situation, finite element method (FEM) can be used as a powerful tool to analyse the problem and to get the approximate solutions. In this study, a higher order shear deformation beam theory is proposed to analyse the thick isotropic uniform beam and a displacement based finite element model is developed using the proposed beam theory. It should be noted that although there are number of versions of higher order theories, only few have worked on the finite element solution for this theory. An exact finite element formulation for the proposed higher order theory using the variational approach is a new aspect in this area of study which would make possible easy use of the higher order theory in analysing the practical beam problems.

1.2. Overview of the finite element method (FEM)

Concept of FEM dates back to 1696. The Brachistochrone problem was one of the earliest problems in Calculus of variations posted by Johann Bernoulli [15] in Acta Eroditorum in 1696. The problem is to find the minimum time trajectory described by an object moving from one point to another in a constant uniform gravitational field. He obtained the solution by dividing the plane into strips and assumes that the particle follows a straight line in each strip.

The history of the modern development of the finite element method began in the 1940s in the field of structural engineering with the work by Hrennikoff [16] in 1941. McHenry [17] in 1943, used one-dimensional elements (bars and beams) to obtain the solution for stresses in continuous solids. In a paper published in 1943, Courant [18] proposed deriving the solution of stresses in a variational form but this had not been widely recognized for many years. Then he proposed piecewise interpolation (or shape) functions which can be used with triangular element as a method to obtain approximate numerical solutions over the region. In 1947 Levy [19]

developed the flexibility or force method of analysis, and in 1953 his work [20] suggested another method called stiffness or displacement method which was a promising alternative for analysing statically redundant structures. However, his equations were cumbersome for hand calculation, and thus the method became popular only after use of computers.

In 1954 Argyris and Kelsey [21] used energy principle to develop matrix based structural analysis. This revealed the importance role of energy principle which would have in the finite element method. In 1956, Turner et al. [22] used two-dimensional elements for the first in their work. They derived stiffness matrices for several two-dimensional elements using direct stiffness method. With the introduction of the high-speed digital computer during 1950s, Turner et al. [22] looked for new and further development in finite element equations.

Although the concepts finite element method were studied and developed by various researchers in the past, Clough [23] was the first to introduce the phrase finite element in 1960 when both triangular and rectangular elements were used for plane stress analysis. In 1961 Melosh [24] developed a flat rectangular-plate bending-element stiffness matrix. Following this, in 1963 Grafton and Strome [25] developed a curved-shell bending element stiffness matrix for axisymmetric shells and pressure vessels.

Martin [26], Gallagher et al. [27], and Melosh [28] extended the finite element method to three-dimensional problems with the development of a tetrahedral stiffness matrix. Further study on the three-dimensional elements were carried out by Argyris [29] in 1964. In 1965, Clough and Rashid [30] and Wilson [31] considered special case of axisymmetric solids.

In 1965 Archer [32] considered dynamic analysis in the development of the consistent-mass matrix, which is applicable to analysis of distributed-mass systems such as bars and beams in structural analysis. In 1963 Melosh found out that the finite element method could be formulated in terms of a variational approach. It made possible that finite element method also could be used to solve non-structural applications. With the introduction of weighted residual method by by Szabo and Lee

[33] in 1969 to derive the previously known elasticity equations used in structural analysis and then by Zienkiewicz and Parekh [34] in 1970 for transient field problems made possible further extension of the method. It was then recognized that when direct formulations and variational formulations are difficult or not possible to use, the method of weighted residuals may at times be appropriate.

From the early 1950s to the present, enormous advances have been made in the application of the finite element method to solve the complicated engineering problems.

1.3. Objectives

The main objective of this study is to develop a higher order shear deformation theory for uniform isotropic beam and to develop an efficient beam element using the higher order beam theory. In addition to that this research focuses on studying stress and strain characteristics of beams having different aspect ratios.

1.4. Methodology

The research methodology includes the following tasks to achieve the research objectives.

- Review of literatures which discuss about derivation of beam theories and beam element associated with those theories.
- Establishing a displacement field which is more physical and describes deformation behaviour more accurately.
- Finding the governing differential equations and boundary conditions of the proposed theory
- Finding the general solutions for primary variables.
- Validations of the proposed theory. The proposed theory should be validated against the two dimensional elasticity solutions.
- Selection of suitable interpolation functions and their order of approximation for the general displacement field.
- Developing the Galerkin's Weak form/Variational statement for the governing differential equations.

- Formulation of finite element by substituting the displacement variables using the approximate solutions.
- Validations and checking the convergence of beam element. Finite element solutions should be compared with corresponding exact theoretical solutions.
- Applications for practical problems (e.g Continuos beams and Frames) would be discussed and solutions should be compared with other finite element solutions.
- A computer program would be developed to get the solutions using present beam element.
- Conclusions based on the research study and recommendation for further work.

1.5. Outline of this Thesis

This thesis consists of six chapters which includes following contents.

Chapter 2: This chapter reviews number of beam theories related to this study. Also it reviews the number of finite element model based on those theories. In addition this chapter discusses some theoretical aspects which are required for the theoretical and finite element formulation of the present study.

Chapter 3: This Chapter includes the theoretical formulation of proposed shear deformation beam theory. Governing Equilibrium equations and boundary conditions are derived using variational principle. Stress resultant- displacement relationships are defined. General solutions for primary variables are obtained for uniform rectangular isotropic beam based on the governing equation of equilibrium.

Chapter 4: This chapter presents a displacement based finite element model for the proposed beam theory. An exact beam element with two nodes having three degree freedom at each node is presented. Explicit terms of the stiffness matrix are derived.

Chapter 5: This chapter present validation of the present theory and the finite element model of the present theory. The finite element solutions are checked for the convergence against the corresponding theoretical solutions. Several numerical examples are discussed using the present beam element and solutions are compared

with the solutions obtained using other beam elements and 2D and 3D models of ‘ABAQUS’

Chapter 6: This chapter presents conclusions of the present study and future areas for consideration in relation to this study.

CHAPTER II

2. LITERATURE REVIEW

2.1. Review of beam theories

Several beam theories are used to represent the kinematics of deformation. To describe the various beam theories, following coordinate system is introduced here. The x-coordinate is taken along the length of the beam, z-coordinate along the thickness (the height) of the beam, and the y-coordinate is taken along the width of the beam. In a general beam theory, all applied loads and geometry are such that the displacements (u,v,w) along the coordinates (x,y,z) are only functions of the x and z coordinates. Among these Euler beam theory (EBT) [1] is earliest and one of the well - known theories which has a major drawback of neglecting effects of transverse shear strain because of the assumption that the plane section is perpendicular to neutral axis of beam before bending, remains plane and perpendicular to axis after the deformation. This theory based on the displacement field;

$$u(x,z) = -z\frac{dw}{dx}$$
$$w(x,z) = w(x) \tag{2.1}$$

This theory provides excellent solution for the analysis of slender beams whereas for moderately short or thick beams, the solutions are not in the acceptable range.

In the development of beam theories, Timoshenko was the first to include the influence of transverse shear strain and rotatory inertia into the newly developed first order shear deformation theory (FSBT) [2]. In the Timoshenko beam theory it is assumed that plane cross section remain plane but not normal to the neutral axis after deformation. . This theory based on the displacement field;

$$u(x,z) = z\phi(x)$$
$$w(x,z) = w(x) \tag{2.2}$$

Since Timoshenko beam theory assumes a constant transverse shear stress distribution through the beam depth, it is necessary to have shear correction factor for

the beam. Cowper [35, 36] analysed the accuracy of Timoshenko beam theory for transverse vibration of simply supported beam with respect to fundamental frequency and reported some values for shear correction factor of beams having various cross sections.

The limitations on the Euler beam theory and the Timoshenko theory led to the development of higher order theory. Many higher order theories are available in the literature for static and dynamic analysis of the beams. Levinson [3] has developed new rectangular beam theory for static and dynamic analysis of the beam where he derived the governing equations of the beam using vector mechanics. He used following displacement field to develop his theory.

$$u(x,z) = z\phi(x) - \frac{4}{3h^2}z^3\left(\frac{dw}{dx} + \phi(x)\right)$$
$$w(x,z) = w(x) \tag{2.3}$$

Bickford [4] used the same displacement function used by the Levinson and derived a variationally consistent shear deformation theory for isotropic beams. Third order plate theory developed by Reddy [5] was specialized into beam theory by Heyliger and Reddy [6] to study the linear and non-linear bending and vibration of isotropic beams. These higher order shear deformation beam theories (HSBT) do not need the shear correction factor since shear stress free boundary condition in top and bottom of the beam are satisfied.

There is another set of refined shear deformation theories using trigonometric and hyperbolic functions to define the displacement function. Touratier [7], Vlasov and Leont'ev [8] and Stein [9] presented trigonometric shear deformation theories. However, those theories do not satisfy shear stress free boundary condition. Ghugal and Shimpi [10] have developed variationaly consistent trigonometric shear deformation theory (TSBT) which satisfies the shear stress free function condition at top and bottom surfaces of the beam.

Ghugal and Sharma [11] have developed variationally consistent hyperbolic shear deformation theory (HPSBT) for static and dynamic analysis of thick isotropic beams.

The above mentioned beam deformation theories can be expressed in a unified mathematical forms as follows [37]

$$u(x,z) = u(x) - z\frac{dw(x)}{dx} + \Phi(z)\left(\frac{dw(x)}{dx} - \phi(x)\right);$$

$$v(x,z) = 0\,; \tag{2.4}$$

$$w(x,z) = w(x)$$

Where u, w, and $\phi(x)$ are three unknown functions, represent the axial displacement, transverse displacement and the total bending rotation of the cross section at any point on the neutral axis, respectively. Also $\Phi(z)$ describes the distribution of transverse shear stress along the thickness of the beam. The mathematical form of this function for the displacement field of the above mentioned theories is as follows [37].

$EBT:\ \Phi(z) = 0$

$FSBT:\ \Phi(z) = z$

$HSBT:\ \Phi(z) = z\left(1 - \frac{4z^2}{3h^2}\right)$

$TSBT:\ \Phi(z) = \frac{h}{\pi}\sin\left(\frac{\pi z}{h}\right)$

$HPSBT:\ \Phi(z) = h\,.\sinh\left(\frac{z}{h}\right) - z.\cosh\left(\frac{1}{2}\right)$

The Figure 2.1 below illustrates the difference between kinematic assumption of Euler-Bernoulli beam theory, Timoshenko beam theory and third order theories.

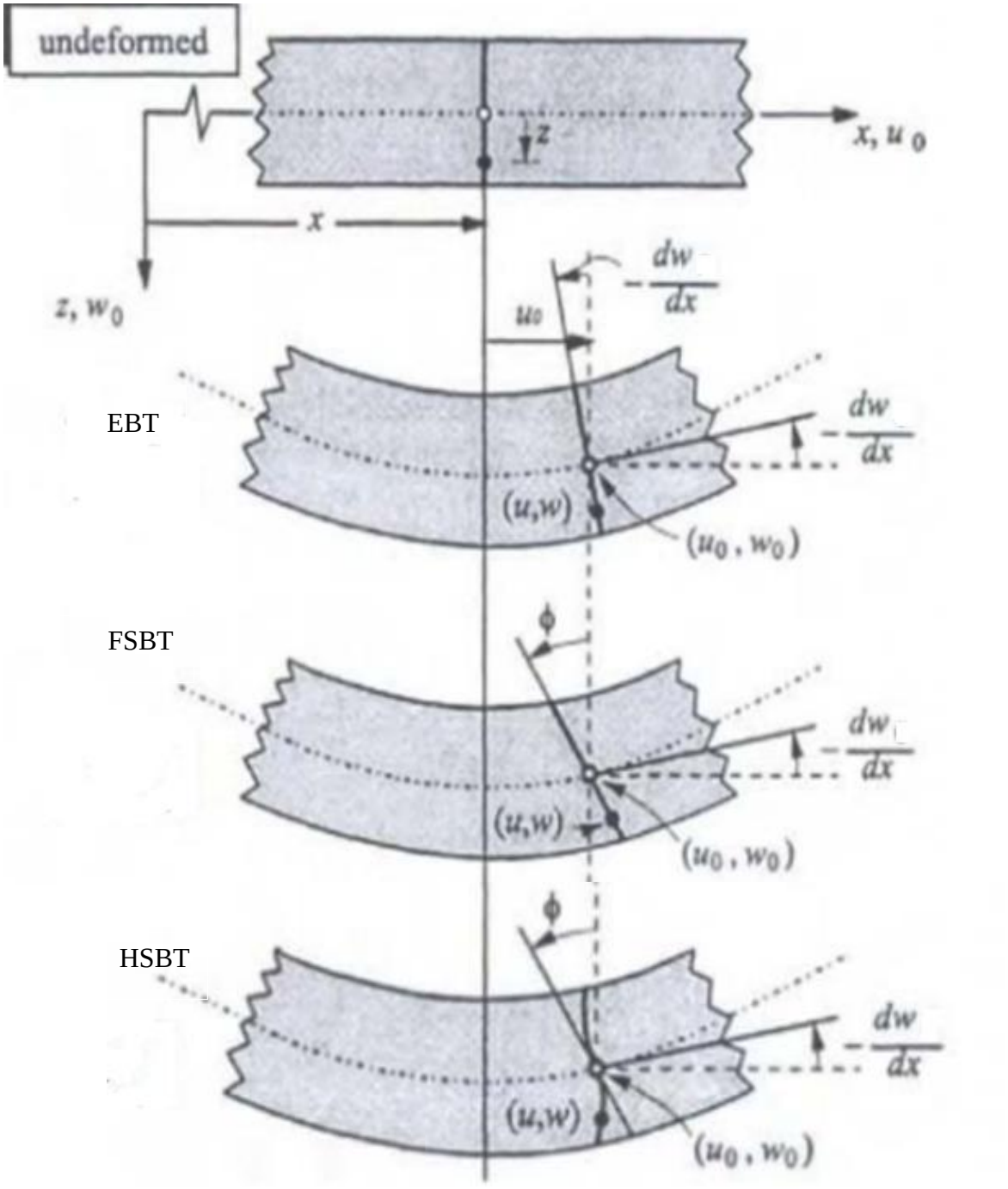

Figure 2.1-Kinematics of various beam theories

2.2. Review of finite element models

The finite element models of Euler-Bernoulli beam theory (EBT) is most common and can be found in several books [38]. Since this finite element model uses Hermite cubic interpolation which is suggested by the general solution of the homogeneous equation, this models gives exact values for the deflection and slope at the nodes [39]. For constant EI and uniformly distributed load of q, the beam element becomes

$$\frac{2EI}{L^3}\begin{bmatrix} 6 & -3L & -6 & -3L \\ -3L & 2L^2 & 3L & L^2 \\ 6 & 3L & 6 & 3L \\ -3L & L^2 & 3L & 2L^2 \end{bmatrix}\begin{Bmatrix} D_1 \\ D_2 \\ D_3 \\ D_4 \end{Bmatrix} = \frac{qL}{12}\begin{Bmatrix} 6 \\ -L \\ 6 \\ L \end{Bmatrix} + \begin{Bmatrix} F_1 \\ F_2 \\ F_3 \\ F_4 \end{Bmatrix} \qquad (2.5)$$

; F_i are the generalized nodal forces.

There are several finite element models based on Timoshenko beam theory in the literature. They differ from each other in the choice of their interpolation function or in weak form used to develop finite element model [39]. These elements can be divided into two classes. According to the literature, a simple element is one which has a total of four degrees of freedom, two at each of the two nodes. A complex element is one which has more than four degrees of freedom, having more than two degrees of freedom at a node or more than two nodes. The first formulation of simple element for a uniform beam was given by McCalley [40].

$$S = \frac{EI}{L^3(1+\Lambda)}\begin{bmatrix} 12 & & & \\ 6L & L^2(4+\Lambda) & & \\ -12 & -6L & 12 & \\ 6L & L^2(2-\Lambda) & -6L & 2L^2 \end{bmatrix};\ \Lambda = \frac{12EI}{GK_sAL^2} \qquad (2.6)$$

This is an exact stiffness matrix developed based on direct flexibility approach. Detailed derivation of this exact stiffness matrix can be found in [37].

The above approach to exact stiffness matrix, has difficulties in developing consistent mass matrix and force matrix. Another approach which is based on the variational principle has been used by several researchers to formulate the element stiffness, mass and force matrices. Here assumed interpolation functions were used to describe the kinematic variables. But using the same order polynomial for both transverse deflection w and cross section rotation ϕ and integrating to get the exact

values resulted in shear locking. To reduce the effect of shear locking, earlier two methods were used by researchers namely reduced integration and consistent interpolation. But these methods to develop Timoshenko elements are not completely free of shear locking [39].

Hughes et al. [41] was the first to develop a 'low-order' two-node element based upon linear polynomials (2 DOF per node) for each of the variables. This element, which was formulated using selective reduced integration, produced reasonably accurate results over a broad range of beam thickness/length ratios. Bending stiffness and one-point and two-point quadrature shear stiffness are separately presented and it is verified that two-point quadrature overestimates the shear stiffness in the case thin beam element hence leads to shear locking.

For linear interpolation of both w and ϕ and for constant values of El, and GAKs, the element equations (with reduced integration) are given in [39] by

$$\frac{2EI}{4L^3\Lambda}\begin{bmatrix} 4 & -2L & -4 & -2L \\ -2L & L^2(1+4\Lambda) & 2L & L^2(1-4\Lambda) \\ -4 & 2L & 4 & 2L \\ -2L & L^2(1-4\Lambda) & 2L & L^2(1+4\Lambda) \end{bmatrix}\begin{Bmatrix} D_1 \\ D_2 \\ D_3 \\ D_4 \end{Bmatrix} = \begin{Bmatrix} f_1 \\ 0 \\ f_2 \\ 0 \end{Bmatrix} + \begin{Bmatrix} F_1 \\ F_2 \\ F_3 \\ F_4 \end{Bmatrix}; \quad (2.7)$$

$$\Lambda = \frac{EI}{GK_sAL^2}$$

$$and\ f_i = \int_0^L q(x)Nidx, \qquad i = 1,2$$

; Ni is linear interpolation functions.

For quadratic interpolation of w and linear interpolation of ϕ and for constant values of El, and GAKs consistent interpolation element matrix is given in [39] by

$$\frac{2EI}{4L^3\Lambda}\begin{bmatrix} 4 & -2L & -4 & -2L \\ -2L & L^2(1+4\Lambda) & 2L & L^2(1-4\Lambda) \\ -4 & 2L & 4 & 2L \\ -2L & L^2(1-4\Lambda) & 2L & L^2(1+4\Lambda) \end{bmatrix}\begin{Bmatrix} D_1 \\ D_2 \\ D_3 \\ D_4 \end{Bmatrix} = \begin{Bmatrix} f_1 + 0.5f_3 \\ -0.125f_3L \\ f_1 + 0.5f_{3_2} \\ 0.125f_3L \end{Bmatrix} + \begin{Bmatrix} F_1 \\ F_2 \\ F_3 \\ F_4 \end{Bmatrix}; \quad (2.8)$$

$$\Lambda = \frac{EI}{GK_sAL^2}$$

$$and\ f_i = \int_0^L q(x)Nidx, \qquad i = 1,2,3$$

; N_i is linear interpolation functions

Completely shear locking free Timoshenko element was developed using inter dependent interpolation between transverse deflection w and cross section rotation ϕ. Derivation of this element can be found in [39]. For constant values of EI and GAKs and uniformly distributed transverse load q, the element equations are given by

$$\frac{2EI}{\mu L^3}\begin{bmatrix} 6 & -3L & -6 & -3L \\ -3L & 2L^2\alpha & 3L & \gamma L^2 \\ -6 & 3L & 6 & 3L \\ -3L & \gamma L^2 & 3L & 2L^2\alpha \end{bmatrix}\begin{Bmatrix} D_1 \\ D_2 \\ D_3 \\ D_4 \end{Bmatrix} = \frac{qL}{12}\begin{Bmatrix} 6 \\ -L \\ 6 \\ L \end{Bmatrix} + \begin{Bmatrix} F_1 \\ F_2 \\ F_3 \\ F_4 \end{Bmatrix};\ \Lambda = \frac{EI}{GK_sAL^2} \quad (2.9)$$

$$\gamma = 1 - 6\Lambda \qquad \alpha = 1 + 3\Lambda \qquad \mu = 1 + 12\Lambda$$

To obtain good results, one must use more than one element in each span of the span if the element is based on reduced integration or consistent interpolation whereas interdependent interpolation element gives the exact values of w and ϕ when only one element per member is used. Therefore to analyse a frame it is convenient to use interdependent interpolation element [39].

Reddy and Heyliger [6] presented higher order finite element based on higher order theory developed by Bickford [4]. In this derivation generalized displacements such as axial displacement (u), and rotation (ϕ) were approximated by linear Lagrange interpolation functions and transverse displacement was approximated by Hermite interpolation functions. For the static linear case with transverse loading only, stiffness matrix based on this higher order theory is given as

$$[S_1] + [S_2] = \frac{2EI}{105L^3}\begin{bmatrix} 30 & -30 & -15L & -15L & 0 & 0 \\ -30 & 30 & 15L & 15L & 0 & 0 \\ -15L & 15L & 10L^2 & 5L^2 & 8L^2 & -8L^2 \\ -15L & 15L & 5L^2 & 10L^2 & -8L^2 & 8L^2 \\ 0 & 0 & 8L^2 & -8L^2 & 34L^2 & -34L^2 \\ 0 & 0 & -8L^2 & 8L^2 & -34L^2 & 34L^2 \end{bmatrix}$$

$$+\frac{8GA}{15}\begin{bmatrix} 1{\cdot}2/L & -1{\cdot}2/L & -0{\cdot}1 & -0{\cdot}1 & -0{\cdot}5 & -0{\cdot}5 \\ -1{\cdot}2/L & 1{\cdot}2/L & 0{\cdot}1 & 0{\cdot}1 & 0{\cdot}5 & 0{\cdot}5 \\ -0{\cdot}1 & 0{\cdot}1 & 2L/15 & -L/30 & -L/12 & -L/12 \\ -0{\cdot}1 & 0{\cdot}1 & -L/30 & 2L/30 & L/12 & -L/12 \\ -0{\cdot}5 & 0{\cdot}5 & -L/12 & L/12 & L/3 & L/6 \\ -0{\cdot}5 & 0{\cdot}5 & -L/12 & -L/12 & L/6 & L/3 \end{bmatrix}, \quad (2.10)$$

where [S_1] represents the bending stiffness matrix and [S_2] represents the shear stiffness matrix.

Kant and Kupta [42] developed a higher order beam element using a higher order shear deformable theory which is based on the Taylor series expansion of the displacement components. In the derivation of the beam element linear shape function is used to define all the displacement components and it is only required to have C_0 continuity in the shape functions. The size of the equation developed for stiffness matrix is 8x8.

Petrolito [43] used Reddy and Bickford [4, 6] higher order shear deformation theory to perform exact stiffness analysis of thick beams. He derived the shape functions for the beam from the solution of the differential equations and then followed the usual finite element method procedure to formulate the beam element. The explicit stiffness terms were not given by Petrolito [43]. Eisenberger [44] derived an exact stiffness matrix analytically, together with the exact end-moment of two common cases, which are required for the exact analysis of structures. Liu [45] formulated a beam element for trigonometric shear deformation theory [7] following the method used by Petrolito [43].

Reddy et al [47, 48] presented common beam element called unified beam element covering elementary theory to higher order theory. The unified beam element was developed based on the relationship between the solution of classical theories and simplified Reddy-Bickford theory [39]. Since the relationships provide an interdependent interpolation of the deflection and rotation, it is required to use only the Hermite cubic interpolation function. Hence element stiffness matrix with order 4x4 is obtained and it gives exact nodal values of generalized displacements for Euler-Bernoulli and Timoshenko beams with uniform cross section and homogeneous material properties.

Reddy [39] suggested two different approaches to formulate the finite element for higher order beam thoery. One is consistent interpolation element where independent polynomial functions are used to define the displacement components. It is suggested to use Hermite cubic polynomial functions to define the transverse

displacement w and quadratic Lagrange polynomials to define the rotation. The obtained matrix would be having an order 7x7. The other method is using the interdependent interpolation based on the simplified polynomials solutions of the governing equilibrium equations. It is required to use only Hermite cubic polynomials to define the displacement components. The resulted stiffness matrix would be having an order of 4x4.

2.3. Theoretical aspects related to formulation of finite element

2.3.1. Strong forms Vs. Weak forms

In solid mechanics each and every physical problem can be represented by system of governing partial differential equations (PDEs). These system of equations are strong forms of system equations. Obtaining the exact solution for a strong-form of the system equation is ideal, but in the case of practical engineering problems those governing equations are generally complex in nature and it is very difficult to get exact solution. Therefore numerical methods are used to get the approximate solution for the problems. Numerical methods for a problem could be formulated either from strong form or weak form of governing equations. In a strong-form numerical method formulation, it is assumed that the approximate unknown function should have sufficient degree of consistency, so that it is differentiable up to the order of the PDEs.

On the other hand the weak-form requires a weaker consistency on the approximate function. We can derive the weak-form of the governing equations by applying an integral operation to the system equation based on a mathematical or physical principle. An approximate solution for a complex system can be obtained from various numerical formulation methods based on the weak-form of the system equation. Formulation based on weak-forms can usually produce a very stable set of discretized system equations that produces much more accurate results .Generally we can use two major principles for constructing weak forms: variational and weighted residual methods [49].

2.3.2. Variational methods and variational principle

The phrase "direct variational methods" refers to methods that make use of variational principles such as the principles of virtual work and the principle of minimum total potential energy in solid and structural mechanics, to determine approximate solutions of problems [38]. In the classical sense a variational principle has to do with finding the extremum (i.e minimum or maximum) or stationary values of a functional with respect to the variables of the problem. The functional includes all the intrinsic features of the problem such as the governing equations boundary and/or initial conditions and constraint conditions if any. In solid, structural mechanics problems the functional represents the total energy of the system, and in other problems it is simply an integral representation of the governing equation.

The principle of minimum total potential energy can be regarded as a substitute to the equations of equilibrium of an elastic body. Also it can be used for the development of displacement finite element models that can be used to determine approximate displacement and stress fields in the body [50].

2.3.3. Weighted residual method

The weighted residual method is a more sophisticated mathematical tool that can be used to develop the weak-form of the system of equations for many types of engineering problems. This section describes general residual technique. Many numerical methods can be based on the general weighted residual method. Readers may refer [38, 49] to get more ideas about weighted residual method.

Consider the following (partial) differential equation (2.11).

$$F(u) + b = 0 \text{ in problem domain } (\Omega). \tag{2.11}$$

Where F is a differential (partial) operator that is defined as a process when F applied to the scalar function u produces a function -b. The boundary condition is given as

$$G(u) = g \text{ on the boundary } (\Gamma) \tag{2.12}$$

Where G is a differential (partial) operator G for the boundary condition

Function u is first approximated by

(2.13)

$u^h(x) = \sum_i^n \alpha_i N_i = N\alpha$

Where N_i is the i^{th} term trial function, α_i is the unknown coefficient for the i^{th} term basis function, and n is the number of basis functions used.

Substituting (2.13) into (2.11) and (2.12), generally would give

$F(u^h) + b \neq 0$

$G(u^h) - g \neq 0$

Hence, the following residual functions R_s and R_b can be obtained respectively, for the system equations defined in the problem domain and the boundary conditions defined on the boundaries.

$$R_s = F(u^h) + b$$
$$R_b = G(u^h) - g \tag{2.14}$$

To make the residual in (2.14) as "small" as possible; it is required to force the residual to zero in an average sense by setting weighted integrals of residuals to zero.

$$\int_{\Omega} \bar{W}_i R_s d\Omega + \int_{\Gamma} \bar{V}_i R_b d\Gamma = 0 \tag{2.15}$$

Where $\bar{W}_i$ and $\bar{V}_i$ are a set of given weight functions for the residuals R_s and R_b respectively.

In the context of FEM the approximate solution, (2.12), can be chosen to satisfy the boundary conditions. In such cases, R_b is zero, and Equation (2.15) becomes

$$\int_{\Omega} \bar{W}_i R_s d\Omega = 0 \tag{2.16}$$

This is the formulation of the weighted residual method that is often used in establishing numerical procedures like FEM.

In the weighted residual method, there are several possible methods of using weight function such as collocation, subdomain, Least square, Moment and Galerkin

Method. Different numerical approximation methods can be obtained by selecting different weight functions. Selection of weight functions will affect its performance.

Although there are different versions of weighted residual method, Galerkin method is regarded so far as the most effective version of the weighted residual method, and is widely used in numerical methods, in particular the finite element method (FEM). There are some considerable advantages of using Galerkin method over other method. First the stiffness matrix derived by the Galerkin method is usually symmetric. In addition, in many cases, Galerkin method leads to the same formulations obtained by the energy principles, and hence has certain physical foundations [49].

In Galerkin method trial functions used for the approximation of the field function are also used as the weight functions.

2.3.4. Euler - Lagrange equations and boundary conditions

A Finite element analyst is interested in identifying suitable functional which gives Euler – Lagrange equations (i.e. Governing differential equations in solid mechanics) and the corresponding boundary conditions. The following section describes the procedure to establish those equations and boundary conditions.

Let y be function of x. Then, $G(y, y', y'')$ is functional. It is required to find

y = y(x), such that the first variance of

$$I = \int_{x1}^{x2} G(y, y', y'')dx \tag{2.17}$$

is made stationary satisfying the boundary conditions specified below.

$$y(x1) = y1$$

$$y(x2) = y2$$

It is stated that the problem of finding y(x) that makes (2.17) stationary with respect to small, admissible variations in y(x) is equivalent to the problem of finding y(x) that satisfies the governing differential equations for this problem [51].

Figure 2.2 shows a typical function y = y(x). The continuous line shows the exact function and dotted line shows an approximate function.

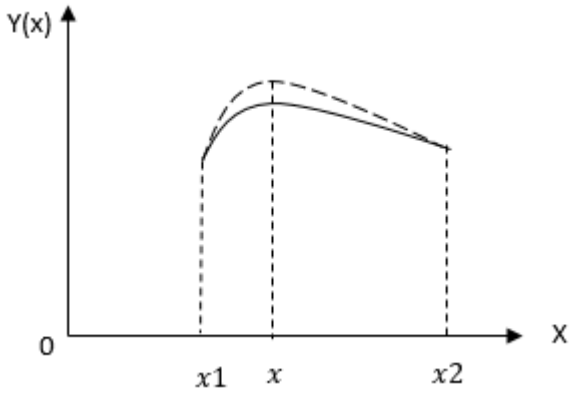

Figure 2.2 - Typical function y(x) and the approximate solution $\bar{y}(x)$

Then $\delta r = \bar{y}(x) - y(x)$

We are interested in finding the solutions with

$$\delta I = 0$$

$$\therefore \int_{x1}^{x2} \left(\frac{\partial G}{\partial y}\delta y + \frac{\partial G}{\partial y'}\delta y' + \frac{\partial G}{\partial y''}\delta y''\right)dx = 0 \tag{2.17}$$

By applying integration by parts to (2.17),

$$\int_{x1}^{x2} \left(\frac{\partial G}{\partial y'}\delta y'\right)dx = \frac{\partial G}{\partial y'}\delta y\Big|_{x1}^{x2} - \int_{x1}^{x2} \frac{d}{dx}\left(\frac{\partial G}{\partial y'}\right)\delta y\, dx$$

$$\int_{x1}^{x2} \left(\frac{\partial G}{\partial y'}\delta y'\right)dx = \frac{\partial G}{\partial y''}\delta y'\Big|_{x1}^{x2} - \frac{d}{dx}\left(\frac{\partial G}{\partial y''}\right)\delta y\Big|_{x1}^{x2} + \int_{x1}^{x2} \frac{d^2}{dx^2}\left(\frac{\partial G}{\partial y'_{,}}\right)\delta y\, dx$$

$$\int_{x1}^{x2} \left(\left(\frac{\partial G}{\partial y'}\right) - \frac{d}{dx}\left(\frac{\partial G}{\partial y'}\right) + \frac{d^2}{dx^2}\left(\frac{\partial G}{\partial y'_{,}}\right)\right)\delta y\, dx + \left(\left(\frac{\partial G}{\partial y'}\right) - \frac{d}{dx}\left(\frac{\partial G}{\partial y''}\right)\right)\delta y\Big|_{x1}^{x2} + \left(\frac{\partial G}{\partial y''}\right)\delta y'\Big|_{x1}^{x2} = 0 \tag{2.18}$$

Since δy is arbitrary, therefore all three terms in equation (2.18) should be zero.

$$\left(\frac{\partial G}{\partial y'}\right) - \frac{d}{dx}\left(\frac{\partial G}{\partial y'}\right) + \frac{d^2}{dx^2}\left(\frac{\partial G}{\partial y'_{,}}\right) = 0 \tag{2.19}$$

$$\left(\left(\frac{\partial G}{\partial y'}\right) - \frac{d}{dx}\left(\frac{\partial G}{\partial y''}\right)\right)\delta y\Big|_{x1}^{x2} = 0 \tag{2.20}$$

$$\left(\frac{\partial G}{\partial y''}\right)\delta y'\Big|_{x1}^{x2} = 0 \tag{2.21}$$

Equation (2.19) known as Euler - Lagrange equations. Equations (2.20) and (2.21) are known as boundary conditions. To satisfy equation (2.20)

$$\delta y(x1) = 0 \; or \; \left(\left(\frac{\partial G}{\partial y'}\right) - \frac{d}{dx}\left(\frac{\partial G}{\partial y''}\right)\right)\Big|_{x1} = 0$$

$$\delta y(x2) = 0 \; or \; \left(\left(\frac{\partial G}{\partial y'}\right) - \frac{d}{dx}\left(\frac{\partial G}{\partial y''}\right)\right)\Big|_{x2} = 0$$

To satisfy equation (2.21)

$$\delta y'(x1) = 0 \; or \; \left(\frac{\partial G}{\partial y''}\right)\Big|_{x1} = 0$$

$$\delta y'(x1) = 0 \; or \; \left(\frac{\partial G}{\partial y''}\right)\Big|_{x2} = 0$$

Conditions like $\delta y(x1) = 0, \delta y(x2) = 0, \delta y'(x1) = 0 \; and \; \delta y'(x2) = 0$ are known as kinematic (essential) boundary conditions. In solid mechanics they usually refer to the displacement requirement at support points.

The conditions like $\left(\left(\frac{\partial G}{\partial y'}\right) - \frac{d}{dx}\left(\frac{\partial G}{\partial y''}\right)\right)\Big|_{x1} = 0, \left(\left(\frac{\partial G}{\partial y'}\right) - \frac{d}{dx}\left(\frac{\partial G}{\partial y''}\right)\right)\Big|_{x2} = 0,$

$\left(\frac{\partial G}{\partial y''}\right)\Big|_{x1} = 0 \; and \; \left(\frac{\partial G}{\partial y''}\right)\Big|_{x2} = 0$ are known as natural(force) boundary conditions. In solid mechanics they usually refer to the conditions like moment and shear force at supports.

Thus first variance of functional for stationary value yields Euler-Lagrange equation, kinematic boundary conditions and natural boundary conditions.

In the case of solid mechanics problem, total potential energy is treated as suitable functional, minimization (first variance) of which yields equation of equilibrium satisfying the boundary conditions [51].

2.3.5. Finite element formulation using minimum total potential energy principle

The principle of minimum potential energy in solid mechanics which may be stated as "Of all the possible displacement configurations a body can assume which satisfy compatibility and boundary conditions, the configuration satisfying equilibrium makes potential energy assume a minimal value" [51]. This variational principle can be directly used to formulate the finite element equations in solid mechanics. This principle can be used in a straightforward manner in the following three simple steps [49].

- Approximating displacement functions in terms of the nodal variables using the interpolation or shape functions; Assume vector D consisting of all the nodal displacements in the problem domain.
- Deriving the total potential energy, Π in terms of the nodal variables **D**. For solids and structures of elastic materials, the total potential energy includes strain energy *U* and the work done by the external forces *V*. This can be expressed as

$$\Pi = U + V$$

- Use the stationary conditions (minimization of total potential energy) to create a set of discretized system equations

$$\delta\Pi = \frac{\partial\Pi}{\partial d_1}\delta D_1 + \frac{\partial\Pi}{\partial d_2}\delta D_2 + \ldots\ldots + \frac{\partial\Pi}{\partial d_n}\delta D_n = 0 \quad \text{Which is equivalent to}$$

$$\frac{\partial\Pi}{\partial D_i} = 0$$

The minimum total potential energy principle requires $\delta\Pi = 0$,

hence $\delta\mathbf{U} + \delta V = 0$. It can also be viewed as principle of virtual work which states " if a solid body is in its equilibrium states, the total virtual work performed by

all the stresses in the body and all the external forces applied on the body vanishes, when the body is subjected to a virtual displacement" [49].

CHAPTER III

3. THEORETICAL FORMULATION

Consider a uniform isotropic thick beam as shown in Figure 3.1, in which the deformed beam cross section neither stays normal to the deformed centroidal axis nor remains a plane. By using the Cartesian coordinate system (x; y; z) indicated in Figure 3.1 where the x-axis is coincident with the centroidal axis of the unreformed beam, the y-axis is the neutral axis, and the z-axis is along the thickness of the beam. The beam is subjected to transverse load of intensity q(x) per unit length of the beam.

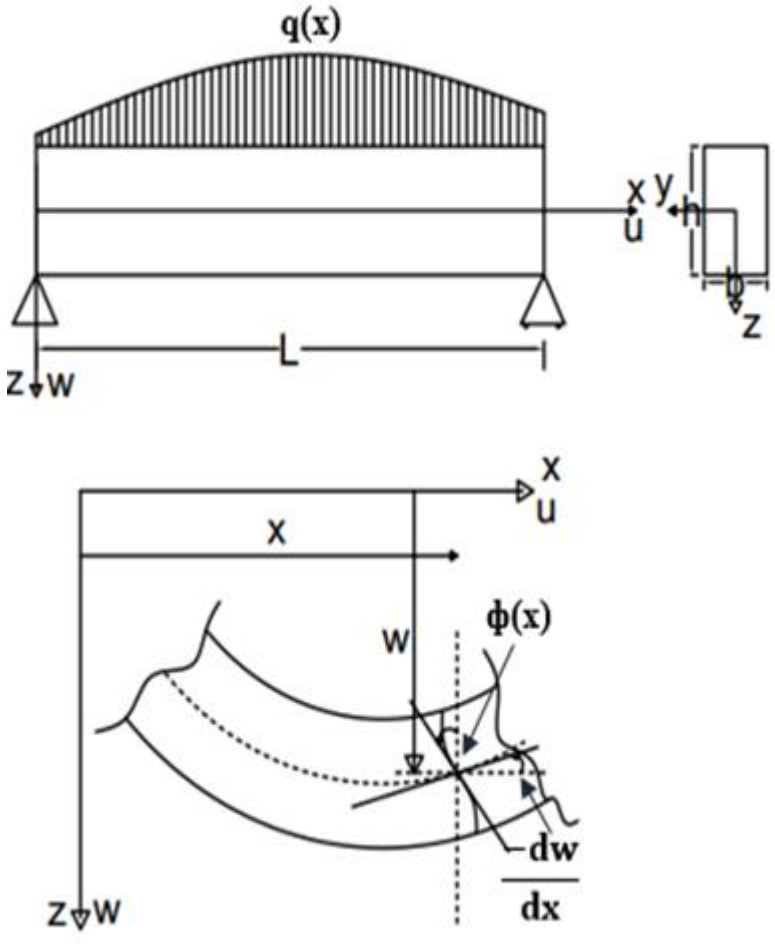

Figure 3.1-The beam under consideration

3.1. Assumptions made in the theoretical formulation

- The in-plane displacement u in x direction consists of two parts:
    a. Displacement due to the bending rotation
    b. Displacement due to shear rotation which is assumed to be hyperbolic in nature with respect thickness coordinate
- The transverse displacement w in z direction is assumed to be a function of x coordinate.
- Transverse normal displacement v is assumed to be identically zero
- One-dimensional constitutive law is used.
- The beam is subjected to lateral load only
- Neutral axis is at the center line of the beam

3.2. Displacement field

Based on the above mentioned assumptions displacement field of the present theory is given as

$$u(x,z) = z\phi(x) - \mu\left(h\,sinh\left(\frac{z}{h}\right) - z\right)\left[\frac{dw}{dx} + \phi(x)\right];\ \mu = \frac{1}{cosh\frac{1}{2} - 1}$$

$$w(x,z) = w(x) \tag{3.1}$$

Where u(x,z) is axial displacement at any point on the line parallel to beam centroidal axis and also w(x) and ϕ(x) are two unknown functions named the transverse displacement and total rotation of the cross section at neutral axis respectively. $\theta(x) = [\frac{dw}{dx} + \phi(x)]$; $\theta(x)$ is rotation of cross section due to shear at neutral axis.

Based on the displacement functions (3.1) above, normal strain and transverse shear strain are obtained using linear theory of elasticity.

$$\varepsilon_{xx} = \frac{\partial u}{\partial x} = z\,\frac{d\phi(x)}{dx} - \mu\left(h\,sinh\left(\frac{z}{h}\right) - z\right)\left[\frac{d^2w}{dx^2} + \phi(x)\right]$$

$$\gamma_{xz} = \frac{\partial u}{\partial z} + \frac{\partial w}{\partial x} = \left[1 - \mu\left(cosh\left(\frac{z}{h}\right) - 1\right)\right]\left[\frac{dw}{dx} + \phi(x)\right] \tag{3.2}$$

Based on the strains defined in (3.2) normal bending and transverse shear stresses are obtained using one-dimensional constitutive law.

$$\sigma_{xx} = E_x \varepsilon_{xx}$$
$$\tau_{xz} = G_{xz} \gamma_{xz} \tag{3.3}$$

3.3. Governing equations and boundary conditions

Using above stress and strain relations in (3.2) and (3.3), strain energy in the system U can be written as

$$U = \int_0^L \int_A \frac{1}{2} (\sigma_{xx} \epsilon_{xx} + \tau_{xz} \gamma_{xz}) \, dA \, dx \tag{3.4}$$

and the gravitational potential energy due to transverse load q is given by

$$V = -\int_0^L q(x) w \, dx \tag{3.5}$$

Applying minimum total potential energy principle

$$\delta \Pi = \delta U + \delta V = 0,$$

it becomes

$$\int_0^L \int_A (\sigma_{xx} \, \delta \epsilon_{xx} + \tau_{xz} \delta \gamma_{xz}) \, dA \, dx - \int_0^L q(x) \delta w \, dx = 0 \tag{3.6}$$

Substituting the strain functions defined in (3.2) into (3.6) will give the following integral statement,

$$\int_0^L \int_A \left\{ \sigma_{xx} \left(z \frac{d\delta\phi}{dx} - \mu \left(h \sinh\left(\frac{z}{h}\right) - z \right) \left(\frac{d^2 \delta w}{dx^2} + \frac{d\delta\phi}{dx} \right) \right) + \tau_{xz} \left(1 - \mu \left(\cosh\left(\frac{z}{h}\right) - 1 \right) \right) \left(\frac{d\delta w}{dx} + \delta\phi \right) \right\} dA \, dx - \int_0^L q(x) \delta w \, dx = 0 \tag{3.8}$$

3.3.1. The stress resultant-displacement relations

Here the stress resultants are defined as follows

$$M_{xx} = \int_A z \, \sigma_{xx} \, dA \tag{3.9}$$

$$Q_x = \int_A \tau_{xz} \, dA \tag{3.10}$$

$$M'_{xx} = \mu \int_A [h\ sinh(\tfrac{z}{h}) - z]\ \sigma_{xx}\ dA \tag{3.11}$$

$$R_x = \mu \int_A [cosh\left(\frac{z}{h}\right) - 1]\tau_{xz}\, dA \tag{3.12}$$

$$V_x = \frac{dM_{xx}}{dx} = Q_x - R_x + \frac{dM'_{xx}}{dx} \tag{3.13}$$

$$\bar{M}_{xx} = M_{xx} - M'_{xx} \tag{3.14}$$

Where M_{xx} and Q_x are the usual bending moment and shear force and M'_{xx} and R_x are the higher order stress resultant. V_x is the effective shear force.

$$M_{xx} = \int_A z\ \sigma_{xx}\ dA$$

$$M_{xx} = \int_A z\, E\left(z\ \frac{d\phi}{dx} - \mu\left(h\ sinh\left(\frac{z}{h}\right) - z\right)\left(\frac{d^2w}{dx^2} + \frac{d\phi}{dx}\right)\right) dA$$

$$M_{xx} = -EI\frac{d^2w}{dx^2} + \mu EI\left(\cosh\left(\frac{1}{2}\right) - 12\left(\cosh\left(\frac{1}{2}\right) - 2\sinh\left(\frac{1}{2}\right)\right)\right)\left(\frac{d^2w}{dx^2} + \frac{d\phi}{dx}\right)$$

$$M_{xx} = -EI\frac{d^2w}{dx^2} + EIA_0\left(\frac{d^2w}{dx^2} + \frac{d\phi}{dx}\right) \tag{3.15}$$

$$M'_{xx} = \mu \int_A [h\ sinh(\tfrac{z}{h}) - z]\ \sigma_{xx}\ dA$$

$$M'_{xx} = \mu \int_A (h\ sinh(\tfrac{z}{h}) - z)\ E\left(z\ \frac{d\phi}{dx} - \mu\left(hsinh\left(\frac{z}{h}\right) - z\right)\left(\frac{d^2w}{dx^2} + \frac{d\phi}{dx}\right)\right) dA$$

$$M'_{xx} = EI(A_0 - 1)\frac{d^2w}{dx^2} + (A_0 - B_0)EI\left(\frac{d^2w}{dx^2} + \frac{d\phi}{dx}\right) \tag{3.16}$$

$$Q_x = \int_A \tau_{xz}\, dA$$

$$Q_x = \int_A G\left(1 - \mu\left(cosh\left(\frac{z}{h}\right) - 1\right)\right)\left(\frac{dw}{dx} + \phi\right) dA$$

$$Q_x = GA\mu\left(\cosh\left(\frac{1}{2}\right) - 2\sinh\left(\frac{1}{2}\right)\right)\left(\frac{dw}{dx} + \phi\right) \tag{3.17}$$

$$R_x = \mu \int_A \left(cosh\left(\frac{z}{h}\right) - 1\right) G \left(1 - \mu \left(cosh\left(\frac{z}{h}\right) - 1\right)\right)\left(\frac{dw}{dx} + \phi\right) dA$$

$$R_x = GA\mu^2 \left(\frac{1}{2}\sinh(1) - \frac{1}{2}\right)\left(\frac{dw}{dx} + \phi\right) - GA\mu^2 \left(\cosh\left(\frac{1}{2}\right) - 2\sinh\left(\frac{1}{2}\right)\right)\left(\frac{dw}{dx} + \phi\right)$$

(3.18)

By substituting the stress resultants defined in (3.9) - (3.14) into (3.8), the following integral form can be obtained.

$$\int_0^L \left(-M'_{xx} \frac{d^2\delta w}{dx^2} + M_{xx} \frac{d\delta \Phi}{dx} - M'_{xx} \frac{d\delta \Phi}{dx} + Q_x \left(\frac{d\delta w}{dx} + \delta\phi\right) - R_x \left(\frac{d\delta w}{dx} + \delta\phi\right) - q(x)\delta w\right) \mathrm{dx} = 0 \quad (3.19)$$

By applying integration by parts to (3.19), we obtain the coupled Euler–Lagrange equations which are the governing differential equations of equilibrium and associated boundary conditions of the beam.

$$\left[-M'_{xx} \frac{d\delta w}{dx} + (M_{xx} - M'_{xx})\delta\phi\right]_0^L + \int_0^L \left(\frac{dM_{xx}}{dx}\frac{d\delta w}{dx} - \left(\frac{dM_{xx}}{dx} - \frac{dM'_{xx}}{dx}\right)\left(\frac{d\delta w}{dx} + \delta\phi\right) + \left(Q_x - R_x\right)\left(\frac{d\delta w}{dx} + \delta\phi\right) - q(x)\delta w\right) dx = 0$$

$$\left[-M'_{xx} \frac{d\delta w}{dx} + (M_{xx} - M'_{xx})\delta\phi + \frac{dM_{xx}}{dx}\delta w\right]_0^L + \int_0^L \left(\left(-\frac{d^2M_{xx}}{dx^2}\delta w - q(x)\delta w\right) - \left(\frac{dM_{xx}}{dx} - \frac{dM'_{xx}}{dx} - Qx + Rx\right)\left(\frac{d\delta w}{dx} + \delta\phi\right)\right) dx = 0 \quad (3.20)$$

Since $\delta w, \frac{d\delta w}{dx}$ and $\delta\phi$ are arbitrary in $0 < x < L$, coefficients of those functions should be zero in (3.20). Setting the coefficients to zero, will give governing equations of equilibrium (3.21) and (3.22) for the problem. Further, at boundary, the conditions given in (3.23) should be satisfied.

Equations of Equilibrium

$$\frac{d^2M_{xx}}{dx^2} = -q(x) \quad (3.21)$$

$$\frac{d(M_{xx} - M'_{xx})}{dx} - \left(Q_x - R_x\right) = 0 \quad (3.22)$$

Boundary conditions

$$\begin{aligned} \frac{dM_{xx}}{dx} = 0 \quad &\text{or} \quad w \text{ is prescribed} \\ \bar{M}_{xx} = 0 \quad &\text{or} \quad \phi \text{ is prescribed} \\ M'_{xx} = 0 \quad &\text{or} \quad -\frac{dw}{dx} \text{ is prescribed} \end{aligned} \tag{3.23}$$

For a uniform rectangular isotropic beam, the equations of equilibrium can be obtained in terms of the displacements w and θ using the stress resultant-displacement relations given in (3.15)-(3.18).

$$EI\frac{d^4w}{dx^4} - A_0EI\left(\frac{d^4w}{dx^4} + \frac{d^3\phi}{dx^3}\right) = q(x) \tag{3.24}$$

$$EIAo\frac{d^3w}{dx^3} - EIB_0\left(\frac{d^3w}{dx^3} + \frac{d^2\phi}{dx^2}\right) + C_0GA\left(\frac{dw}{dx} + \phi\right) = 0 \tag{3.25}$$

Where

$$\mathrm{A_o} = \mu\left\{\cosh\left(\tfrac{1}{2}\right) - 12\left[\cosh\left(\tfrac{1}{2}\right) - 2\sinh\left(\tfrac{1}{2}\right)\right]\right\} \approx 8.0234 \times 10^{-1}$$

$$\mathrm{B_o} = \mu^2\left\{\cosh(\tfrac{1}{2})^2 - 24\cosh\left(\tfrac{1}{2}\right)\left[\cosh\left(\tfrac{1}{2}\right) - 2\sinh\left(\tfrac{1}{2}\right)\right] + 6[\sinh(1) - 1]\right\} \approx 6.5138 \times 10^{-1}$$

$$\mathrm{C_o} = \mu^2\left\{\cosh\left(\tfrac{1}{2}\right)\left[\cosh\left(\tfrac{1}{2}\right) - 2\sinh\left(\tfrac{1}{2}\right)\right] - \tfrac{1}{2}[\sinh(1) - 1]\right\} \approx 5.3649 \times 10^{-1}$$

3.4. General solutions for static flexure of beams

By integrating and rearranging (3.24) and (3.25), the following differential forms are obtained

$$\frac{d^3w}{dx^3} - \mathrm{A_0}\left(\frac{d^3w}{dx^2} + \frac{d^2\phi}{dx^2}\right) + \mathrm{V(x)} = 0 \tag{3.26}$$

$V_x = -(\int q(x)dx + C_1)$; V_x is effective shear force at section x.

$$\frac{d^3w}{dx^3} - \frac{A_0}{B_0}\left(\frac{d^3w}{dx^3} + \frac{d^2\phi}{dx^2}\right) + \mathrm{k}\left(\frac{dw}{dx} + \phi\right) = 0 \tag{3.27}$$

$\mathrm{k} = \frac{GAC_0}{EIA_0}$

Using (3.26) and (3.27), following differential equation can be obtained in terms of $\theta = \left(\frac{dw}{dx} + \phi\right)$ only.

$$\frac{d^2\theta}{dx^2} - \lambda^2\theta + \frac{V(x)}{E\,I\,m} = 0 \tag{3.28}$$

$$m = \frac{B_o}{A_o} - A_o$$

$$\lambda^2 = \frac{k}{m} = \frac{GAC_o}{E\,I\,(B_o - A_o^2)}$$

Solving the (3.28) for θ and substituting the result into (3.26) will give following general solutions for displacements

$$\theta = C_2\cosh(\lambda x) + C_3\sinh(\lambda x) + \frac{V_x}{E\,I\,m} \tag{3.29}$$

$$EIw = \int\int\int\int q(x)\,dxdxdxdx + EI\frac{A_0}{\lambda}\left[C_2\sinh(\lambda x) + C_2\cosh(\lambda x)\right] + C_1\frac{x^3}{6} + C_4\frac{x^2}{2} + C_5 x + C_6 \tag{3.30}$$

Where C_i for $i = 1,2,\ldots.6$ are unknown parameters.

Since six boundary conditions are available, those six unknown constants can be determined for the specific problems. Numerical examples are discussed in chapter V to validate the present beam theory. Solution obtained using present theory are compared with the solutions available from the other beam theories and two dimensional elasticity solutions.

CHAPTER IV

4. FINITE ELEMENT FORMULATION

4.1. Derivation of shape functions

In traditional formulation of the finite element, the displacement variables are approximated using polynomials which should satisfy certain requirements in order to converge to the actual solution as the number of elements is increased [38]. The approximation function for the variable should be

- continuous over the element and differentiable, as required by the weak form.
- a complete polynomial (i.e: all lower order terms up to the highest order term used) and
- an interpolant of the primary variables at the nodes of the finite element (i.e: imposing the continuity of the solution across the inter-element boundary)

However, later a new approach was followed by researchers for the choice of approximation function in certain finite element formulation which makes possible to get the exact finite element solutions of the differential equations at nodal points. In this approach primary variables are approximated by the solution of the adjoint differential equation [52]. IIE beam element using FSBT in [39] follows same approach which gives exact nodal values.

Assuming that there is no applied transverse load in (3.24) and (3.25), adjoint differential equation can be obtained. These coupled equations are uncoupled in order to get the homogeneous solutions for the equations. The uncoupled equations of equilibrium are

$$\frac{d^6w}{dx^6} - \lambda^2 \frac{d^4w}{dx^4} = 0 \tag{4.1}$$

$$\frac{d^5\Phi}{dx^5} - \lambda^2 \frac{d^3\Phi}{dx^3} = 0 \tag{4.2}$$

$$\lambda^2 = \frac{GAC_o}{EI(B_o - A_o^2)}$$

The solutions for the differentials equations (4.1) and (4.2) can be written as follows

$$\mathrm{w(x)} = C_1 \sinh(\lambda x) + C_2 \cosh(\lambda x) + C_3 x^3 + C_4 x^2 + C_5 x + C_6 \quad (4.3)$$

$$\Phi\mathrm{(x)} = C_7 \sinh(\lambda x) + C_8 \cosh(\lambda x) + C_9 x^2 + C_{10} x + C_{11} \quad (4.4)$$

Where $C_i \; for \; i = 1,2 \ldots \ldots 11$ are unknown parameters .

Since the theory is only having six boundary conditions, only six of the parameters can be independent. Substituting (4.3) and (4.4) into (3.25), gives the following relationships between the parameters:

$$\frac{dw}{dx} = C_1 \lambda \cosh(\lambda x) + C_2 \lambda \sinh(\lambda x) + 3C_3 x^2 + 2C_4 x + C_5 \quad (4.4)$$

$$\frac{d^3 w}{dx^3} = C_1 \lambda^3 \cosh(\lambda x) + C_2 \lambda^3 \sinh(\lambda x) + 6C_3 \quad (4.5)$$

$$\frac{d^2 \phi}{dx^2} = C_7 \lambda^2 \sinh(\lambda x) + C_8 \lambda^2 \cosh(\lambda x) + 2C_9 \quad (4.6)$$

$$EIAo \frac{d^3 w}{dx^3} - EIB_0 \left(\frac{d^3 w}{dx^3} + \frac{d^2 \phi}{dx^2} \right) + C_0 GA \left(\frac{dw}{dx} + \phi \right) = 0$$

Substituting (4.4), (4.5) and (4.6), into above equations gives the following relationships between the unknown parameters:

$$(EIAo - EIB_0)\ (C_1 \lambda^3 \cosh(\lambda x) + C_2 \lambda^3 \sinh(\lambda x) + 6C_3\ ) + C_0 GA(C_1 \lambda \cosh(\lambda x) + C_2 \lambda \sinhh(\lambda x) + 3C_3 x^2 + 2C_4 x + C_5) = EIB_0(C_7 \lambda^2 \sinh(\lambda x) + C_8 \lambda^2 \cosh(\lambda x) + 2C_9\ ) - C_0 GA(C_7 \sinh(\lambda x) + C_8 \cosh(\lambda x) + C_9 x^2 + C_{10} x + C_{11})$$

Equating the coefficient of each term, gives relationship between those unknown parameters.

<u>$\cosh(\lambda x)$:</u>

$$(\lambda^3 (EIAo - EIB_0) + C_0 GA\lambda) C_1 = (EIB_0 \lambda^2 - C_0 GA\lambda) C_8$$

$$C_8 = \lambda \left(\frac{1}{A_0} - 1 \right) C_1$$

$C_8 = 0.2463\lambda C_1$

sinhh(λx) :

$C_7 = 0.2463\lambda C_2$

x^2 :

$3C_0GAC_3 = -C_0GAC_9$

$C_9 = -3C_3$

x :

$2C_0GAC_4 = -C_0GAC_{10}$

$C_{10} = -2C_4$

Constant:

$(EIAo - EIB_0)6C_3 + C_0GAC_5 = 2EIB_0C_9 - C_0GAC_{11}$

$C_{11} = -\left(\frac{EIAo}{C_0GA}C_3 + C_5\right)$

$C_{11} = -\left(8.9728\frac{EI}{GA}C_3 + C_5\right) = C_{11} = -(8.9728\,R\,C_3 + C_5)\ ;\ R = \frac{EI}{GA}$

Substituting these relations between these parameters into (4.4), gives following interpolation functions having six unknown parameters. Here interpolation functions are inter-dependant on each other (inter-dependent interpolation-IIE) which makes the size of the stiffness matrix smaller with higher accuracy in solutions comparing to the independent approximation for primary variables [52].

$$w(x) = C_1\sinh(\lambda x) + C_2\cosh(\lambda x) + C_3x^3 + C_4x^2 + C_5x + C_6 \quad (4.7)$$

$$\Phi(x) = 0.2463\lambda C_1\cosh(\lambda x) + 0.2463\lambda C_2\sinh(\lambda x) - 3C_3x^2 - 2C_4x - (8.9728\,R\,C_3 + C_5) \quad (4.8)$$

Therefore within the element shown in Figure 4.1, the interpolation can be written as

$$w(x) = \{A_1\}.\{C\} \tag{4.9}$$

$$\Phi(x) = \{A_2\}.\{C\} \tag{4.10}$$

Where

$$\{A_1\} = \{\sinh(\lambda x)\,, \cosh(\lambda x)\,, x^3, x^2, x, 1\} \tag{4.11}$$

$$\{A_2\} = \{0.2463\lambda \cosh(\lambda x)\,, 0.2463\lambda \sinh(\lambda x), \\ -(3x^2 + 8.9728\,R), -2x, -1{,}0\} \tag{4.12}$$

$$\{C\} = \{C_1, C_2, C_3, C_4, C_5, C_6\}^{\mathrm{T}} \tag{4.13}$$

The element has two nodes each with three degrees of freedom, one displacement (transverse displacement) and two rotations (total rotation and bending rotation of the cross section). The element nodal degrees of freedom are taken as

$$\{D\} = \{w(0), -w'(0), \Phi(0), w(L), -w'(L), \Phi(L)\}^T \tag{4.14}$$

Using (4.9) and (4.10), {D} can be written as

$$\begin{Bmatrix} w(0) \\ -w'(0) \\ \Phi(0) \\ w(L) \\ -w'(L) \\ \Phi(L) \end{Bmatrix} = \begin{bmatrix} 0 & 1 & 0 & 0 & 0 & 1 \\ -\lambda & 0 & 0 & 0 & -1 & 0 \\ 0.2463\lambda & 0 & -8.9728\,R & 0 & -1 & 0 \\ \sinh(\lambda L) & \cosh(\lambda L) & L^3 & L^2 & L & 1 \\ -\lambda\cosh(\lambda L) & -\lambda\sinh(\lambda L), & -3L^2 & -2L & -1 & 0 \\ 0.2463\lambda\cosh(\lambda L) & 0.2463\lambda\sinh(\lambda L) & -(3L^2 + 8.9728\,R) & -2L & -1 & 0 \end{bmatrix} \begin{Bmatrix} C_1 \\ C_2 \\ C_3 \\ C_4 \\ C_5 \\ C_5 \end{Bmatrix}$$

$$\{\mathrm{D}\} = [\mathrm{B}].\{\mathrm{C}\} \tag{4.15}$$

Where

$$[B] = [A_1(0), A'_1(0), A_2(0), A_1(L), A'_1(L), A_2(L)]^T \tag{4.16}$$

Solving (4.15) for C

$$\{C\} = [B]^{-1}\{D\} \tag{4.17}$$

Substituting (4.17) into equations (4.9) and (4.10), gives

$$w(x) = [N_1].\{D\} \tag{4.18}$$

$$\Phi(x) = [N_2].\{D\} \tag{4.19}$$

Where

$$[N_1] = \{A_1\}.[B]^{-1} \tag{4.20}$$

$$[N_2] = \{A_2\}.[B]^{-1} \tag{4.21}$$

are shape function matrices.

4.2. Construction of weak form

The weak forms of the governing equations are developed using Galerkin method. Assume that $W_1 \, and \, W_2$ and are two weight functions used to form the weighted integral form of the differential equations.

Considering the differerential equation (3.11);

$$\int_0^L W_1 \left(\frac{d^2 M_{xx}}{dx^2} + q(x)\right) dx = 0 \tag{4.22}$$

$$\int_0^L \left(-\frac{dW_1}{dx}\frac{d\,M_{xx}}{dx} + W_1\, q(x)\right) dx + \left(W_1 \frac{d\,M}{dx}\right)\Big|_0^L = 0$$

$$\int_0^L \left(\frac{d^2 W_1}{dx^2} M_{xx} + W_1\, q(x)\right) dx + \left(W_1 \frac{d\,M}{dx}\right)\Big|_0^L - \left(\frac{dW_1}{dx} M\right)\Big|_0^L = 0$$

$$\int_0^L \left(\frac{d^2 W_1}{dx^2}\left(-EI\frac{d^2 w}{dx^2} + EIA_0\left(\frac{d^2 w}{dx^2} + \frac{d\phi}{dx}\right)\right) + W_1\, q(x)\right) dx + \left(W_1 \frac{d\,M}{dx}\right)\Big|_0^L - \tag{4.25}$$

$$\left(\frac{dW_1}{dx} M\right)\Big|_0^L = 0$$

Considering the differerential equation (3.12);

$$\int_0^L W_2 \left(\frac{d\bar{M}_{xx}}{dx} - (Q_x - R_x)\right) dx = 0 \tag{4.26}$$

$$\int_0^L \left(-\frac{dW_2}{dx}\bar{M}_{xx} - W_2 (Q_x - R_x)\right) dx + (W_2 \bar{M})\Big|_0^L = 0$$

$$\int_0^L \left(-\frac{dW_2}{dx}\bar{M}_{xx} - W_2 (Q_x - R_x)\right) dx + (W_2 \bar{M})\Big|_0^L = 0$$

$$\int_0^L \left(-\frac{dW_2}{dx}\left(-EIA_0\frac{d^2w}{dx^2} + EIB_0\left(\frac{d^2w}{dx^2} + \frac{d\phi}{dx}\right)\right) - W_2 GAC_0\left(\frac{dw}{dx} + \phi\right)\right) dx +$$
$$(W_2 \bar{M})\Big|_0^L = 0 \tag{4.27}$$

Equations (4.25) and (4.27) are weak form of governing differential equations (3.11) and (3.12) respectively.

4.3. Finite element model

General finite element model for this beam problem is developed by substituting approximations of primary variables into the weak forms (4.25) and (4.27). In Galerkin based finite element model, the weight functions in the weak form are equal to interpolation functions which are used to approximate the primary variables.

Here the weight functions W_1 and W_2 should be equal to $[N_1]^T$ and $[N_2]^T$ respectively. Substituting all these into the weak forms (4.25) and (4.27), gives;

$$\int_0^L \left(\frac{d^2[N_1]^T}{dx^2}\left(-EI\frac{d^2N_1.D}{dx^2} + EIA_0\left(\frac{d^2N_1.D}{dx^2} + \frac{dN_2.D}{dx}\right)\right) + [N_1]^T q(x)\right) dx + \tag{4.28}$$
$$\left([N_1]^T \frac{d\,M}{dx}\right)\Big|_0^L - \left(\frac{d[N_1]^T}{dx} M\right)\Big|_0^L = 0$$

$$\int_0^L \left(\frac{d^2N_1^T}{dx^2}\left(-EI\frac{d^2N_1.D}{dx^2} + EIA_0\left(\frac{d^2N_1.D}{dx^2} + \frac{dN_2.D}{dx}\right)\right) + N_1^T q(x)\right) dx + \left(N_1^T \frac{d\,M}{dx}\right)\Big|_0^L -$$
$$\left(\frac{dN_1^T}{dx} M\right)\Big|_0^L = 0$$

$$\int_0^L \left(EI(1-A_0)\frac{d^2N_1^T}{dx^2}\frac{d^2N_1.D}{dx^2} - EIA_0\frac{d^2N_1^T}{dx^2}\frac{dN_2.D}{dx}\right)dx = \int_0^L N_1^T q(x)dx + \left(N_1^T\ \frac{d\,M}{dx}\right)\Big|_0^L - \left(\frac{dN_1^T}{dx}M\right)\Big|_0^L \tag{4.29}$$

$$\int_0^L \left(-\frac{dN_2^T}{dx}\left(-EIA_0\frac{d^2N_1.D}{dx^2} + EIB_0\left(\frac{d^2N_1.D}{dx^2} + \frac{dN_2.D}{dx}\right)\right) - N_2^T GAC_0\left(\frac{dN_1.D}{dx} + N_2.D\right)\right)dx + (N_2^T\bar{M})\Big|_0^L = 0 \tag{4.30}$$

$$\int_0^L \left(-EIA_0\frac{dN_2^T}{dx}\frac{d^2N_1.D}{dx^2} + EIB_0\frac{dN_2^T}{dx}\frac{d^2N_1.D}{dx^2} + EIB_0\frac{dN_2^T}{dx}\frac{dN_2.D}{dx} + GAC_0N_2^T\frac{dN_1.D}{dx} + GAC_0N_2^TN_2.D\right)dx = (N_2^T\bar{M})\Big|_0^L \tag{4.31}$$

Combining (4.30) and (4.31) will give the required set of algebraic equations.

$$\int_0^L \left(EI(1-A_0)\frac{d^2N_1^T}{dx^2}\frac{d^2N_1.D}{dx^2} - EIA_0\frac{d^2N_1^T}{dx^2}\frac{dN_2.D}{dx} - EIA_0\frac{dN_2^T}{dx}\frac{d^2N_1.D}{dx^2} + EIB_0\frac{dN_2^T}{dx}\frac{d^2N_1.D}{dx^2} + EIB_0\frac{dN_2^T}{dx}\frac{dN_2.D}{dx} + GAC_0N_2^T\frac{dN_1.D}{dx} + GAC_0N_2^TN_2.D\right)dx = \int_0^L N_1^T q(x)dx + \left(N_1^T\ \frac{d\,M}{dx}\right)\Big|_0^L - \left(\frac{dN_1^T}{dx}M\right)\Big|_0^L + (N_2^T\bar{M})\Big|_0^L \tag{4.32}$$

Equation (4.32) can be expressed as the following finite element model form;

$$[S]\{D\} = \{f\} + \{F\} \tag{4.33}$$

Where

$$S_{ij} = \int_0^L \left(EI(1-A_0)\frac{d^2N_{1i}^T}{dx^2}\frac{d^2N_{1j}}{dx^2} - EIA_0\frac{d^2N_{1i}^T}{dx^2}\frac{dN_{2j}}{dx} - EI(A_0-B_0)\frac{dN_{2i}^T}{dx}\frac{d^2N_{1j}}{dx^2} + EIB_0\frac{dN_{2i}^T}{dx}\frac{dN_{2j}}{dx} + GAC_0N_{2i}^T\frac{dN_{1j}}{dx} + GAC_0N_{2i}^TN_{2j}\right)$$

$$f_i = \int_0^L N_{1i}^T\, q(x)dx$$

$$F_i = \{-V(0), M'(0), -\bar{M}(0), -V(L), M'(L), -\bar{M}(L)\}^T$$

This gives a 6x6 symmetric stiffness matrix. The element stiffness depends on parameters such as Poisson's ratio (υ) and aspect ratio (L/h).

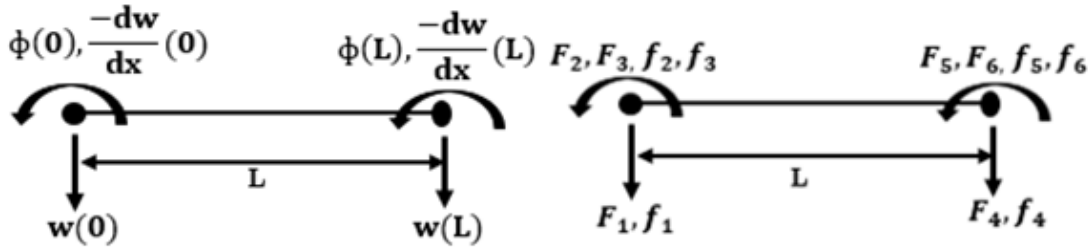

Figure 4.1-Genralized displacements and generalised forces on a typical element

4.3.1. Stiffness matrix terms

$$S_{11} = \frac{2*E*I}{K^2} * \left(9.3196 * \lambda^2 * L^3 + 9.4384 * 10^3 * L - 1.8877 * \frac{10^4}{\lambda}\right)$$

$$S_{12} = -\frac{2*E*I}{K^2} * \left(9.2103 * 10^{-1} * \lambda^2 * L^4 + 7.4775 * \lambda * L^3 + 9.3278 * 10^2 * L^2 + 5.7074 * 10^3 * \frac{L}{\lambda} - 1.5146 * \frac{10^4}{\lambda^2}\right)$$

$$S_{23} = \frac{2*E*I}{K^2*L} * \left(-5.92380 * 10^{-3} * \lambda^3 * L^7 + 4.9266 * 10^{-1} * \lambda^2 * L^6 - 9.7381 * \lambda * L^5 + 6.4168 * 10^2 * L^4 - 5.0338 * 10^3 * \frac{L^3}{\lambda} + 1.39980 * 10^5 * \frac{L^2}{\lambda^2} - 5.17480 * 10^5 * \frac{L}{\lambda^3} + 5.05330 * \frac{10^5}{\lambda^4}\right)$$

$$S_{13} = \frac{2*E*I}{K^2} * \left(-3.7388 * \lambda^2 * L^4 + 7.4775 * \lambda * L^3 - 3.7864 * 10^3 * L^2 + 1.5146 * 10^4 * \frac{L}{\lambda} - 1.5146 * \frac{10^4}{\lambda^2}\right)$$

$$S_{22} = \frac{2*E*I}{K^2*L} * \left(5.9238 * 10^{-3} * \lambda^3 * L^7 + 1.2136 * 10^{-1} * \lambda^2 * L^6 + 1.3477 * 10^1 * \lambda * L^5 + 1.3564 * 10^2 * L^4 + 7.2656 * 10^3 * \frac{L^3}{\lambda} + 9.8995 * 10^3 * \frac{L^2}{\lambda^2} - 1.1233 * 10^5 * \frac{L}{\lambda^3} + 1.2449 * \frac{10^5}{\lambda^4}\right)$$

$$S_{25} = \frac{2*E*I}{K^2*L} * \left(6.0682 * 10^{-2} * \lambda^2 * L^6 + 1.478 * \lambda * L^5 + 36.727 * L^4 + 1.4354 * 10^3 * \frac{L^3}{\lambda} - 2.8039 * 10^4 * \frac{L^2}{\lambda^2} + 1.1233 * 10^5 * \frac{L}{\lambda^3} - 1.2449 * \frac{10^5}{\lambda^4}\right)$$

$$S_{26} = \frac{2*E*I}{K^2*L} * \left(2.4633 * 10^{-1} * \lambda^2 * L^6 + 2.2608 * \lambda * L^5 + 1.1873 * 10^2 * L^4 + 2.0402 * 10^3 * \frac{L^3}{\lambda} - 1.3699 * 10^5 * \frac{L^2}{\lambda^2} + 5.17480 * 10^5 * \frac{L}{\lambda^3} - 5.0533 * \frac{10^5}{\lambda^4}\right)$$

$$S_{33} = \frac{2*E*I}{K^2*L} * \left(5.9238 * 10^{-3} * \lambda^3 * L^7 + 1.9998 * \lambda^2 * L^6 + 5.9993 * \lambda * L^5 + 2.5137 * 10^3 * L^4 - 5.0634 * 10^3 * \frac{L^3}{\lambda} + 5.0674 * 10^5 * \frac{L^2}{\lambda^2} - 2.0391 * 10^6 * \frac{L}{\lambda^3} + 2.0513 * \frac{10^6}{\lambda^4}\right)$$

$$S_{36} = -\frac{2*E*I}{K^2*L} * \left(-9.9992 * 10^{-1} * \lambda^2 * L^6 + 5.9996 * \lambda * L^5 - 5.1232 * 10^2 * L^4 + 7.0887 * 10^3 * \frac{L^3}{\lambda} + 4.9459 * 10^5 * \frac{L^2}{\lambda^2} - 2.0391 * 10^6 * \frac{L}{\lambda^3} + 2.0513 * \frac{10^6}{\lambda^4}\right)$$

$$K = \left(1.2463 * \lambda * L^3 + 1.2623 * 10^3 * \frac{L}{\lambda} - 2.5246 * \frac{10^3}{\lambda^2}\right)$$

$S_{11} = -S_{14} = S_{44}$ $S_{12} = S_{15} = -S_{24} = -S_{45}$ $S_{13} = S_{16} = -S_{34} = -S_{46}$
$S_{23} = S_{56}$ $S_{22} = K_{55}$ $S_{26} = S_{35}$ $S_{33} = S_{66}$

Although the stiffness terms look complex and longer, substitution of Poisson's ratio (υ) and aspect ratio (L/h) gives a simple 6x6 matrix.

- For L/h =1 and υ =0.3

$$S = \frac{EI}{L^3}\begin{bmatrix} 3.1795 & -0.4558L & -1.1339L & -3.1795 & -0.4558L & -1.1339L \\ & 0.2418L^2 & 0.1837L^2 & 0.4558L & 0.0263L^2 & 0.0040L^2 \\ & & 1.1855L^2 & 1.1339L & 0.0040L^2 & -0.2393L^2 \\ & & & 3.1795 & 0.4558L & 1.1339L \\ & & & & 0.2418L^2 & 0.1837L^2 \\ & & & & & 1.1855L^2 \end{bmatrix}$$

- For L/h =10 and υ =0.3

$$S = \frac{EI}{L^3}\begin{bmatrix} 11.6408 & -1.2023L & -4.6182L & -11.6408 & -1.2023L & -4.6182L \\ & 1.5375L^2 & -0.7387L^2 & 1.2023L & 0.0851L^2 & 0.3184L^2 \\ & & 3.8500L^2 & 4.6182L & 0.3184L^2 & 1.1883L^2 \\ & & & 3.1795 & 1.2023L & 4.6182L \\ & & & & 1.5375L^2 & -0.7387L^2 \\ & & & & & 3.8500L^2 \end{bmatrix}$$

There is a significant difference in the stiffness value estimated when the aspect ratio is different for the element. Therefore when the classical Euler-Bernoulli beam element is used for the thick or short beam analysis, it tends to estimate higher stiffness value and lower deformation.

4.3.2. Load vector

For uniform distributed load of q, the load vector f is given by,

$$f_i = \begin{Bmatrix} 0.5 * q * L \\ -q * \dfrac{821 * \lambda^2 * L^2 + 20000 * \lambda * L - 40000}{49852 * \lambda^2} \\ -q * \dfrac{2500 * \lambda^2 * L^2 - 15000 * \lambda * L + 30000}{37389 * \lambda^2} \\ 0.5 * q * L \\ q * \dfrac{821 * \lambda^2 * L^2 + 20000 * \lambda * L - 40000}{49852 * \lambda^2} \\ q * \dfrac{2500 * \lambda^2 * L^2 - 15000 * \lambda * L + 30000}{37389 * \lambda^2} \end{Bmatrix}$$

4.4. Using the finite element model for 2D frame analysis.

When the finite element model is used for the 2D frame analysis, axial displacement due to axial force also need to be included. The displaced field (3.1) is extended to take into account the effect of axial force as follows;

$$u(x,z) = u(x) + z\,\phi(x) - \mu\left(h\sinh\left(\frac{z}{h}\right) - z\right)\left[\frac{dw}{dx} + \phi(x)\right];\ \mu = \frac{1}{\cosh\frac{1}{2} - 1}$$

$$w(x,z) = w(x) \tag{4.33}$$

Where;

u_0 is axial displacement due to axial force at the centre line. Other terms are defined same as before.

With same procedure followed in the previous section (3.3), set of governing equations of equilibrium and boundary conditions can be obtained.

In addition to equation of equilibrium obtained section (3.3), there is one more governing equation

$$\frac{dP}{dx} = -p(x) \tag{4.34}$$

Where;

$p(x)$ is distributed axial load acting on the beam. P is resultant axial force in an arbitrary section of the beam.

The additional boundary condition becomes

$$P = 0 \quad \text{or} \quad \phi \text{ is prescribed} \tag{4.35}$$

The stress resultant P is defined as

$$P = \int_A \sigma_{xx} dA$$

$$P = \int_{-\frac{h}{2}}^{h/2} Eb\left(\frac{d\,u(x)}{dx} + z\,\frac{d\phi}{dx} - \mu\left(h\sinh\left(\frac{z}{h}\right) - z\right)\left(\frac{d^2w}{dx^2} + \frac{d\phi}{dx}\right)\right)dz$$

$$P = EA\frac{d\,u(x)}{dx} \tag{4.36}$$

Other stress resultants are same as defined in section (3.4).

Linear Lagrangian interpolation can be used to approximate the displacement variable u_0. Since the approximation also represents homogeneous solution of the governing equations of equilibrium, the formulation based on this approximation also will give

exact nodal displacement. Additional stiffness terms due to axial displacement is same as in the classical finite elements. The final stiffness matrix is 8x8 matrix. For uniformly distributed axial load the finite element model can be written as follows

$$\begin{bmatrix} EA/L & 0 & 0 & 0 & -EA/L & 0 & 0 & 0 \\ 0 & * & * & * & 0 & * & * & * \\ 0 & * & * & * & 0 & * & * & * \\ 0 & * & * & * & 0 & * & * & * \\ -EA/L & 0 & 0 & 0 & EA/L & 0 & 0 & 0 \\ 0 & * & * & * & 0 & * & * & * \\ 0 & * & * & * & * & * & * & * \\ 0 & * & * & * & * & * & * & * \end{bmatrix} \begin{Bmatrix} u_0\,(0) \\ * \\ * \\ * \\ u_0\,(L) \\ * \\ * \\ * \end{Bmatrix} = \begin{Bmatrix} pL/2 \\ * \\ * \\ * \\ pL/2 \\ * \\ * \\ * \end{Bmatrix} + \begin{Bmatrix} P(0) \\ * \\ * \\ * \\ * \\ * \\ * \\ P(L) \end{Bmatrix}$$

*these refer to similar terms derived in the previous sections (4.3.1)

4.4.1. Transformation from local system to global system

Analysis of 2D frame for displacements and stresses requires, setting of global coordinate system and referring all quantities of individual elements to common global coordinate system in order to assemble the element and impose boundary conditions on the whole structure.

The local coordinates (x_e, y_e, z_e) of a typical element are related to the global coordinates (x, y, z) by

$$\begin{Bmatrix} x_e \\ y_e \\ z_e \end{Bmatrix} = \begin{bmatrix} cos\alpha & 0 & sin\alpha \\ 0 & 1 & 1 \\ -sin\alpha & 0 & cos\alpha \end{bmatrix} \begin{Bmatrix} x \\ y \\ z \end{Bmatrix} \tag{4.37}$$

Where α angle is measured clockwise from the global x - axis to the element x_e- axis and y and y_e, axes are parallel to each other and they are out of the plane of the paper (see Figure 4.2).

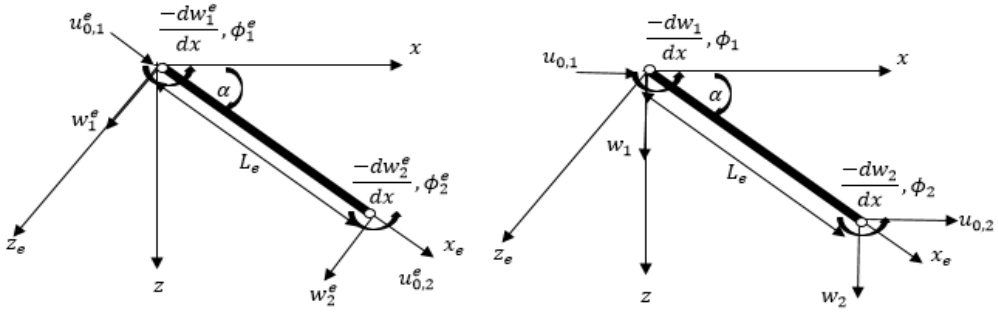

Figure 4.2-Generalised displacements in the local and global coordinates

The nodal degrees of freedom in the local coordinate system are related to nodal degrees of freedom in the global coordinate system using the following transformation matrix [T].

$$\begin{Bmatrix} u_{0,1}^e \\ w_1^e \\ \frac{-dw_1^e}{dx} \\ \phi_1^e \\ u_{0,2}^e \\ w_2^e \\ \frac{-dw_2^e}{dx} \\ \phi_2^e \end{Bmatrix} = \begin{bmatrix} cos\alpha & sin\alpha & 0 & 0 & & & & \\ -sin\alpha & cos\alpha & 0 & 0 & & & & \\ 0 & 0 & 1 & 0 & & & & \\ 0 & 0 & 0 & 1 & & & & \\ & & & & cos\alpha & sin\alpha & 0 & 0 \\ & & & & -sin\alpha & cos\alpha & 0 & 0 \\ & & & & 0 & 0 & 1 & 0 \\ & & & & 0 & 0 & 0 & 1 \end{bmatrix} \begin{Bmatrix} u_{0,1} \\ w_1 \\ \frac{-dw_1}{dx} \\ \phi_1 \\ u_{0,2} \\ w_2 \\ \frac{-dw_2}{dx} \\ \phi_2 \end{Bmatrix}$$

$$\{D^e\} = [T].\{D\} \tag{4.38}$$

Similarly the element force vectors in the local and global system are related by

$$\{f^e\} + \{F^e\} = [T](\{f\} + \{F\}) \tag{4.39}$$

Substituting (4.38) and (4.39) into the finite element relations $[S_e]\{d_e\} = \{f^e\} + \{F^e\}$ in the local coordinate system, gives;

$$[S_e][T].\{D\} = [T](\{f\} + \{F\}) \tag{4.40}$$

Pre multiplying (4.40) both sides by $[T]^T = [T]^{-1}$, gives;

$$[S].\{D\} = \{f\} + \{F\} \tag{4.41}$$

Where $[S] = [T]^T[S_e][T]$

CHAPTER V

5. RESULTS AND DISCUSSION

5.1. Validation of the proposed theory

The following numerical examples are considered for the validation of the present theory. A simply supported beam problem and a cantilever beam problem with different aspect ratios are solved for displacements and stresses and results are compared with solutions predicted by other beam theories and two dimensional elasticity solution.

5.1.1. Numerical examples I

Example 1

The first problem is of a simply supported beam of different aspect ratios (L/h) carrying an uniformly distributed load of qkN/m (see Figure 5.1).

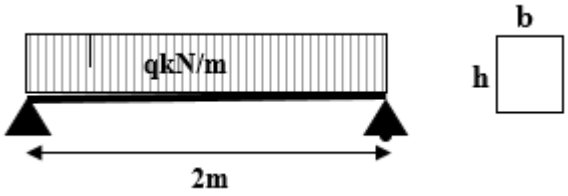

Figure 5.1-simply supported beam problem

The numerical data for this example are:

a) q = 5kN/m , E = $2*10^8$ N/m^2, L = 2m, h = 1m, b = 0.3m and Poisson's ratio υ = 0.3.

b) q = 3kN/m , E = $2*10^8$ N/m^2, L = 2m, h = 0.5m, b = 0.3m and Poisson's ratio υ = 0.3.

c) q = 2kN/m , E = $2*10^8$ N/m^2, L = 2m, h = 0.2m, b = 0.2m and Poisson's ratio υ = 0.3.

The boundary conditions associated with simply supported beam for the present beam theory are as follows:

$M'_{xx} = \bar{M}_{xx} = w = 0$ at x = 0 and x = L

$M'_{xx} = \bar{M}_{xx} = 0 \rightarrow \frac{d\phi}{dx} = \frac{d^2w}{dx^2} = 0$ at x = 0 and x = L

From the general solutions of the present beam theory, expression for w and ϕ as follows:

$$w(x) = \frac{qL^4}{24EI}\left(\frac{x^2}{L^2} - \frac{x^3}{L^3} + \frac{x^4}{L^4}\right) + \frac{qA_0^2L^2}{2C_0GA}\left(\frac{x}{L} - \frac{x^2}{L^2} - \frac{2}{(\lambda L)^2}\left(1 - \frac{cosh\,\lambda(L/2-x)}{\cosh(\lambda L/2)}\right)\right)$$

$$\theta(x) = \frac{A_0qL}{2C_0GA}\left(\left(1 - \frac{x}{L}\right) - \frac{2sinh\,\lambda(L/2-x)}{(\lambda L)\cosh(\lambda L/2)}\right)$$

Other theoretical solutions are from [1] and [53]

Euler Beam theory (EBT):

$$w(x) = \frac{qL^4}{24EI}\left(\frac{x^2}{L^2} - 2\frac{x^3}{L^3} + \frac{x^4}{L^4}\right)$$

First order shear deformation beam theory (FSBT):

$$w(x) = \frac{qL^4}{24EI}\left(\frac{x^2}{L^2} - \frac{x^3}{L^3} + \frac{x^4}{L^4}\right) + \frac{qL^2}{2K_sGA}\left(\frac{x}{L} - \frac{x^2}{L^2}\right)$$

$$\theta(x) = \frac{qL}{2K_sGA}\left(1 - 2\frac{x}{L}\right)$$

Higher order shear deformation beam theory (HSBT):

$$w(x) = \frac{qL^4}{24EI}\left(\frac{x^2}{L^2} - \frac{x^3}{L^3} + \frac{x^4}{L^4}\right) + \frac{6qL^2}{10GA}\left(\frac{x}{L} - \frac{x^2}{L^2} - \frac{2}{(\lambda L)^2}\left(1 - \frac{\cosh\,\lambda(L/2-x)}{\cosh(\lambda L/2)}\right)\right)$$

$$\theta(x) = \frac{3qL}{4GA}\left(\left(1 - \frac{x}{L}\right) - \frac{2\sinh\,\lambda(L/2-x)}{(\lambda L)\cosh(\lambda L/2)}\right)$$

2D Elasticity solution:

$$w(x,y) = -\frac{q}{2EI}\left\{\frac{y^4}{12} - \frac{h^2y^2}{8} + \frac{h^3y}{12} + \upsilon\left(\frac{(l^2-x^2)y^2}{2} + \frac{y^4}{6} - \frac{h^2y^2}{20}\right)\right\} - \frac{q}{2EI}\left\{\frac{l^2x^2}{2} - \frac{x^4}{12} - \frac{h^2x^2}{20} + \frac{\left(1+\frac{1}{2}\upsilon\right)h^2x^2}{4}\right\} + \frac{5ql^4}{24EI}\left\{1 + \frac{3h^2}{20l^2}\left(\frac{4}{5} + \frac{\upsilon}{2}\right)\right\}$$

$$\theta(x,y) = -\frac{q}{2GI}\left(\frac{h^2}{4} - y^2\right)x$$

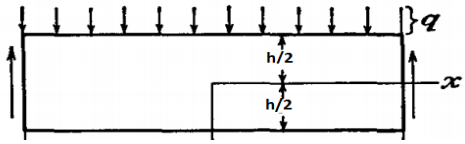

Figure 5.2 -The coordinate system for 2D elasticity solution for example 1(a)

Solutions are represented in the graphical forms from Figure 5.3 to Figure 5.12

For part (a)

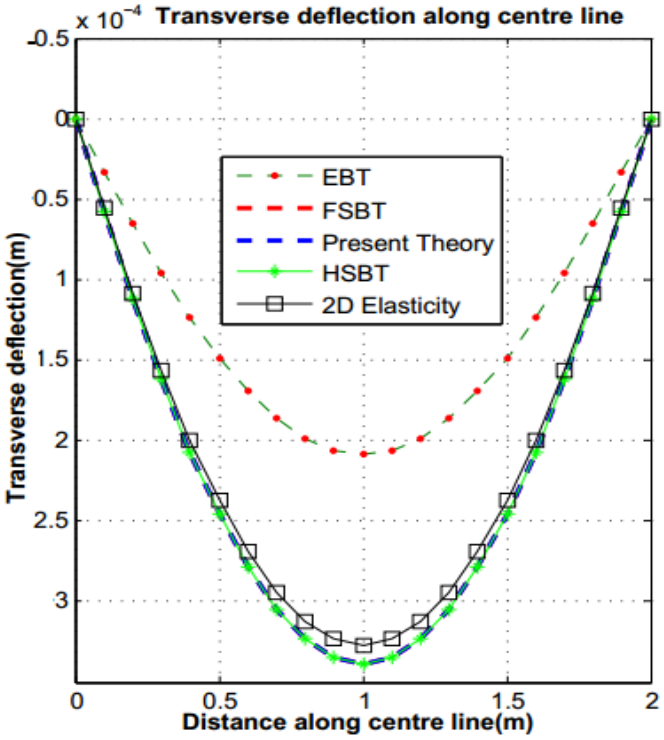

Figure 5.3-Transverse displacement along centre line for example 1(a)

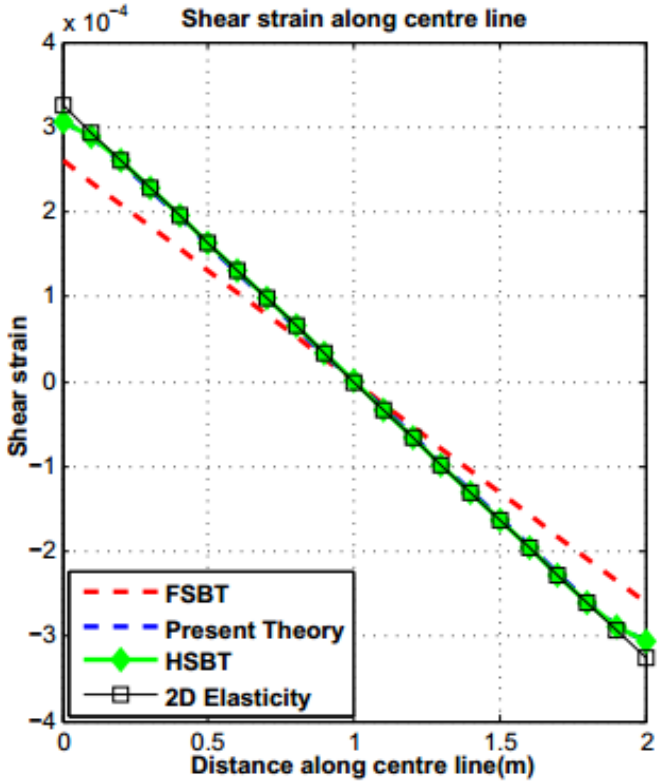

Figure 5.4-Shear strain along centre line for example 1(a)

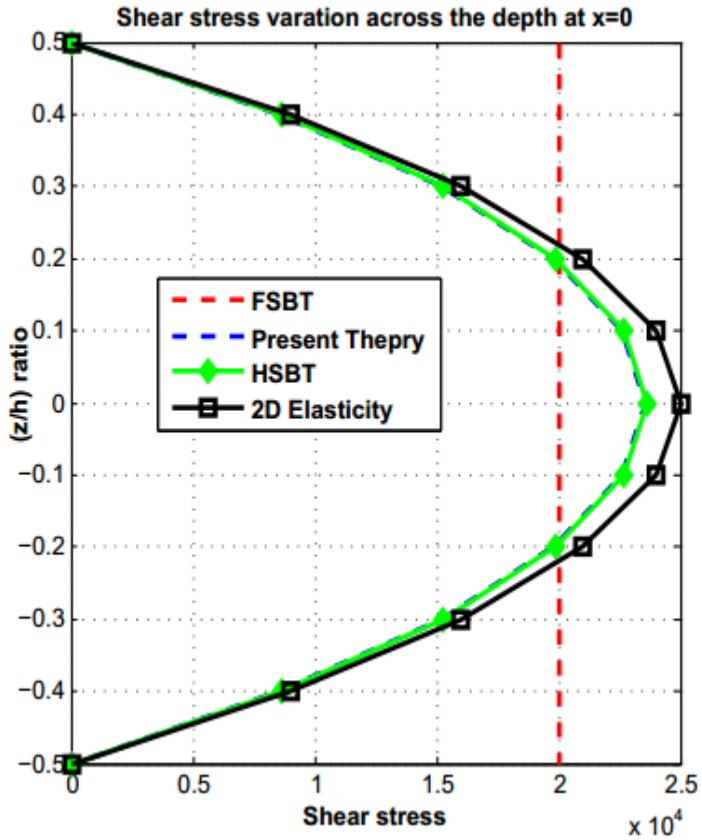

Figure 5.5-Shear stress variation across the depth at x = 0 for example 1(a)

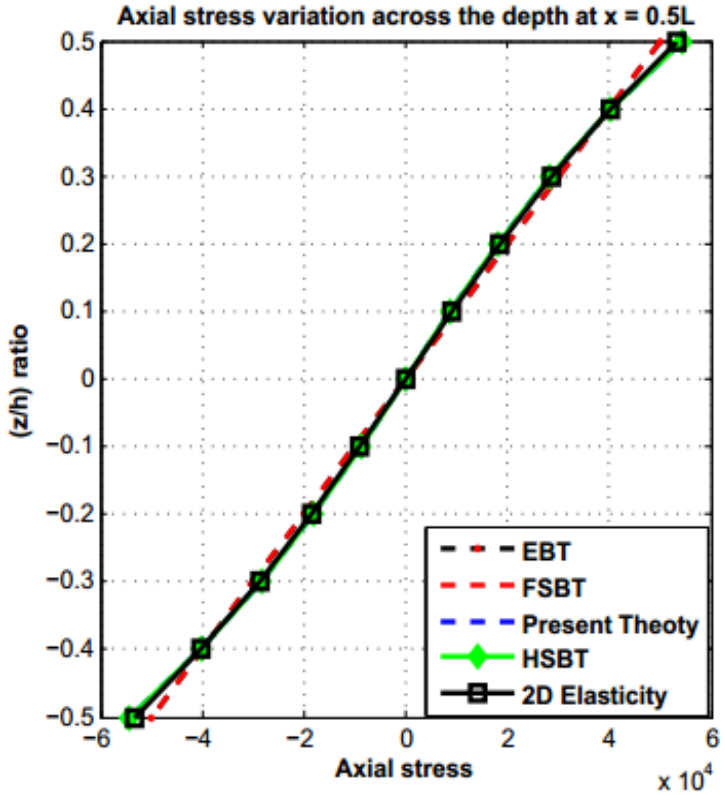

Figure 5.6-Axial stress variation across the depth at x = 0.5L for example 1(a)

For part (b)

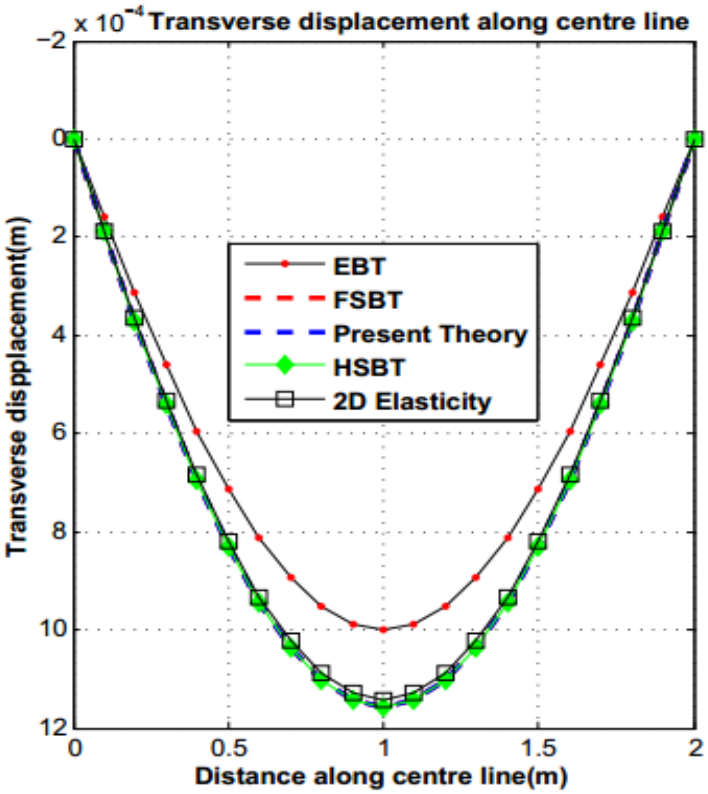

Figure 5.7-Transverse displacement along centre line for example 1(b)

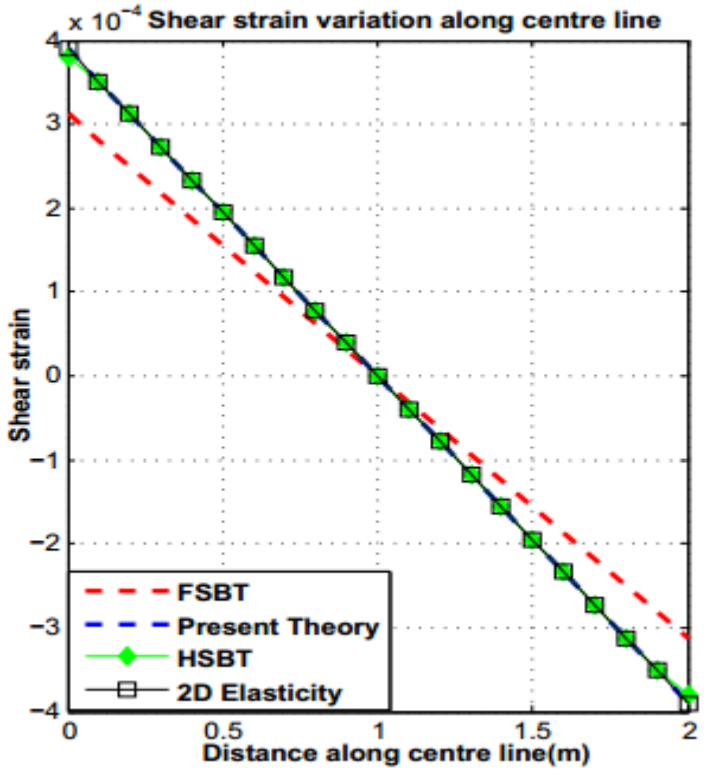

Figure 5.8-Shear strain variation along centre line for example 1(b)

For part (c)

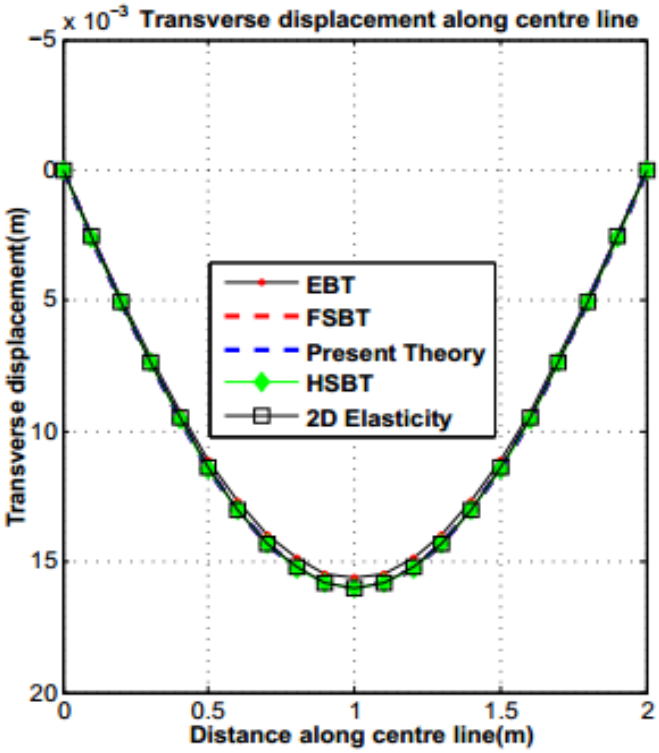

Figure 5.9-Transverse displacement along centre line for example 1(c)

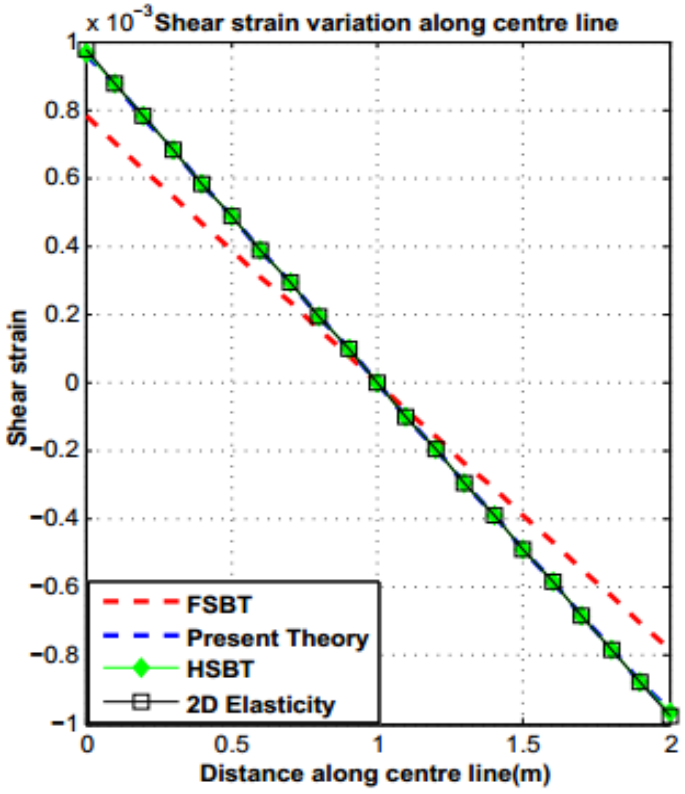

Figure 5.10-Shear strain variation along centre line for example 1(c)

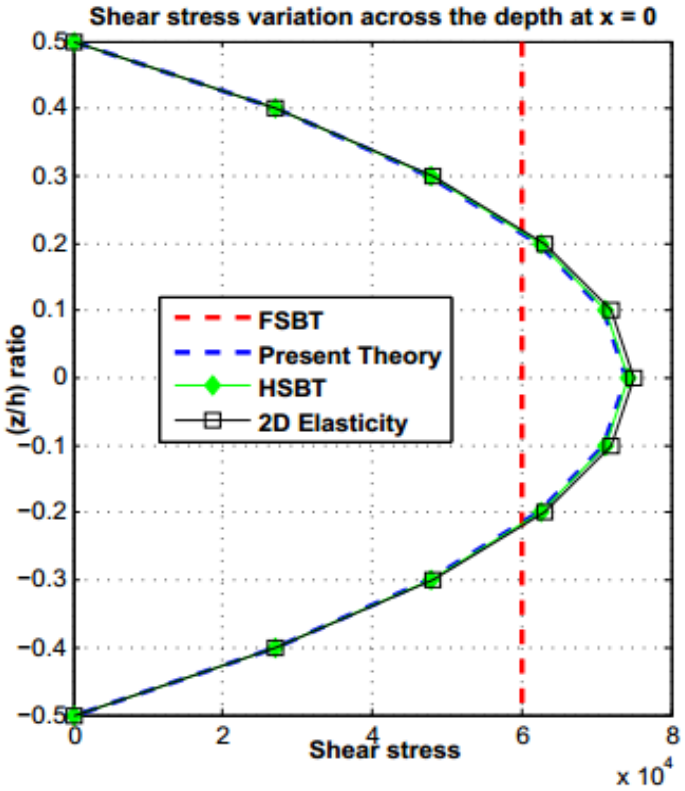

Figure 5.11-Shear stress variation across the depth at x = 0 for example 1(c)

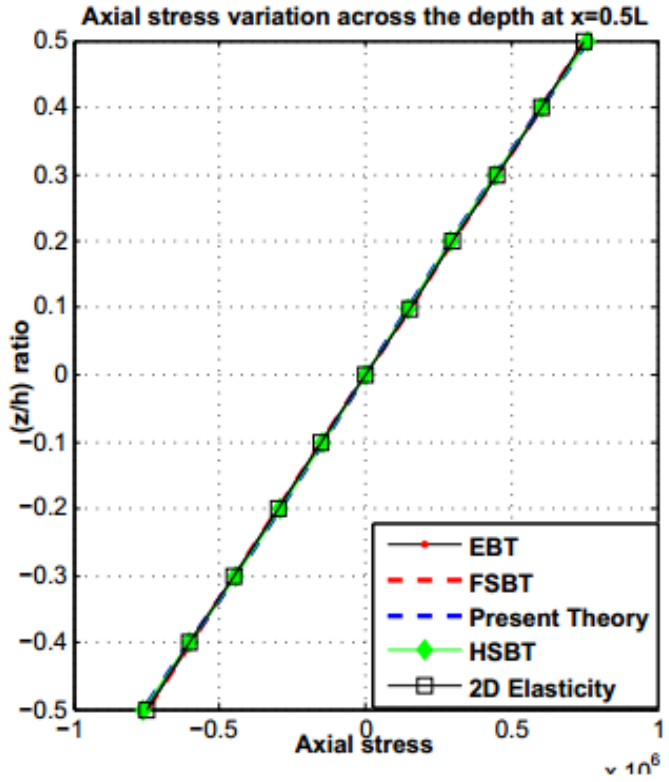

Figure 5.12-Axial stress variation across the depth at x = 0.5L for example 1(c)

The tables 1-3 below give the maximum value of transverse displacement ($\boldsymbol{w}$), axial stress ($\boldsymbol{\sigma_{xx}}$), shear rotation of cross section ($\boldsymbol{\theta}$) and transverse shear stress ($\boldsymbol{\tau_{xz}}$) for each aspect ratios of the beam.

Table 5.1. Maximum value for displacements and stresses for example 1(a)

Model	$\boldsymbol{w(10^{-4}m)}$	$\boldsymbol{\sigma_{xx}(10^{4}Nm^{-2})}$	$\boldsymbol{\theta(10^{-4})}$	$\boldsymbol{\tau_{xz}(10^{4}Nm^{-2})}$
EBT	2.0833	5.0000	-	-
FSBT	3.3833	5.0000	2.6000	2.0000
Present	3.3833	5.4310	3.0602	2.3538
HSBT	3.3833	5.4333	3.0692	2.3609
Exact	3.2708	5.3333	3.2500	2.5000

Table 5.2. Maximum value for displacements and stresses for example 1(b)

Model	$\boldsymbol{w(10^{-3}m)}$	$\boldsymbol{\sigma_{xx}(10^{5}Nm^{-2})}$	$\boldsymbol{\theta(10^{-4})}$	$\boldsymbol{\tau_{xz}(10^{4}Nm^{-2})}$
EBT	1.0000	1.2000	-	-
FSBT	1.1560	1.2000	3.1200	2.4000
Present	1.1560	1.2259	3.7801	2.9077
HSBT	1.1560	1.2260	3.7915	2.9165
Exact	1.1425	1.2220	3.9000	3.0000

Table 5.3. Maximum value for displacements and stresses for example 1(c)

Model	$\boldsymbol{w(10^{-3}m)}$	$\boldsymbol{\sigma_{xx}(10^{5}Nm^{-2})}$	$\boldsymbol{\theta(10^{-4})}$	$\boldsymbol{\tau_{xz}(10^{4}Nm^{-2})}$
EBT	15.625	7.5000	-	-
FSBT	16.015	7.5000	7.8000	6.0000
Present	16.015	7.2586	9.6122	7.3940
HSBT	16.015	7.2600	9.6415	7.4165
Exact	15.981	7.5200	9.7500	7.5000

Example 2:

This problem is of a cantilever beam of different aspect ratios (L/h) carrying a tip load of P.

The numerical data for this example are:

a) P = 5kN, E = $2*10^8$ N/m^2, L = 2m, h = 1m, b = 0.3m and Poisson's ratio υ = 0.3.

b) P = 100N, E = $2*10^8$ N/m^2, L = 2m, h = 0.2m, b = 0.2m and Poisson's ratio υ = 0.3.

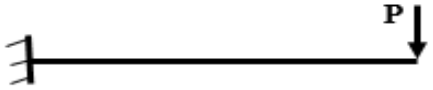

Figure 5.13-Cantilever beam problem

The boundary conditions associated with cantilever beam for present beam theory as follows:

$w = \frac{d\,w}{dx} = \phi$ at x = 0

$M'_{xx} = \bar{M}_{xx} = \frac{dM_{xx}}{dx} = 0$ at x = L

From the general solutions of the present beam theory, expression for w and ϕ as follows:

$$w(x) = \frac{PL^3}{6EI}\left(3\frac{x^2}{L^2} - \frac{x^3}{L^3}\right) + \frac{PA_0^2L}{C_0GA}\left(\frac{x}{L} + \frac{1}{(\lambda L)}\left(\frac{\sinh\lambda(\mathrm{L}-\mathrm{x})}{\cosh(\lambda L)} - \tanh(\lambda L)\right)\right)$$

$$\theta(x) = \frac{A_0P}{5C_0GA}\left(1 - \frac{\cosh\lambda(\mathrm{L}-\mathrm{x})}{\cosh(\lambda L)}\right)$$

Other theoretical solutions are from [1] and [53]

Euler Beam theory (EBT):

$$w(x) = \frac{PL^3}{6EI}\left(3\frac{x^2}{L^2} - \frac{x^3}{L^3}\right)$$

First order shear deformation beam theory (FSBT):

$$w(x) = \frac{PL^3}{6EI}\left(3\frac{x^2}{L^2} - \frac{x^3}{L^3}\right) + \frac{Px}{K_sGA}$$

$$\theta(x) = \frac{P}{K_sGA}$$

Higher order shear deformation beam theory (HSBT):

$$w(x) = \frac{PL^3}{6EI}\left(3\frac{x^2}{L^2} - \frac{x^3}{L^3}\right) + \frac{6PL}{5GA}\left(\frac{x}{L} + \frac{1}{(\lambda L)}\left(\frac{\sinh \lambda(\mathrm{L-x})}{\cosh(\lambda L)} - \tanh(\lambda L)\right)\right)$$

$$\theta(x) = \frac{3P}{10GA}\left(1 - \frac{cosh\lambda(\mathrm{L-x})}{\cosh(\lambda L)}\right)$$

2D Elasticity solution:

$$w(x,y) = \frac{\upsilon Pxy^2}{2EI} + \frac{Pl^3}{6EI}\left(2 - 3\frac{Px}{l} + \frac{x^3}{l^3}\right) + \frac{Ph^2}{8GI}(l-x)$$

$$\theta(x,y) = \frac{-P}{2IG}\left(\frac{h^2}{4} - y^2\right)$$

For part (a):

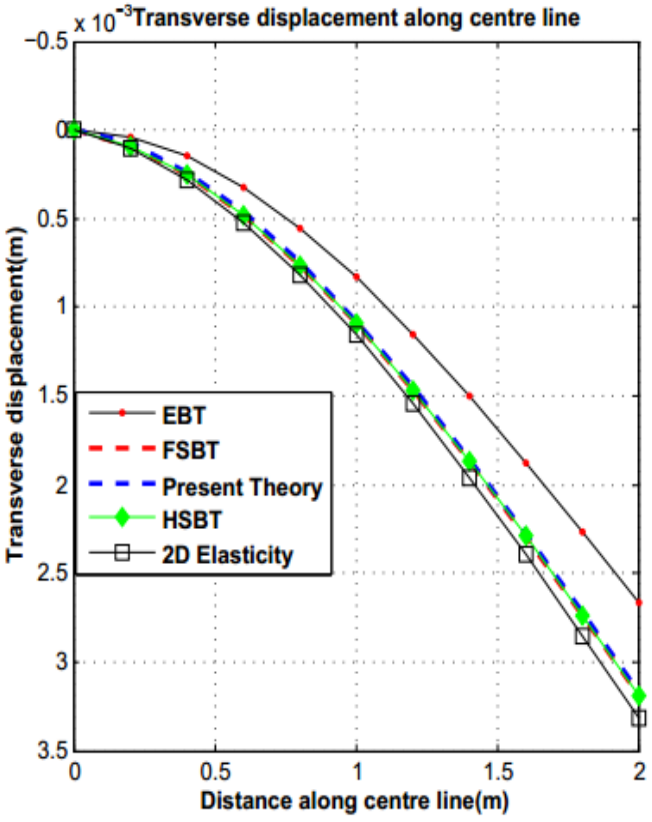

Figure 5.14-Transverse displacement along centre line for example 2(a)

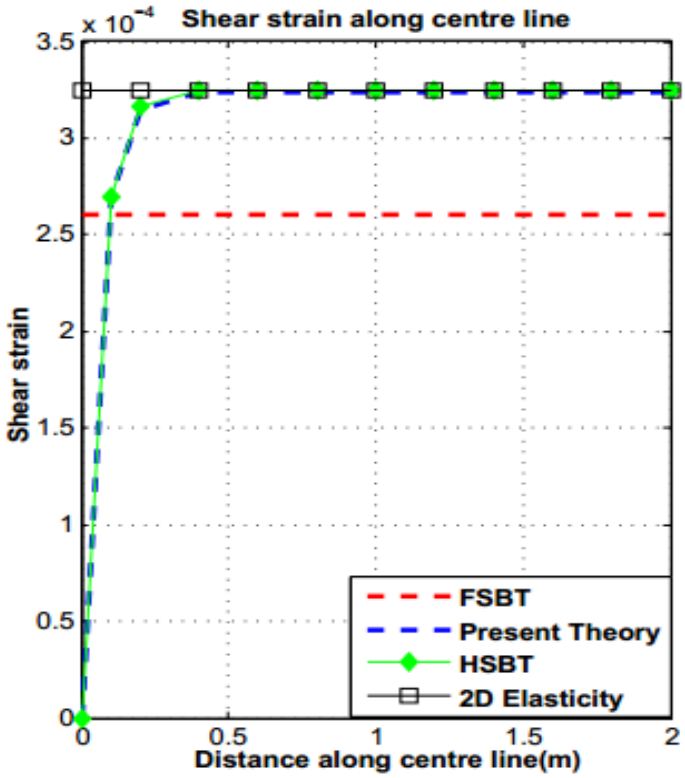

Figure 5.15-Shear strain along centre line for example 2(a)

For part (b):

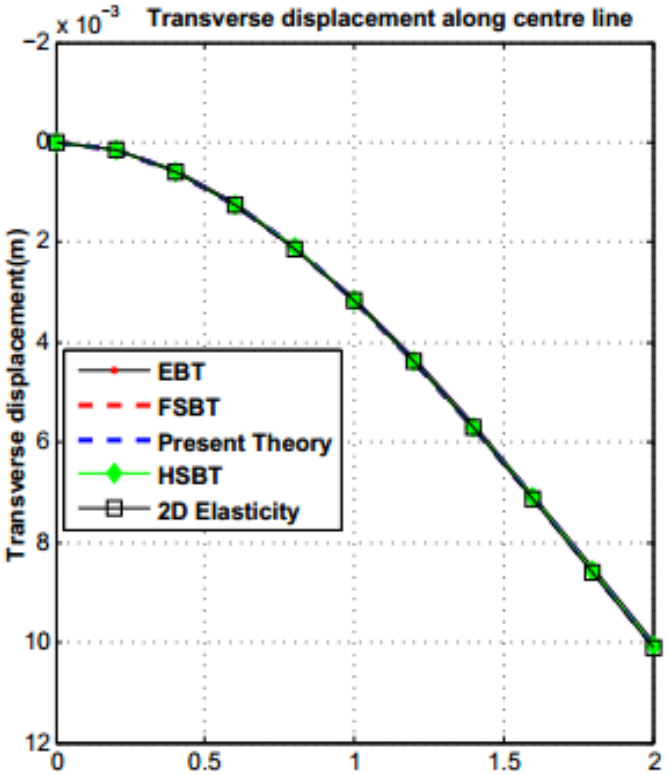

Figure 5.16-Transverse displacement along centre line for example 2(b)

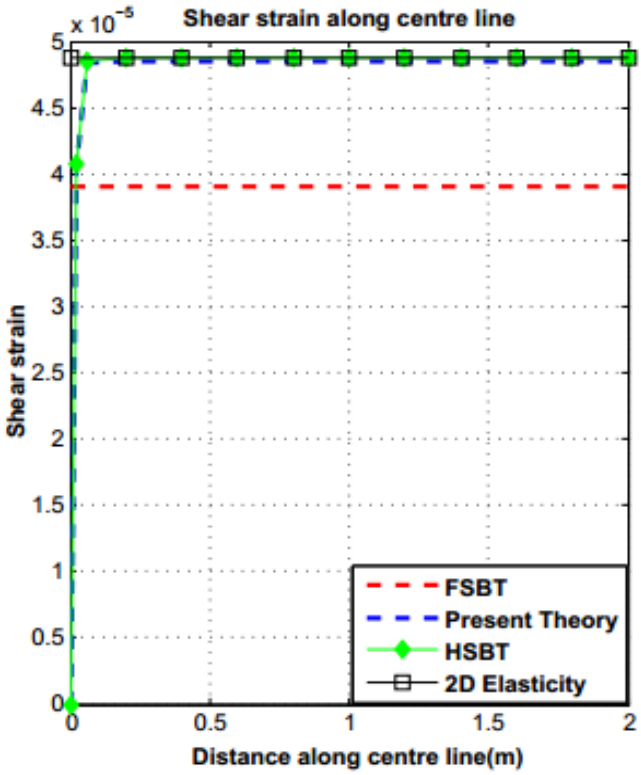

Figure 5.17-Shear strain along centre line for example 2(b)

5.1.2. Comparisons and findings of the theoretical solutions

From the above numerical examples (1) and (2), it can be clearly seen from the Figure 5.3 and Figure 5.7 that classical Euler-beam theory predicts significantly different values than other theoretical values for transverse displacement when the beam becomes thick. But the values are closer to other theoretical values when the aspect ratio (L/h) becomes larger (Figure 5.9). In example (1.a) (aspect ratio 2), it under estimates the maximum value for transverse displacement (see Table 5.1) by 36% and in example (1.b) and (1.c), it underestimates the maximum value by 12.5% and 2.2% (see Table 5.2 and Table 5.3) respectively compared to 2D elasticity solution. From the second example also (Figure 5.14 and Figure 5.16), same behaviour can be observed.

In the case of present theory, HSBT and FSBT, all these theories predicts almost same values to each other and much closer value to two dimensional elasticity solution for transverse displacement. In example 1, all these theories (i.e present theory, HSBT and FSBT) over estimates the maximum transverse displacement by 3.4%, 1.2% and 0.2% in 1(a), 1(b) and 1(c) respectively. In the second example, present theory, HSBT, and

FSBT under estimate the tip deflection by 4% and 0.2% in example 2(a) and 2(b) respectively when it is compared to two dimensional elasticity solution. It should be noted that in all these cases, FSBT uses a shear correction factor (K_s) of 5/6.

It can be seen from Figure 5.5 and Figure 5.11 that present theory and HSBT gives the parabolic shear variation while satisfying the shear boundary conditions at top and bottom of the beam. However in example 1(a), both present theory and HSBT under-estimate the maximum shear rotation (Table 1) by 5.8% and (5.6%) respectively compared to 2D elasticity solution. This error percentage reduces with increase in the aspect ratio of the beam. When the aspect ratio of the beam is four (example 1(b) & Table 2), these percentage are 3.1% and 2.8% respectively. In the second example both in part 2(a) and part 2(b), these theories predict almost same shear rotation along the beam as predicted by 2D elasticity theory.

It can be noted from maximum values for stresses given in Table 5.1, Table 5.2 and Table 5.3 that shear stress starts to dominate when the beam becomes thicker. When the aspect ratio of the beam is two, (example1 part (a)),the ratio between the maximum shear stress and maximum flexural stress is around 48% but when the aspect ratios are four (Table 5.2) and ten (Table 5.3), these percentages are 25% and 10% respectively. Also it can be noted from Figure 5.6 that when the beam becomes deeper, the axial stress distribution across the section of the beam becomes nonlinear even in the linear elastic analysis. But this behaviour couldn't be captured by EBT and FSBT.

In brief, among those one dimensional beam theories discussed here, present theory and HSBT are most suitable to analyse the deep beams since they give more close values to the solutions predicted by two dimensional elastic theory for deformations and stresses. But in the most of the cases, it is not possible to get the analytical solutions, a suitable finite element model is required to get the solutions using this theory.

5.2. Validation of the finite element model

Number of numerical examples are considered to illustrate the different scenarios and the finite element solutions for those problems are obtained using the proposed finite element model. Convergence of finite element solutions are checked

against corresponding analytical solutions of theory where it is obtainable. In the cases where the analytical solutions are not available, finite element solutions of the problem compared against the solutions obtained using other beam elements and two and three dimensional model of 'ABAQUS' software (version 14.1). However, 'ABAQUS' program solutions are validated against two dimensional elasticity solution for simple beam problem. The problems are discretized into different number of elements to get some ideas on the convergent rate and performance of the present finite element model.

MATLAB program is used to get the finite element solutions of the present finite element model. First stiffness matrix and load vectors were calculated in the symbolic form using "symbolic tool box" of MATLAB. These matrices were developed using exact integration. The stiffness values defined in the section 4.3.1 derived after some simplifications to the matrices obtained from exact integration. Then a program developed to analyse a general beam problem. The MATLAB program consists of several user-defined functions created in different M-Files to handle different tasks. This program includes a main function which calls several other built-in functions and user-defined functions to complete different tasks. This program includes functions to get the input data from user, to calculate local stiffness matrix, to assemble the global stiffness matrix, to calculate local load vector, to assemble global load vector and to interpolate and plot the variables.

5.2.1. Numerical examples II

Example 03

Consider the example 1(a) in section (5.1.1), the finite element solution of this problem obtained using different number of elements (number of elements are indicated within the bracket). Also, the beam is analysed using an exact finite element model (2.9) (finite element based on the interdependent interpolation) of the FSBT.

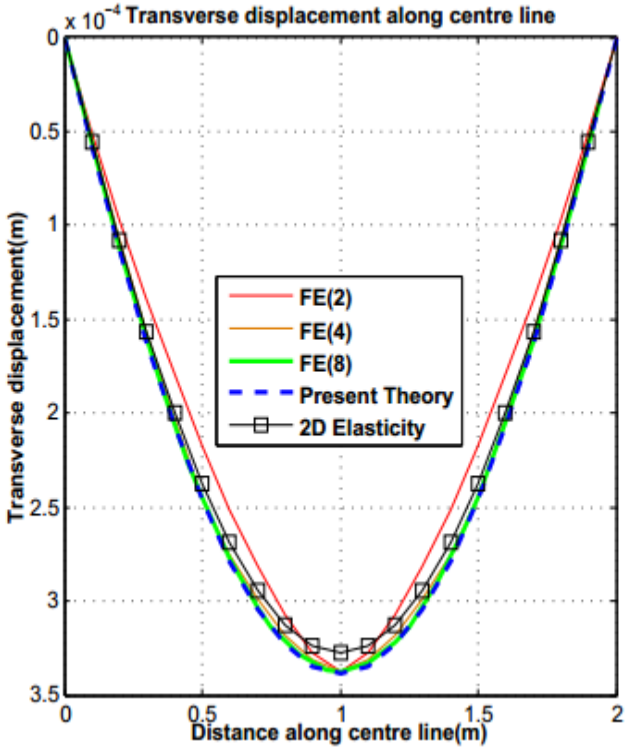

Figure 5.18 -Transverse displacement along centre line using present FE for example 1(a)

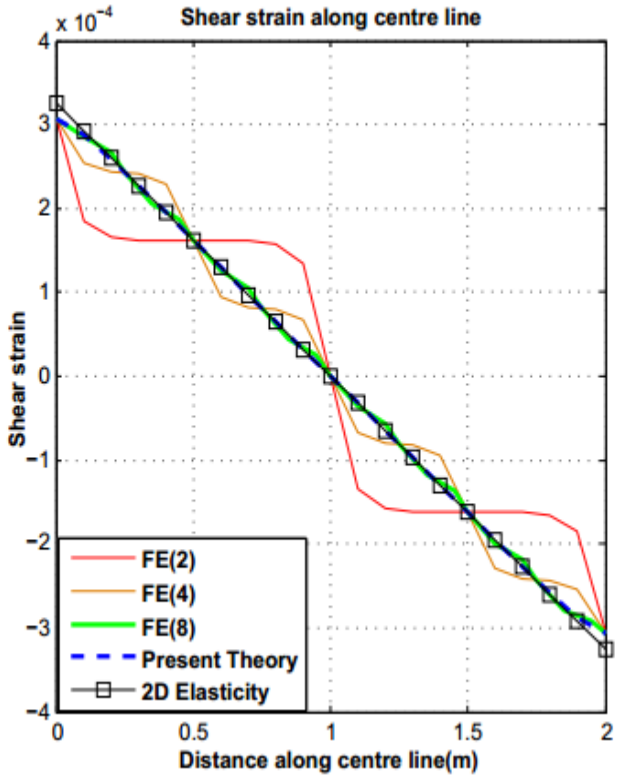

Figure 5.20 -Transverse displacement along centre line using present FE for example 1(a)

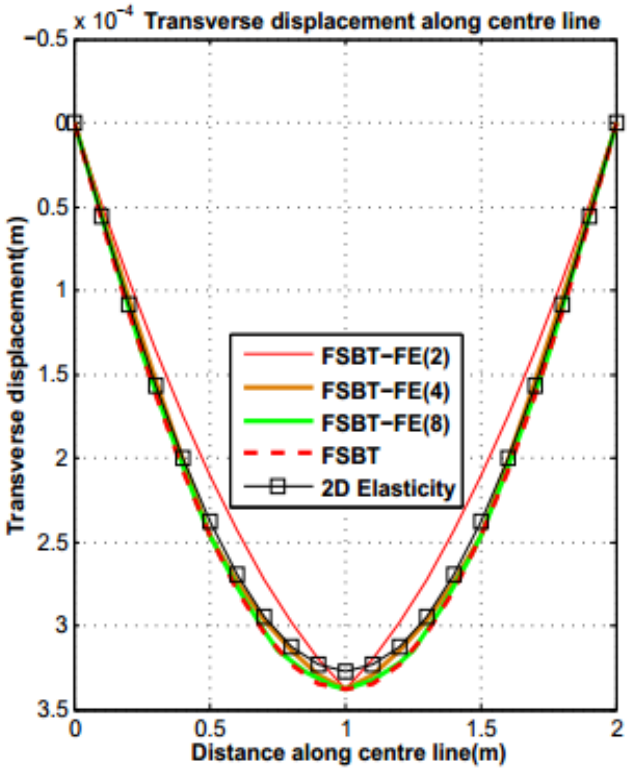

Figure 5.19 -Transverse displacement along centre line using FSBT-FE for example 1(a)

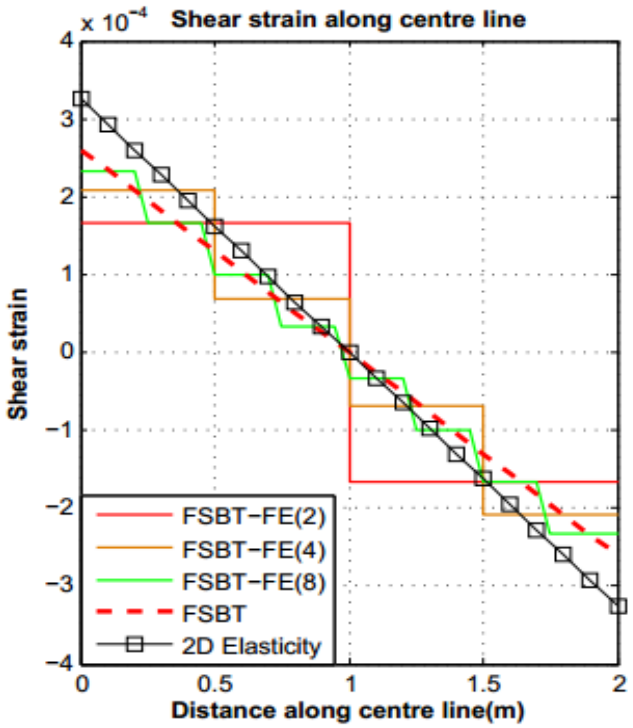

Figure 5.21-Shear strain along centre line using FSBT-FE for example 1(a)

Finite element solution and corresponding analytical solution for transverse displacement are very close to each other with four elements. But when the number of element is eight, finite element solution for transverse displacement is almost same as the corresponding theoretical solution. But this improvement in the results is very small compare to improvement obtained in the results by increasing the element from two to four (Figure 5.18). However in the case of shear rotation, the finite element solution of the present theory converges to corresponding analytical solution when the number of the element used is eight (Figure 5.19). On the other hand, by comparison of Figure 5.18 and Figure 5.20, it can be noted that the finite element solution of FSBT for transverse displacement doesn't differ very much in terms of convergent rate and accuracy from the finite element solution of the present theory. Both the finite element models follows same pattern in the convergence of the solution for transverse displacement since they have same order of approximation. But in the case of shear rotation, it can be seen from Figure 5.19 and Figure 5.21 that present finite element model converges to corresponding theoretical solution much faster than finite element

model of the FSBT. This could be due to use of hyperbolic function in the approximation of the finite element solution of the present theory and also due to the additional degrees of freedom of rotation which makes possible that the shear rotations estimated at the nodal points are also to be exact to the theoretical solution.

In addition, following points also can be noted related to the finite element solutions. Both the finite element models gives exact nodal values for transverse displacement regardless of discretisation of the member. But only the present finite element model gives the exact nodal values for shear rotation due to additional degree of freedom used for rotations.

The Figure 5.22 below show finite element solution for transverse displacement of thin beam (Example 1(c)) using the present finite element model.

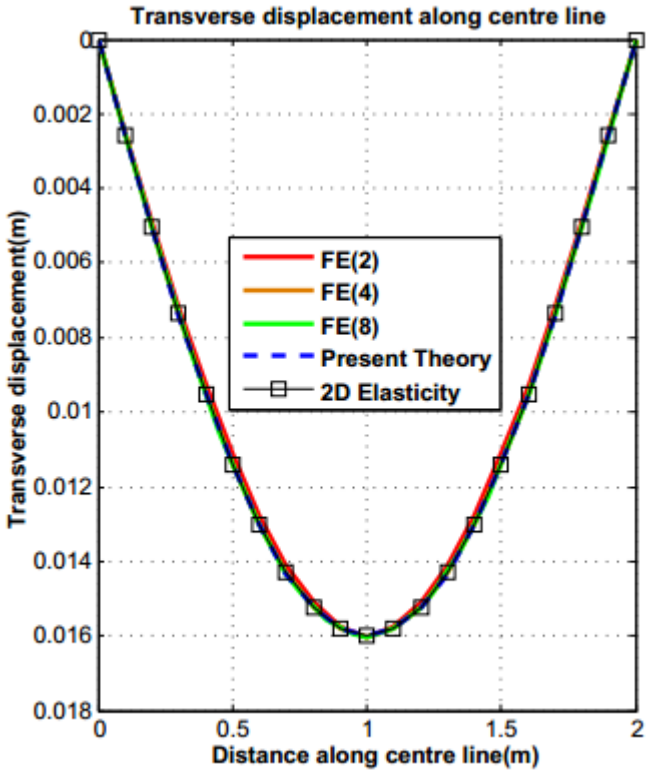

Figure 5.22-Transverse displacement along centre line using present FE for example 1(c)

Even with only two elements, finite element solution converges to exact analytical solutions of the corresponding theory. Since the approximations for primary

variables are interdependent and they represent homogeneous solution of the governing equations, here we do not have the problem of ‘Shear Locking’ when the beam becomes thin which was earlier found in the traditional formulation of the finite element models using FSBT [39]. However, since finite element model of EBT performs very well for the thin beams and it is much easier in applying to the thin beam problems, the present finite element model may not be desired in these instances.

In the following problems, solutions are compared against solution obtained from ‘ABAQUS’ software since the analytical solutions for this problems are not available. But before this comparison, the solutions from the ‘ABAQUS’ software is validated against analytical solutions of simply supported beam problems in example 1(a) and 1(b).

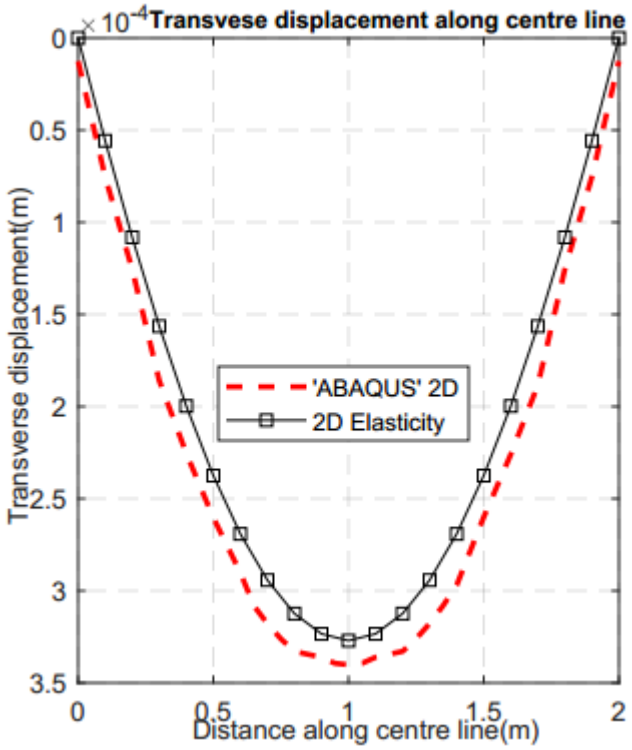

Figure 5.23- Transverse displacement along centre line using ABAQUS for example 1(a)

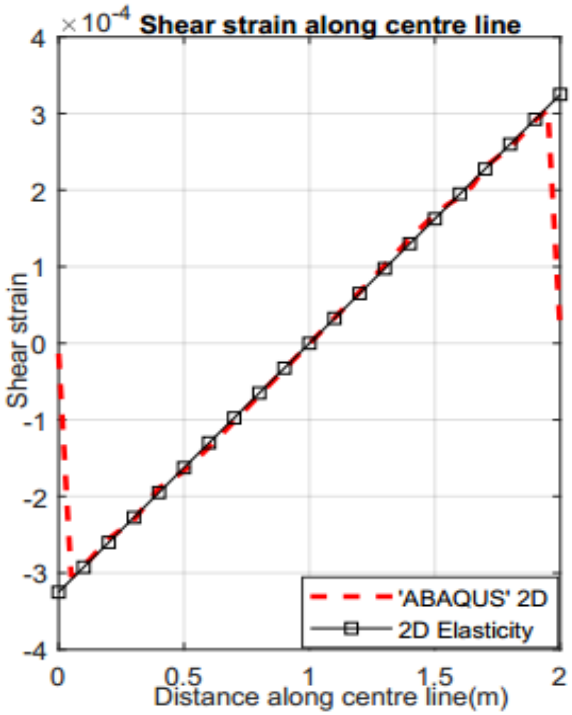

Figure 5.25- Shear strain along centre line using ABAQUS for example 1(a)

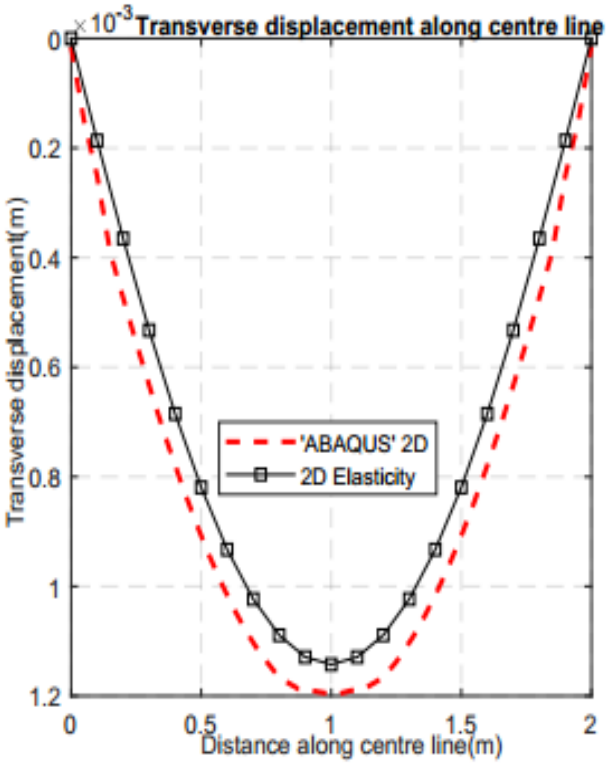

Figure 5.24- Transverse displacement along centre line using ABAQUS for example 1(b)

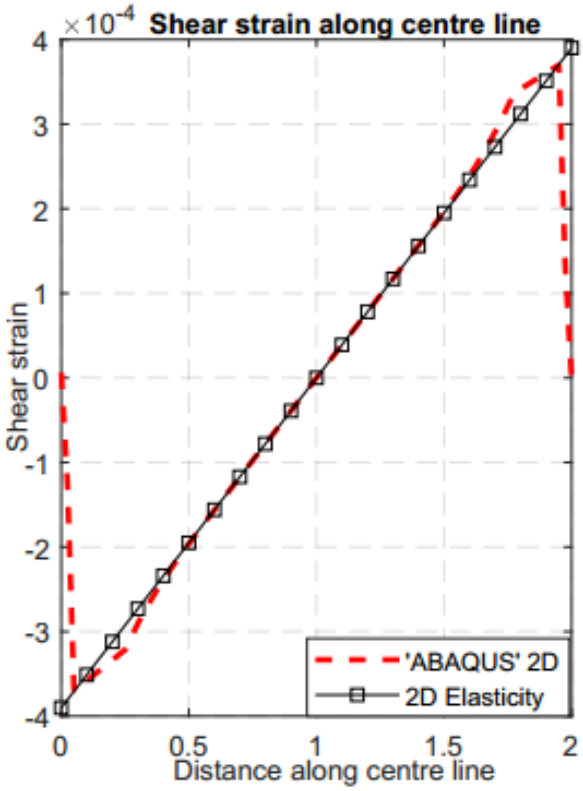

Figure 5.26- Shear strain along centre line using ABAQUS for example 1(b)

The comparison of displacements in Figure 5.23 to Figure 5.26, shows that solutions obtained from ‘ABAQUS’ are reasonable predictions. Therefore ABAQUS can be used for comparison against present beam element when the analytical solutions are not available.

Example 04

This problem is of a stepped beam shown in the Figure 5.23 below. The numerical data for this example are: $E = 2*10^8 N/m^2$ and Poisson's ratio $\upsilon = 0.3$. The beam discretised into 4, 6 and 14 elements in following manner.

Placing nodes at 0, 0.75m, 1.5m, 2.5m, 3.5m (4 elements)

Placing the nodes at 0, .75m, 1.5m, 2m, 2.5m, 3m and 3.5m distance from the fixed support (6 elements) and

Placing the nodes at 0.25m regular interval (14 elements)

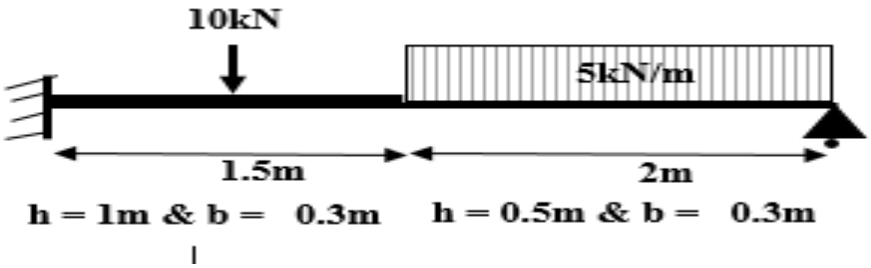

Figure 5.27-Stepped beam problem

Solutions obtained using the present finite element model is compared against the solutions obtained using the two dimensional solid model (CPS3 -3 node linear plane stress triangle) of 'ABAQUS'. This model uses approximately 2100 elements with the approximate element size of 0.05m (Figure 5.26). The results obtained for transverse displacement and shear rotation are presented in the Figure 5.24 and Figure 5.25

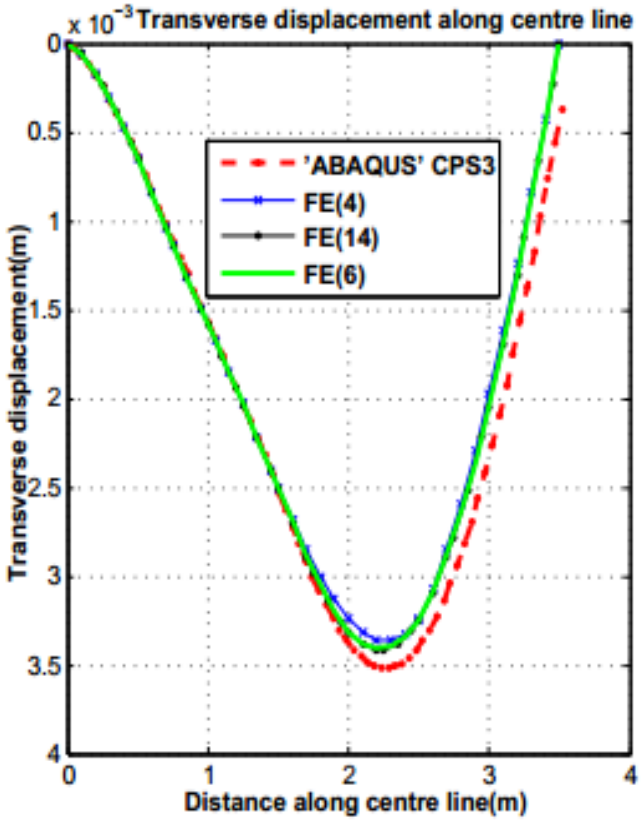

Figure 5.29 - Transverse displacement along centre line for example 4

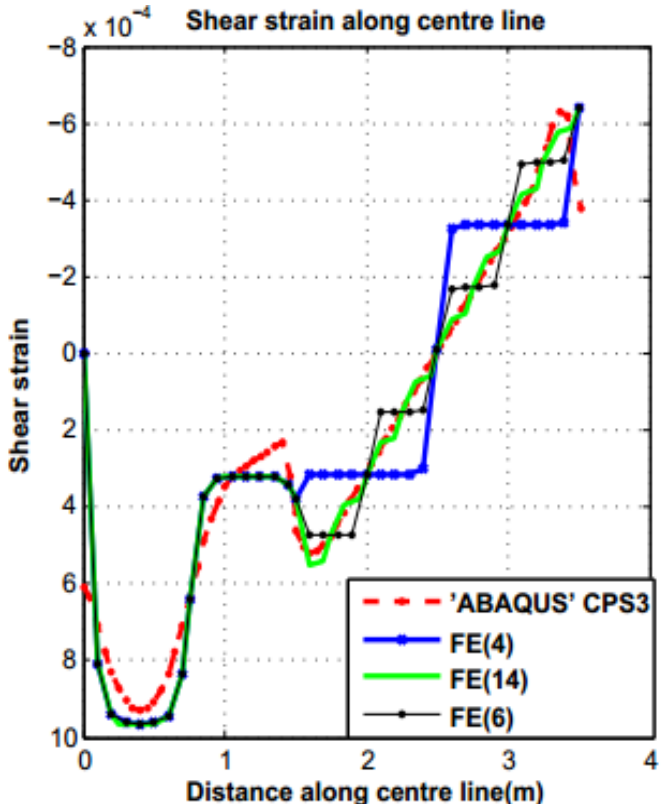

Figure 5.28 - Shear strain along centre line for example 4

Predicted results using the present finite element show close agreement with the results obtained using two dimensional model of 'ABAQUS'. As in the previous cases, there is no much improvement in the predicted transverse displacement when the number of elements are increased (Figure 5.24). But predicted shear strain variation converges to predicted results using 2D model when the number of elements is 14 (Figure 5.25). 2D model predicts maximum transverse displacement of 3.52mm at about 2.28m from the fixed support, whereas the present finite element predicts the maximum transverse displacement as 3.42mm at about 2.25m from the fixed support. However, predicted shear strain using the present finite element has the same trend with the predicted results from 2D model.

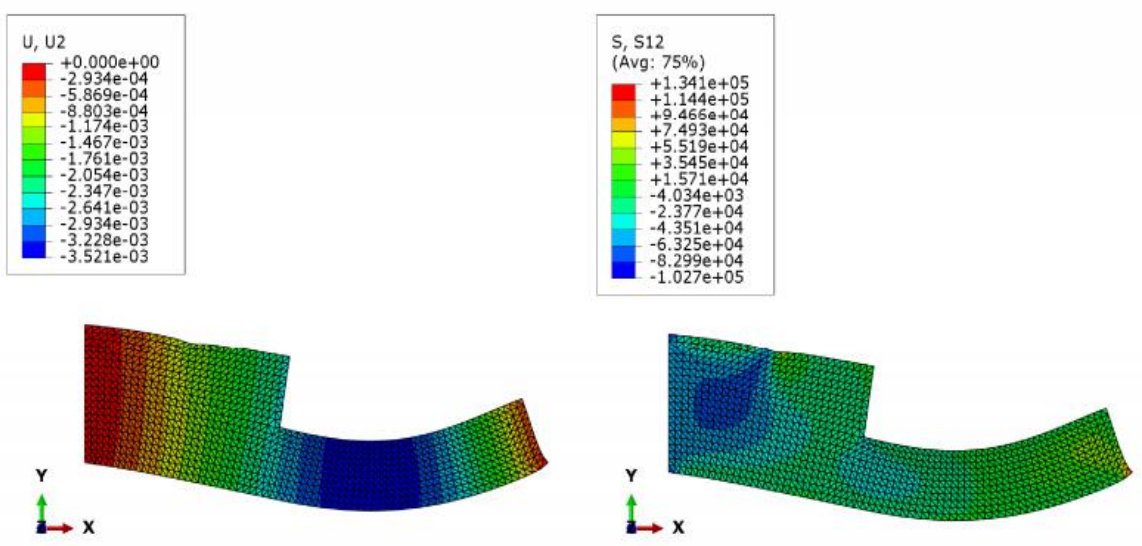

Figure 5.30 - Results for tranverse diplacement and shear strain uisng 'ABAQUS' 2D model

Example 05

This problem is of a thick isotropic continuous beam shown in Figure 5.27. The numerical data for this example are E = $2x10^8$ N/m^2, b = 0.3m, h = 1m and υ = 0.3. The beam is analysed using the present beam element and with a 3D solid model developed using 'ABAQUS' software. The 3D solid model uses 19212 number of 8-node linear brick elements (C3D8R) with the approximate mesh size of 0.05m. The beam is discretised into two different ways using the present finite element as follows

Placing the nodes at 0, 2m, 4m, 5.5m, 7m and 8m distance from the fixed support (5 elements).

Placing the nodes at 0.5m interval (16 elements)

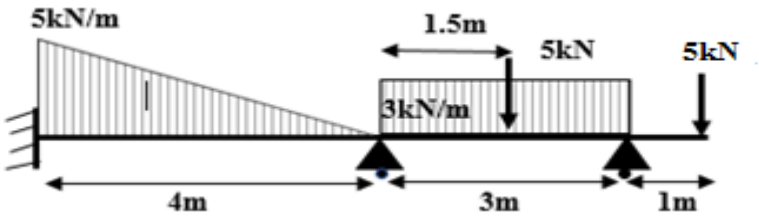

Figure 5.31- Continuos beam probelem

The results are shown in Figure 5.28 and Figure 5.29. It can be observed a good agreement between the results obtained using present finite element and 3D solid model. Although there is an improvement in the predicted transverse displacement when the number of present finite element is increased from 5 to 16, this doesn't make great impact on the results. The overall trend is the same as in both the discretizations. Predicted maximum transverse displacement between the spans and at tip of the cantilever are very close to each other. Predicted transverse displacements using the present finite element with 16 elements are 0.53mm, 0.61mm and 0.69mm at about 1.8m, 5.5m, and 8m respectively from the fixed support whereas 3D model predicts 0.56mm, 0.625mm and 0.706mm at about 1.8m, 5.45m and 8m respectively. It can be seen from Figure 5.30 that at the centre line above the supports, transverse displacements are not zero, while at the bottom fibres of the beam above the supports, displacements are zero. But it can't be captured by the present theory which assumes that transverse deflection of every coordinate in a cross section is equal to the transverse deflection at neutral axis. However it can be seen from the displacement contour map of 3D model in Figure 5.30, that this assumption is valid to a great extent.

Predicted shear strain values using present element with 16 elements has close agreement with the results of 3D model. Present finite element gives some ideas on effect of the shear in the isotropic beam which may be useful in the preliminary study.

However the 3D model in Figure 5.30, gives clear insight of shear effect in the beam. It clearly indicates the critical areas which are susceptible to shear concentration.

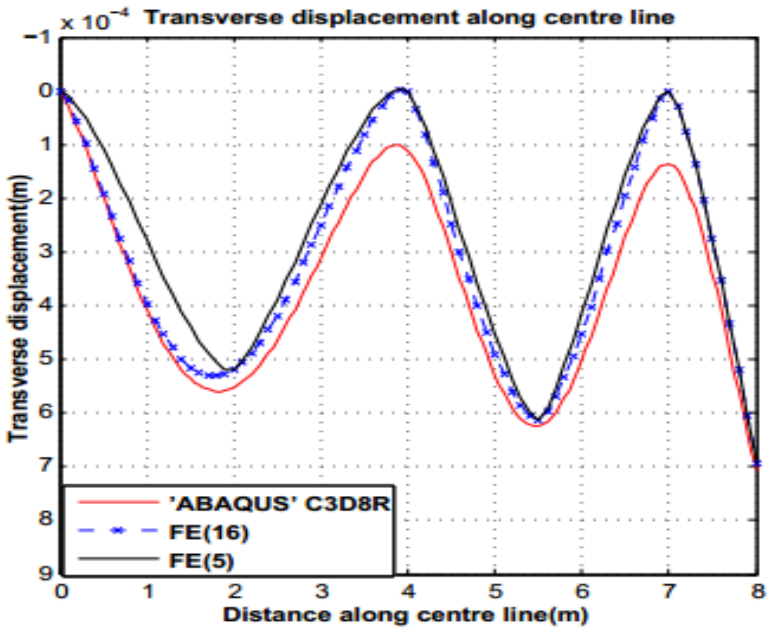

Figure 5.32 -Transverse displacement along centre line for example 5

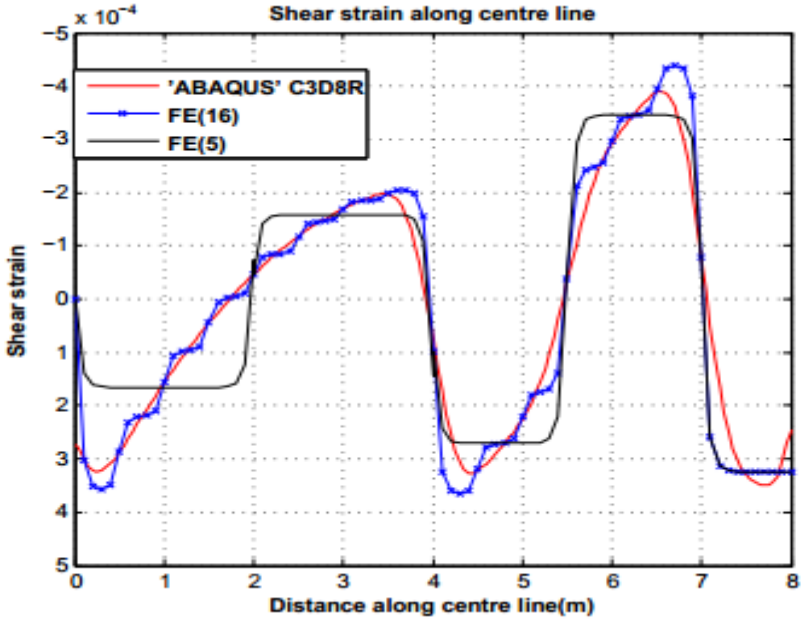

Figure 5.33 - Shear strain along centre line for example 5

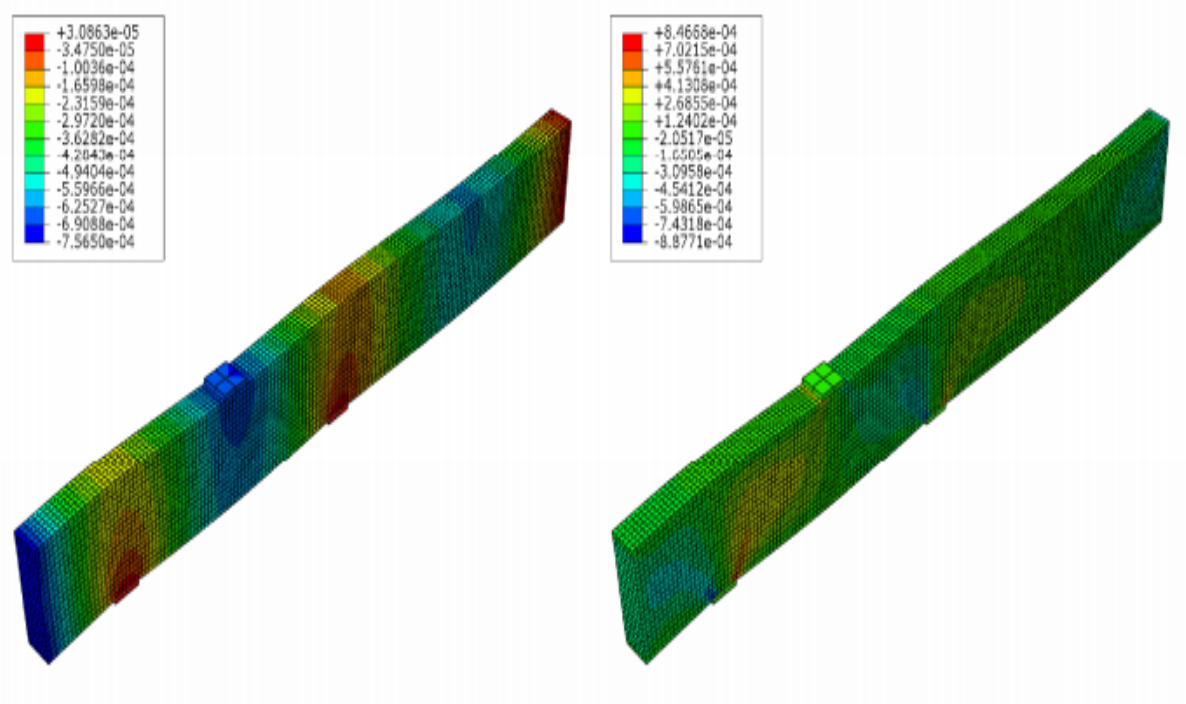

Figure 5.34 - Results for tranverse diplacement and shear strain uisng 'ABAQUS' 3D model

The Figure 5.32 below shows the axial stress variation of the deep beam. It can be seen from the figure that the neutral surface does not remain at centroidal axis. Comparing this with the result of thin beam in the Figure 5.31, the differences in the stress variation of the deep beam can be clearly identified. In elastic range of loading there could be multiple neutral axis in deep beam [55]. Also development compression strut between loading and support can also be seen from the Figure 5.32.

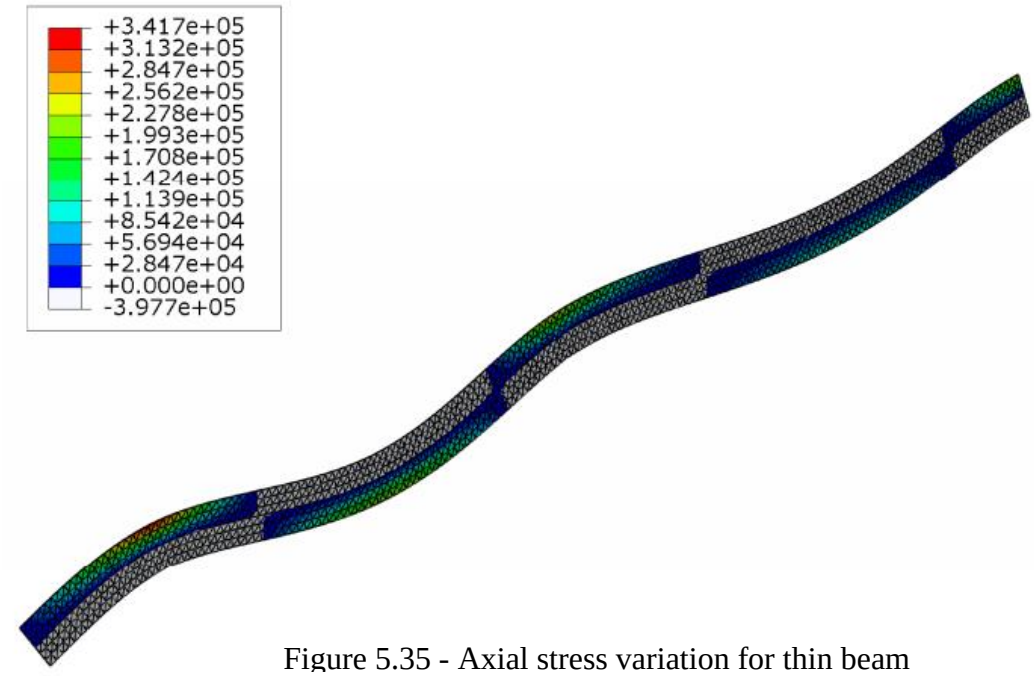

Figure 5.35 - Axial stress variation for thin beam

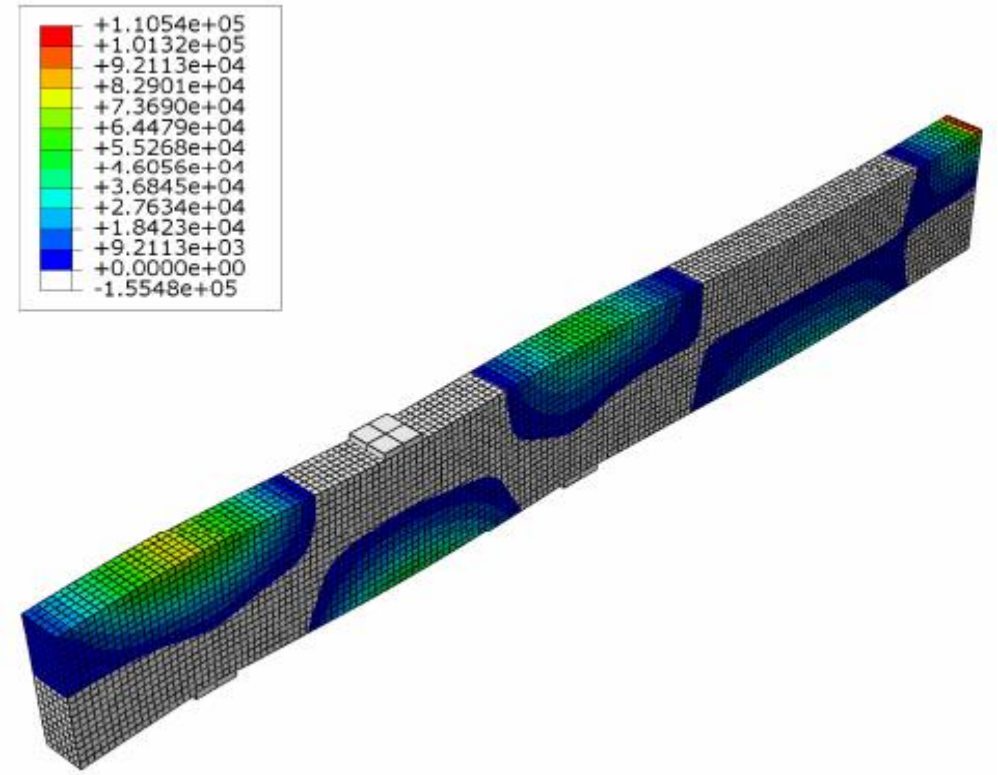

Figure 5.36 - Axial stress variation for deep beam

CHAPTER VI

6. CONCLUSIONS AND FUTURE WORKS

6.1. Conclusions

A hyperbolic shear deformation beam theory for analysing thick isotropic beam is presented here which gives parabolic shear stress variation across the thickness of the beam while satisfying shear boundary conditions at top and bottom of the beam. Also this theory does not need a shear correction factor. It can be observed from the study of beams with several aspect ratios using this theory that effect of shear rotation greatly contributes to transverse displacement of deep beams. Also this makes the shear stress to dominate over axial stress and the axial stress variation across depth of beam becomes nonlinear at lower aspect ratios although this is a linear elastic analysis. But these effects are diminished when the aspect ratio increases.

The characteristics of the present hyperbolic shear deformation theory are similar to that of HSBT and also this theory produces almost same values in the case of deformations and stresses. Also the present theory gives very close values to the solutions of two dimensional elastic theory.

The displacement based finite element model for this theory is obtained by approximating the primary variable using the homogeneous solution of the governing equilibrium equations. This enables the finite element model to give exact nodal displacement regardless of the discretization of the member. Also this exact formulation enables that finite element solutions converge much quicker to the corresponding analytical solutions of the proposed theory.

The solutions of the present finite element model for thick isotropic beam are compared with the solutions of 2D and 3D model of 'ABAQUS' software when the analytical solutions are not available for the problems. Present finite element solutions show good agreement with solutions of 2D and 3D models. This assures that present finite element is suitable for the preliminary analysis of deep isotropic beam.

The element stiffness of this beam element depends on number of additional parameters such as (L/h) ratio and Poisson's ratio (υ) compare to other beam elements

but these effects can be ignored for slender beams. Although this element is most suitable for analysing thick beams, it can be also used to analyse the thin beams without having the problem of shear locking. But in the case of very thin beams, stiffness matrix tends to be singular since the shear rotation is negligible. (i.e total rotation of the cross section is equal to the bending rotation of the cross section)

6.2. Future work

Present finite model is can only be used for uniform isotropic beam. However, in practice, we encounter various problems which have varying parameters. Extending this element to handle the axially varying parameters will provide more scope for this finite element in practical beam problems.

One of theoretical assumption of the present theory is neutral axis passes through the centroid of the section. But in the case of deep beams the assumption is not completely valid. This reduces the accuracy of stress distribution across the depth of the beam. More realistic way is to have arbitrary neutral surface in the case of deep beams.

This present finite element model is only applicable to linear elastic analysis. But for large displacement and rotations, geometric nonlinearities should be considered. Further, here material is assumed to be linear, but material could be non-linear elastic.

REFERENCES

[1] C. M. Wang, J. N. Reddy and K. H. Lee, “Shear deformable beam and plates -Relationship with classical solutions” Oxford: Elsevier Science Ltd, 2000.

[2] S. Timoshenko, “On the correction for shear of the differential equation for transverse vibrations of prismatic bars,” *Philosoph. Mag,* vol. 6, p. 742–746, 1921.

[3] M. Levinson, “A new rectangular beam theory,” J. Sound Vibration, vol. 74, no. 1, p. 81–87, 1981.

[4] W. B. Bickford, “ A consistent higher order beam theory,” *Development of Theoretical and Applied Mechanics, SECTAM,* vol. 11, pp. 137-150, 1982.

[5] J. N. Reddy, “A simple higher-order theory for laminated composite plates,” J. Appl. Mech, vol. 51, no. 4, p. 745–752, 1984.

[6] P. R. Heyliger and J. N. Reddy, “A higher order beam finite element for bending and vibration problems,” J. Sound Vibration, vol. 126, no. 2, p. 309–326, 1988.

[7] M. Touratier, “An efficient standard plate theory,” *Int. J. Eng. Sci.,* vol. 29, no. 8, p. 901–916, 1991.

[8] V. Z. Vlasov and U. N. Leont’ev, Beams, Plates and Shells on Elastic foundation, Jerusalem: (Translated from Russian) Israel Program for Scientific Translation Ltd, 1996.

[9] M. Stein, “Vibration of beams and plate strips with three-dimensional flexibility,” Transaction ASME Journal of Applied Mechanics, vol. 56, no. 1, p. 228–231, 1989.

[10] Y. M. Ghugal and R. P. Shimpi, “ A review of refined shear deformation theories for isotropic and anisotropic laminated beams,” Journal of Reinforced Plastics and Composites, vol. 21, p. 775–813, 2002.

[11] Y. M. Ghugal and R. Sharma, “A hyperbolic shear deformation theory for flexure and free vibration of thick beams,” Int. J. Comput. Methods, vol. 6, no. 4, p. 585–604, 2009.

[12] Eurocode 2: Design of concrete structures Part 1-1: General rules and rules for buildings NEN-EN-1992-1-1.

[13] ACI 318-08 “Building Code Requirements for Structural Concrete and Commentary”.

[14] R. Patel, S. K. Dubey and K. K. Pathak, “Effect of depth span ratio on the behaviour of the beams,” Int J Adv Struct Eng, vol. 56, no. 6, 2014.

[15] J. Bernoulli, “Problema novum ad cujus solutionem Mathematici invitantur,” (A new problem to whose solution mathematicians are invited.) *Acta Eruditorum* , 1696.

[16] A. Hrennikoff, “Solution of Problems in Elasticity by the Frame Work Method,” *Journal of Applied Mechanics,* vol. 8, no. 4, pp. 169-175, 1941.

[17] D. McHenry, “A Lattice Analogy for the Solution of Plane Stress Problems,” *Journal of Institution of Civil Engineers,* vol. 21, pp. 59-82, 1943.

[18] R. Courant, “Variational Methods for the Solution of Problems of Equilibrium and Vibrations,” *Bulletin of the American Mathematical Society,* vol. 49, pp. 1-23, 1943.

[19] S. Levy, “Computation of Influence Coefficients for Aircraft Structures with Discontinuities and Sweepback,” *Journal of Aeronautical Sciences,* vol. 14, no. 10, pp. 547-560, 1947.

[20] S. Levy, “Structural Analysis and Influence Coefficients for Delta Wings,” *Journal of Aeronautical Sciences,* vol. 20, no. 7, pp. 449-454, 1953.

[21] J. H. Argyris and S. Kelsey, Energy Theorems and Structural Analysis, London: Butterworths,, 1960.

[22] M. J. Turner, R. W. Clough, H. C. Martin and L. J. Topp, “Stiffness and Deflection Analysis of Complex Structures,” *Journal of Aeronautical Sciences,* vol. 23, no. 9, p. 805–824, 1956.

[23] R. W. Clough, “The Finite Element Method in Plane Stress Analysis,” in *Proceedings,American Society of Civil Engineers, 2nd Conference on Electronic Computation*, Pittsburgh, 1960.

[24] R. J. Melosh, “A Stiffness Matrix for the Analysis of Thin Plates in Bending,” *Journal of the Aerospace Sciences,* vol. 28, no. 1, pp. 34-42, 1961.

[25] P. E. Grafton and D. R. Strome, “Analysis of Axisymmetric Shells by the Direct Stiffness Method,” *Journal of the American Institute of Aeronautics and Astronautics,* vol. 1, no. 10, p. 2342–2347, 1963.

[26] H. C. Martin, “Plane Elasticity Problems and the Direct Stiffness Method,” *The Trend in Engineering,* vol. 13, pp. 5-19, 1961.

[27] R. H. P. J. Gallagher and P. P. Bijlaard, “Stress Analysis of Heated Complex,” *Journal of the American Rocket Society,* vol. 32, pp. 700-707, 1962.

[28] R. J. Melosh, “Structural Analysis of Solids,” *Journal of the Structural Division, Proceedings of the American Society of Civil Engineers,* pp. 205-223, 1963.

[29] J. H. Argyris, “Recent Advances in Matrix Methods of Structural Analysis,” *Progress in Aeronautical Science,* vol. 4, 1964.

[30] R. W. Clough and Y. Rashid, “Finite Element Analysis of Axisymmetric Solids,” *Journal of the Engineering Mechanics Division, Proceedings of the American Society of Civil Engineers,* vol. 91, p. 71–85, 1965.

[31] E. L. Wilson, “Structural Analysis of Axisymmetric Solids,” *Journal of the American Institute of Aeronautics and Astronautics,* vol. 3, no. 12, p. 2269–2274, 1965.

[32] J. S. Archer, “Consistent Matrix Formulations for Structural Analysis Using FiniteElement Techniques,” *Journal of the American Institute of Aeronautics and Astronautics,* vol. 3, no. 10, p. 1910–1918, 1965.

[33] B. A. Szabo and G. C. Lee, “Derivation of Stiffness Matrices for Problems in Plane Elasticity by Galerkin’s Method,” *International Journal of Numerical Methods in Engineering,* vol. 1, p. 301–310, 1969.

[34] O. C. Zienkiewicz and C. J. Parekh, “Transient Field Problems: Two-Dimensional and Three-Dimensional Analysis by Isoparametric Finite Elements,” *International Journal of Numerical Methods in Engineering,* vol. 2, no. 1, p. 61–71, 1970.

[35] G. R. Cowper, “The shear coefficient in Timoshenko’s beam theory,” *ASME J. appl. Mech.,* vol. 33, pp. 335-340 , 1966.

[36] G. R. Cowper, “On the accuracy of Timoshenko’s beam theory,” *ASCE Journal of Engineering Mechanics Division,* vol. 94, no. 6, 1968.

[37] H. Darijani and H. Mohammadabadi, “A new deformation beam theory for static and dynamic analysis of microbeams,” *International journal of mechanical sciences,* vol. 89, pp. 31-39, 2014.

[38] R. J.N., An Introduction to the Finite Element Method, New York: McGraw-Hill, 1993.

[39] R. J.N, “On locking-free shear deformable beam finite elements,” *Comput. Methods Appl. Mech. Engrg.,* vol. 149, pp. 113-132, 1997.

[40] R. B. McCalley, “Rotatory Inertia Correction for Mass Matrices,” General Electric Knolls Atomic Power Laboratory, Schenectady, NY, 1963.

[41] T. J. Hughes, R. Taylor and W. Kanoknukulchoii, “A simple and efficient plate element for bending,” *Int. J. Numer. Meth. Engng,* vol. 11, pp. 1529-1543, 1977.

[42] T. Kant and A. Gupta, “A finite element model for a higher order shear deformable beam theory,” *Journal of Sound and Vibration,* vol. 125, no. 2, pp. 193-202, 1988.

[43] J. Petrolito, “Stiffness analysis of beams using higher-order theory,” *Coput.Structures,* vol. 55, no. 1, p. 33–39, 1995.

[44] M. Eisenberger, “An exact high order beam element,” *Coput.Structures,* vol. 81, p. 147–152, 2003.

[45] Y. Liu, “A beam element using Touratier theory,” *Int.J.Comput.Methods Eeng. Sci.Mech,* vol. 11, p. 142–145, 2010.

[46] K. P. Soldatos, “A transverse shear deformation theory for homogeneous monoclinic plates,” *Acta Mech,* vol. 94, no. 3, p. 195–220, 1992.

[47] J. N. Reddy, “Unified finite elements based on the classical and shear deformation theories of beams and axisymmetric circular plates,” *Commun. Numer. Methods Engrg.,* 1997.

[48] J. N. Reddy, “Exact relationships between the bending solutions of the Euler-Bernoulli beam theory and shear deformable beam theories,” *Int. J. Solids Struct.,* 1997.

[49] L. G. R. and Y. T. Gu, An Inroduction to MeshFree Methods and Their Progamming, Dordrecht: Springer, 2005.

[50] P. Seshu, Textbook of Finite Element Analysis, New Delhi: PHI Learning, 2012.

[51] S. S. Bhavikatti, Finite Element Analysis, New Delhi: New Age International, 2005.

[52] O. C. Zienkiewicz and R. L. Taylor, The Finite Element Method-Volume 1: The Basis, Oxford: Butterworth-Heinemann, 2000.

[53] S. P. Timoshenko and J. N. Goodier, Theory of Elasticity, Singapore: McGraw-Hill, 1970.

[54] K. Amar, Introduction to Finite Element Analysis Using MATLAB and ABAQUS, Boca Raton: CRC Press, 2013.

[55] M. Mohammad, M. Z. Bin Jumaat, M. Chemrouk, A. Ghasemi, S. J. S. Hakim, and R. Najmeh, “An experimental investigation of the stress-strain distribution in high strength concrete deep beams,” *Procedia Eng.*, vol. 14, pp. 2141–2150, 2011.

APPENDIX A

A.1. MATLAB program for stiffness matrix

```
syms A L D  E I G h W v V R q; % symbolic variables
syms x;


IM=eye(6,6);
IM2=eye(3,3);

U=1/(cosh(0.5)-1);
Ao=0.1024*U;
Bo=0.01061*U^2;
Co=(8.7385*10^-3)*U^2;

V=W*h; %V-cross sectional area, W-width, h-depth
R=(E*I)/(G*V); %elastic modulus, I-second moment of area, G-shear
modulus
A = (71.3945/R)^0.5;

W=12*I/h^3;

G=E/(2*(1+v));

B=[0,1,0,0,0,1;
    -A 0 0 0 -1 0;
    0.2463*A,0,-8.9728*R,0,-1,0;
    sinh(A*L),cosh(A*L),L^3,L^2,L,1;
    -A*cosh(A*L),-A*sinh(A*L),-3*L^2,-2*L,-1,0;
    0.2463*A*cosh(A*L),0.2463*A*sinh(A*L),-8.9728*R-3*L^2,-2*L,-
1,0];

D=(12463*A*L^3*sinh(A*L) + 179456*A*R*L*sinh(A*L) + 358912*R-
358912*R*cosh(A*L));

C=B\IM;

%display(C);

A1=[sinh(A*x),cosh(A*x),x^3,x^2,x,1];
A2= [0.2463*A*cosh(A*x),0.2463*A*sinh(A*x),-8.9728*R-3*x^2,-2*x,-
1,0];

N1= A1*C;% N1 & N2 are shape functtion matrices
N2= A2*C;
%display(N1);
%display(N2);


dN1 =diff(N1,x);
%display(dN1);
```

```
dN2 = diff(N2,x);
%display(dN2);
ddN1=diff(dN1,x);
%display(ddN1);
K1=sym('K1',6);K2=sym('K2',6);K=sym('K',6);K4=sym('K4',6);
%K(1,1)=1;
for i= 1:1:6
    for j=1:1:6
K1(i,j) = int((E*I/R*Co*dN1(i)*dN1(j)+(Bo+1-
2*Ao)*E*I*ddN1(i)*ddN1(j)),x,0,L);
   end;
end;
for i= 1:1:6
   for j=1:1:6

K2(i,j) = int((E*I/R*Co*dN1(i)*N2(j)-(Ao-
Bo)*E*I*ddN1(i)*dN2(j)),x,0,L);
   end;
end;
%for i= 1:1:6
    %for j=1:1:6
%K3(i,j) = int((G*V*Co*dN1(i)*N2(j)-(Ao-
Bo)*E*I*ddN1(i)*dN2(j)),x,0,L);
  %end;
%end;
for i= 1:1:6
   for j=1:1:6
K4(i,j) = int((E*I/R*Co*N2(i)*N2(j)+ Bo*E*I*dN2(i)*dN2(j)),x,0,L);
   end;
end;
K=(K1+K2+transpose(K2)+K4);
simplify(K);
display(K);

for r=1:1:6
Q(r)= q*int(N1(r),x,0,L); %Q is load vestor for uniformly distriuted
load q
end;
```

A.2. MATLAB program to analyse the general beam problem

beam_main.m

```
% beam_main.m
%
% LINEAR STATIC ANALYSIS OF A CONTINUOUS BEAM
%
clc % Clear screen
clear % Clear all variables in memory
%
% variables are declared as global so that they can be shared
% by other functions in the same project
%
global nond noel none nodof eldof n geomco connect F q ...
propt nf El_loads Jt_loads force nd_disp
%
display('Executing beam program.m');
%
% Open file for output of results
%
display('Results printed to file : beam_results.txt ');
fid_r=fopen('beam_results.txt','w');
%
%
% Choosing the data for analysis
%
beam_data % load beam data from the input file
%
%
KK =zeros(n) ; % Initialize global stiffness
% matrix to zero
%
F=zeros(n,1); % Initialize global force vector to zero
F = form_beamF(F); % Form global force vector

%
%
for i=1:nel
 kl=beamk(i); % Form element matrix
%
g=beamg(i) ; % Retrieve the element steering
% vector
%
KK =formKK(KK, kl,g); % assemble global stiffness
% matrix
%
end
display(KK);
%
%%%%%%%%%%%% End of assembly %%%%%%%%%%%
%
%
 delta = KK\F ; % solve for unknown primary variables
%
% Get nodal displacements at each node
%
```

```
for i=1:nond
    for j=1:nodof
        nd_disp(i,j) = 0;
        if nf(i,j)~= 0;
            nd_disp(i,j) = delta(nf(i,j)) ;
        end
    end
end
%
% Calculate the forces acting on each element
% in local coordinates, and store them in the
% vector force().
%
display(nd_disp);
for i=1:noel
    kl=beamk(i); % Form element stiffness matrix
    g=beamg(i) ; % Retrieve the element steering vector
    for j=1:eldof
            if g(j)==0
                ed(j)= 0.; % displacement = 0.for restrained freedom
            else
                ed(j) = delta(g(j));
            end
    end
    fl=kl*ed';% Element force vector in global XY
    f0 = El_loads(i,:);
    force(:,i) = fl-f0';

end
%
print_beam_results;
%
fclose(fid_r);
%deformed_shape;
%shearstrain;
```

beam_data.m

```
% File: beam_data.m
%
%
global nond noel none nodof eldof n geomco connect F q ...
propt nf El_loads Jt_loads force nd_disp %

format short e
%
%%%%%%%%%%%%%%% Beginning of data input %%%%%%%%%%%%%%%%
nond = 17; % Number of nodes in the member:
noel = 16; % Number of elements in the member:
none=2;%Number of nodes per element:
nodof =3 ; % Number of degrees of freedom per node
eldof = none*nodof; % calculate  degrees of freedom per element
%
q=zeros(nel,2); %uniformly distributed load
q=[-2500/2,5000;....
```

```
    -2500/2,4375;...
    -2500/2,3750;....
    -2500/2,3125;
    -2500/2,2500;....
    -2500/2,1875;
    -2500/2,1250;....
    -2500/2,625;
    0 3000;....
    0 3000;....
    0 3000;....
    0 3000;....
    0 3000;....
    0 3000;....
    0 0;...
    0 0];
% Nodes coordinates X
geomco=zeros(nnd,1);
geomco= [ 0,0.5,1,1.5,2,2.5,3,3.5,4,4.5,5,5.5,6,6.5,7,7.5,8]; ... %

%
% Element connectivity
%
connect=zeros(nel,2);
connect = [1 2;2 3;3 4;4 5;5 6;6 7;7 8;8 9;9 10;10 11;11 12;12 13;13
14;14 15;15 16;16 17] ;

%
% properties of the element <Elastic Modulus,Width of beam,Depth of
%beam>
%
%
propt=zeros(nel,3);
propt = [2*10^8 0.3 1;....
    2*10^8 0.3 1;....
    2*10^8 0.3 1;...
    2*10^8 0.3 1;....
    2*10^8 0.3 1;....
    2*10^8 0.3 1;...
    2*10^8 0.3 1;....
    2*10^8 0.3 1;....
    2*10^8 0.3 1;....
    2*10^8 0.3 1;...
    2*10^8 0.3 1;....
    2*10^8 0.3 1;....
    2*10^8 0.3 1;....
    2*10^8 0.3 1;...
    2*10^8 0.3 1];
%
%Applying the boundary conditions
%
nf = ones(nond, nodof); % Initialize the matrix nf to 1
nf(1,1) = 0;nf(1,2)=0;nf(1,3)=0; % Prescribed nodal freedom of node
nf(9,1) = 0;
nf(15,1)=0;
%
% Counting of the free degrees of freedom
```

```
%
n=0;
for i=1:nond
    for j=1:nodof
        if nf(i,j) ~= 0
            n=n+1;
            nf(i,j)=n;
        end
    end
end
%
%
%%
% loading
%
Jt_loads= zeros(nond, 3);
Jt_loads=[0,0,0;0,0,0;0,0,0;0,0,0;0,0,0;0,0,0;0,0,0;0,0,0;0,0,0;0,0,0;0,0,
0;0,0,0;5000,0,0;0,0,0;0,0,0;0,0,0;0,0,0;0,0,0;20000,0,0];

%Enter the external Moment components and Loads applied on the nodes

El_loads= zeros(nel,6);
for i=1:nel
    El_loads(i,:)= beaml(i);
end



%
%%%%%%%%%%%%%%%%%% End of data input for member %%%%%%%%%%%%


function[g] = beamg(i)
%
% This function forms the steering vector for element i
%
global connect nf
%
% get the nodes of element i
%
node1=connect(i,1);
node2=connect(i,2);
%
%
g=[nf(node1,1); nf(node1,2);nf(node1,3);
nf(node2,1);nf(node2,2);nf(node2,3)];

%%%%%%%%%%%%%% end function beamg %%%%%%%%%%
```

beamk

```
function[kl] = beamk(i)
%
% Creating the element stiffness matrix in local coordinates
%
global nond noel none nodof eldof
```

```
global geomco connect propt nf load
%
% retrieve the nodes of element i
%
node1=connect(i,1);
node2=connect(i,2);
%
%
% Retrieve the x and y coordinates of nodes 1 and 2
%
x1=geomco(node1); x2=geomco(node2);
%
% calculate length of element i from the coordinates
%
L = abs(x2-x1);
%

% Get section properties of element i
%
b=propt(i,2);
h=propt(i,3);
A=18.0166/h;
I=b*h^3/12;
E = propt(i,1);
%
%Get numerical value for stiffness terms
%
D =(1.2463*A*L^3 + 1.2623*10^3*L/A-2.5246*10^3/A^2);
S11 = (2*E*I*(9.3196*A^2*L^3 + 9.4384*10^3*L - 1.8877*10^4/A))/D^2 ;
S12 = -(2*E*I*(9.2103*10^-
1*A^2*L^4+7.4775*A*L^3+9.3278*10^2*L^2+5.7074*10^3*L/A -
1.5146*10^4/A^2))/D^2 ;

S23 = (2*E*I*(-5.92380*10^-3*A^3*L^7+4.9266*10^-1*A^2*L^6 -
9.7381*A*L^5+ 6.4168*10^2*L^4-(5.0338*10^3*L^3)/A +(1.39980*10^5
*L^2)/A^2 -(5.17480*10^5*L)/A^3 +5.05330*10^5/A^4 ))/(D^2*L) ;

S13 = (2*E*I*(-3.7388*A^2*L^4 +7.4775*A*L^3-
3.7864*10^3*L^2+1.5146*10^4*L/A-1.5146*10^4/A^2))/D^2 ;

S22 = (2*E*I*(5.9238*10^-3*A^3*L^7+ 1.2136*10^-1*A^2*L^6
+1.3477*10^1*A*L^5 +1.3564*10^2*L^4+ (7.2656*10^3*L^3)/A+
(9.8995*10^3*L^2)/A^2-(1.1233*10^5*L)/A^3 +
1.2449*10^5/A^4))/(D^2*L) ;

S25 = (2*E*I*(6.0682*10^-2*A^2*L^6 + 1.478*A*L^5+36.727*L^4+
(1.4354*10^3*L^3)/A -(2.8039*10^4*L^2)/A^2 +(1.1233*10^5*L)/A^3 -
1.2449*10^5/A^4))/(D^2*L) ;

S26 = (2*E*I*(2.4633*10^-1*A^2*L^6 +2.2608*A*L^5 +1.1873*10^2*L^4+
(2.0402*10^3*L^3)/A -1.3699*10^5*L^2/A^2+5.17480*10^5*L/A^3-
5.0533*10^5/A^4))/(D^2*L);

S33 = (2*E*I*(5.9238*10^-3*A^3*L^7+1.9998*A^2*L^6 +5.9993*A*L^5 +
2.5137*10^3*L^4-5.0634*10^3*L^3/A + (5.0674*10^5*L^2)/A^2 -
(2.0391*10^6*L)/A^3+2.0513*10^6/A^4))/(D^2*L);
```

```
S36= - (2*E*I*(-9.9992*10^-1*A^2*L^6 +5.9996*A*L^5-5.1232*10^2*L^4+
(7.0887*L^3*10^3)/A + (4.9459*10^5*L^2)/A^2 -
(2.0391*10^6*L)/A^3+2.0513*10^6/A^4))/(D^2*L);

S44=S11;
S14=-S11;
S41=-S11;

S15=S12;
S24=-S12;
S45=-S12;
S21=S12;
S51=S12;
S42=-S12;
S54=-S12;

S16=S13;
S34=-S13;
S46=-S13;
S31=S13;
S61=S13;
S43=-S13;
S64=-S13;

S56=S23;
S32=S23;
S65=S23;

S55=S22;

S52=S25;

S35=S26;
S62=S26;
S53=S26;

S66=S33;

S63=S36;

%Element stiffness matrix for element i
kl=[S11,S12,S13,S14,S15,S16;
    S21,S22,S23,S24,S25,S26;
    S31,S32,S33,S34,S35,S36;
    S41,S42,S43,S44,S45,S46;
    S51,S52,S53,S54,S55,S56;
    S61,S62,S63,S64,S65,S66];
%
% Endfunction beamk
```

beaml

```
function[Ele_loads] = beaml(i)

% get the nodes of element i
%
global connect geomco propt q
syms x
node1=connect(i,1);
node2=connect(i,2);
%
%
x1=geomco(node1); x2=geomco(node2);
%
% Calculating  length of element i from the coordinate
%
L = abs(x2-x1);
%

% get section properties of element i
%
h=propt(i,3);
A=18.0166/h;
T=q(i,1);
LD1=[T/A^2 + (L^2*T)/4 - (26983223*A^3*L^3*T +
(62315*A^5*L^5*T)/2)/(- 640119552*A^2*coth(A*L) + 311575*A^5*L^3 +
320059776*A^3*L),.....
    -(L*T*(- 1576614456576*coth(A*L) + 65692269024*A^3*L^3 +
51160615*A^5*L^5 - 2412290531712*A*L +
797865343904*A^2*L^2*coth(A*L) +
934725000*A^4*L^4*coth(A*L)))/(24926*A^2*(311575*A^3*L^3-
640119552*coth(A*L) + 320059776*A*L )),.....
    (2500*L*T*(3840717312*coth(A*L) - 160029888*A^3*L^3 -
124630*A^5*L^5 - 3840717312*A*L + 1276500204*A^2*L^2*coth(A*L) +
560835*A^4*L^4*coth(A*L)))/(37389*A^2*(311575*A^3*L^3 -
640119552*coth(A*L) + 320059776*A*L)),.....
    (L^2*T)/4 - T/A^2 + (26983223*A^3*L^3*T + (62315*A^5*L^5*T)/2)/(
- 640119552*A^2*coth(A*L) + 311575*A^5*L^3 + 320059776*A^3*L),....
    (L*T*(28758010993152*coth(A*L)+ 118921538048*A^3*L^3 +
153481845*A^5*L^5 - 20780201016576*A*L +
4279926680000*A^2*L^2*coth(A*L) +
4362050000*A^4*L^4*coth(A*L)))/(49852*A^2*(311575*A^3*L^3 -
640119552*coth(A*L) + 320059776*A*L)),.....
    -(2500*L*T*(1280239104*coth(A*L)  - 54589596*A^3*L^3 -
62315*A^5*L^5 - 1280239104*A*L + 427992668*A^2*L^2*coth(A*L) +
436205*A^4*L^4*coth(A*L)))/(12463*A^2*(311575*A^3*L^3 -
640119552*coth(A*L) + 320059776*A*L))];

LD2=[ (L*q(i,2))/2,-q(i,2)*((821*A^2*L^2 + 20000*A*L -
40000)/(49852*A^2) ),-q(i,2)*((2500*A^2*L^2 - 15000*A*L +
30000)/(37389*A^2)),(L*q(i,2))/2,q(i,2)*((821*A^2*L^2 + 20000*A*L -
40000)/(49852*A^2)),q(i,2)*((2500*A^2*L^2 - 15000*A*L +
30000)/(37389*A^2))];

El_loads=LD1+LD2;
display(El_loads);
```

```
% End of function beaml
```

form_beamF

```
function[F] = form_beamF(F)
%
% Getting  the global force vector
%
global nond nodof noel eldof
global nf El_loads Jt_loads
%
for i=1:nond
    for j=1:nodof
        if nf(i,j)~= 0
        F(nf(i,j)) = Jt_loads(i,j);
        end
    end
end
%
%
for i=1:noel
    g=beamg(i) ; % Get element steering vector
        for j=1:eldof
            if g(j)~= 0
            F(g(j))= F(g(j)) + El_loads(i,j);
            end
        end
end
%%%%%%%% End of function form_beamF %%%%%%%%
```

formKK

```
function[KK]= formKK(KK, kg, g)
%
% assembling the global stiffness matrix
%
global eldof
%
%
for i=1:eldof
    if g(i) ~= 0
     for j=1: eldof
         if g(j) ~= 0
             KK(g(i),g(j))= KK(g(i),g(j)) + kg(i,j);
         end
     end
    end
end
%
%%%%%%%%%%%% end function form_KK %%%%%%%%%%%%


%
```

deflection.m

```
global nond noel none nodof eldof n geomco connect F q ...
propt nf El_loads Jt_loads force nd_disp
syms x;
fid3=fopen('deflection.txt','w');
%
%
for i=1:1:noel
    node1=i;node2=i+1;
    x1=geomco(node1); x2=geomco(node2);
%
% calculating the length of element i
%
    L = abs(x2-x1);
    h=propt(i,3);
    R=0.2167*h^2;
    A=18.0166/h;
    IM=eye(6,6);


  B=[0,1,0,0,0,1;
    -A 0 0 0 -1 0;
    0.2463*A,0,-8.9728*R,0,-1,0;
      sinh(A*L),cosh(A*L),L^3,L^2,L,1;
      -A*cosh(A*L),-A*sinh(A*L),-3*L^2,-2*L,-1,0;
      0.2463*A*cosh(A*L),0.2463*A*sinh(A*L),-8.9728*R-3*L^2,-2*L,-
      1,0];
C1=B\IM;

C=simplify(C1);
   format long
     y=0:0.1:L;
    A1=[sinh(A*y),cosh(A*y),y.^3,y.^2,y,1];
    A2= [0.2463*A*cosh(A*y),0.2463*A*sinh(A*y),-8.9728*R-3*y.^2,-
2*y,-1,0];
    A3=[A*cosh(A*y),A*sinh(A*y),3*y.^2,2*y,1,0];
    N1=
sinh(A*y)*C(1,1)+cosh(A*y)*C(2,1)+y.^3*C(3,1)+y.^2*C(4,1)+y*C(5,1)+C
(6,1);
    N2=
sinh(A*y)*C(1,2)+cosh(A*y)*C(2,2)+y.^3*C(3,2)+y.^2*C(4,2)+y*C(5,2)+C
(6,2);
    N3=
sinh(A*y)*C(1,3)+cosh(A*y)*C(2,3)+y.^3*C(3,3)+y.^2*C(4,3)+y*C(5,3)+C
(6,3);
    N4=
sinh(A*y)*C(1,4)+cosh(A*y)*C(2,4)+y.^3*C(3,4)+y.^2*C(4,4)+y*C(5,4)+C
(6,4);
    N5=
sinh(A*y)*C(1,5)+cosh(A*y)*C(2,5)+y.^3*C(3,5)+y.^2*C(4,5)+y*C(5,5)+C
(6,5);
    N6=
sinh(A*y)*C(1,6)+cosh(A*y)*C(2,6)+y.^3*C(3,6)+y.^2*C(4,6)+y*C(5,6)+C
(6,6);
```

```
    fn = -
(nd_disp(i,1)*N1+nd_disp(i,2)*N2+nd_disp(i,3)*N3+nd_disp(i+1,1)*N4+n
d_disp(i+1,2)*N5+nd_disp(i+1,3)*N6);
    %display(fn);

       x=x1+y;
  for i=1:1:6
    fprintf(fid3,' %8.8f\t %8.8f\r\n',x(i),fn(i));
  end
    plot(x,fn);
    hold on;
end
hold off;

%%%%End of deflection.m %%%%%%
```

shearstrain.m

```
global nond noel none nodof eldof n geomco connect F q ...
propt nf El_loads Jt_loads force nd_disp
syms x;
fid2=fopen('shearstrain.txt','w');
%fprintf(fid2, 'Disatance\t\t strain\r\n');
for i=1:1:noel
    node1=i;node2=i+1;
    x1=geomco(node1); x2=geomco(node2);
%
% calculating the length of element i
%
    L = abs(x2-x1);
    h=propt(i,3);
    R=0.2167*h^2;
    A=18.0166/h;
    %D=(12463*A*L^3*sinh(A*L) + 179456*A*R*L*sinh(A*L) + 358912*R-
358912*R*cosh(A*L));
    IM=eye(6,6);


 B=[0,1,0,0,0,1;
    -A 0 0 0 -1 0;
    0.2463*A,0,-8.9728*R,0,-1,0;
sinh(A*L),cosh(A*L),L^3,L^2,L,1;
-A*cosh(A*L),-A*sinh(A*L),-3*L^2,-2*L,-1,0;
0.2463*A*cosh(A*L),0.2463*A*sinh(A*L),-8.9728*R-3*L^2,-2*L,-1,0];
C1=B\IM;

C=simplify(C1);
   format long
     y=0:0.1:L;
    A1=[sinh(A*y),cosh(A*y),y.^3,y.^2,y,1];
    A2= [0.2463*A*cosh(A*y),0.2463*A*sinh(A*y),-8.9728*R-3*y.^2,-
2*y,-1,0];
    A3=[A*cosh(A*y),A*sinh(A*y),3*y.^2,2*y,1,0];
```

```
    N1=
A*cosh(A*y)*C(1,1)+A*sinh(A*y)*C(2,1)+3*y.^2*C(3,1)+2*y*C(4,1)+C(5,1
);
    N2=
A*cosh(A*y)*C(1,2)+A*sinh(A*y)*C(2,2)+3*y.^2*C(3,2)+2*y*C(4,2)+C(5,2
);

N3=A*cosh(A*y)*C(1,3)+A*sinh(A*y)*C(2,3)+3*y.^2*C(3,3)+2*y*C(4,3)+C(
5,3);
    N4=
A*cosh(A*y)*C(1,4)+A*sinh(A*y)*C(2,4)+3*y.^2*C(3,4)+2*y*C(4,4)+C(5,4
);

N5=A*cosh(A*y)*C(1,5)+A*sinh(A*y)*C(2,5)+3*y.^2*C(3,5)+2*y*C(4,5)+C(
5,5);

N6=A*cosh(A*y)*C(1,6)+A*sinh(A*y)*C(2,6)+3*y.^2*C(3,6)+2*y*C(4,6)+C(
5,6);

    fn1 =
(nd_disp(i,1)*N1+nd_disp(i,2)*N2+nd_disp(i,3)*N3+nd_disp(i+1,1)*N4+n
d_disp(i+1,2)*N5+nd_disp(i+1,3)*N6);

     M1= 0.2463*A*cosh(A*y)*C(1,1)+0.2463*A*sinh(A*y)*C(2,1)+(-
8.9728*R-3*y.^2)*C(3,1)-2*y*C(4,1)-C(5,1);
    M2= 0.2463*A*cosh(A*y)*C(1,2)+0.2463*A*sinh(A*y)*C(2,2)+(-
8.9728*R-3*y.^2)*C(3,2)-2*y*C(4,2)-C(5,2);
    M3=0.2463*A*cosh(A*y)*C(1,3)+0.2463*A*sinh(A*y)*C(2,3)+(-
8.9728*R-3*y.^2)*C(3,3)-2*y*C(4,3)-C(5,3);
    M4= 0.2463*A*cosh(A*y)*C(1,4)+0.2463*A*sinh(A*y)*C(2,4)+(-
8.9728*R-3*y.^2)*C(3,4)-2*y*C(4,4)-C(5,4);
    M5=0.2463*A*cosh(A*y)*C(1,5)+0.2463*A*sinh(A*y)*C(2,5)+(-
8.9728*R-3*y.^2)*C(3,5)-2*y*C(4,5)-C(5,5);
    M6=0.2463*A*cosh(A*y)*C(1,6)+0.2463*A*sinh(A*y)*C(2,6)+(-
8.9728*R-3*y.^2)*C(3,6)-2*y*C(4,6)-C(5,6);
     fn2 =
(nd_disp(i,1)*M1+nd_disp(i,2)*M2+nd_disp(i,3)*M3+nd_disp(i+1,1)*M4+n
d_disp(i+1,2)*M5+nd_disp(i+1,3)*M6);
    %display(fn);
   %
display(N1);display(N2);display(N3);display(N4);display(N5);display(
N6);
    x=x1+y;
    fn=-fn2-fn1;
  for i=1:1:6
    fprintf(fid2,' %8.8f\t %8.8f\r\n',x(i),fn(i));
  end
    plot(x,fn);
    hold on;
end
hold off;
fclose(fid2);
```